Check for updates

Materials Horizons



Accepted Manuscript

This article can be cited before page numbers have been issued, to do this please use: S. Kiyabu, A. Shkatulov, A. Ahmed, S. Greene, H. P. Huinink and D. Siegel, *Mater. Horiz.*, 2025, DOI: 10.1039/D5MH01794G.



This is an Accepted Manuscript, which has been through the Royal Society of Chemistry peer review process and has been accepted for publication.

Accepted Manuscripts are published online shortly after acceptance, before technical editing, formatting and proof reading. Using this free service, authors can make their results available to the community, in citable form, before we publish the edited article. We will replace this Accepted Manuscript with the edited and formatted Advance Article as soon as it is available.

You can find more information about Accepted Manuscripts in the <u>Information for Authors</u>.

Please note that technical editing may introduce minor changes to the text and/or graphics, which may alter content. The journal's standard <u>Terms & Conditions</u> and the <u>Ethical guidelines</u> still apply. In no event shall the Royal Society of Chemistry be held responsible for any errors or omissions in this Accepted Manuscript or any consequences arising from the use of any information it contains.



Heat is a central component of the world's energy ecosystem. Examples of heat's prevalence include combustion engines, which convert heat into mechanical work, while heat from solar energy, geothermal wells, and the burning of fossil-fuels is used to condition the air and water in homes, offices, and factories. In the U.S., approximately 10% of the energy consumed can be traced to residential heating and cooling alone. More generally, energy generation and use exhibit inefficiencies associated with large thermal losses -- 66% of the energy produced in the U.S. in 2023 did no useful work and was lost to the environment as heat. Hence, technologies that capture, manage, and re-use heat have the potential to yield significant improvements in energy efficiency and expedite decarbonization. Thermal energy storage (TES) is one such technology. TES is predicted to reduce energy costs by 5-15% and peak electrical power demand by 13-33% globally. Despite these benefits, the development of TES systems remains in its infancy due to deficiencies in the underlying storage materials. This review introduces materials and mechanisms for low-temperature TES, emphasizing those that store heat using thermochemical reactions. Benefits, challenges, and high-priority research directions for thermochemical TES materials are described in detail.

Data availability statement:

No primary research results, software or code have been included and no new data were generated or analysed as part of this review.

View Article Online DOI: 10.1039/D5MH01794G

ARTICLE

Materials for thermochemical energy storage and conversion: Attributes for low-temperature applications

Received 00th January 20xx. Accepted 00th January 20xx

DOI: 10.1039/x0xx00000x

Steven Kiyabu, at Aleksandr Shkatutov, b, ct Alauddin Ahmed, a Samuel M. Greene, d Hendrik P. Huinink, c,* and Donald J. Siegeld,e,*

The development of systems that can efficiently store and manage thermal energy - i.e., heat - would improve the efficiencies of numerous processes throughout multiple sectors of the global economy. Nevertheless, the developent of these thermal storage devices remains at a relatively early stage. To engage more researchers in the development of these devices and to accelerate their commercialization, this review presents an introduction to the properties of thermal storage materials that absorb and release heat through thermochemical reactions. Thermochemical materials typically exhibit the largest energy densities among all approaches to materials-based heat storage. Nevertheless, they suffer from limited reaction rates and poor cycle life. An additional challenge is the multi-scale nature of the energy storage process, which ranges from atomistic interactions that govern the storage of heat through alteration of chemical bonds, to mesoscale processes that control the transport of mass and heat. Following an overview of general concepts related to thermal energy storage, emphasis is placed on describing properties relevant for low-temperature applications. These applications include domestic heat storage/amplification (hot water heating), adsorptive cooling (air conditioning), and heat-moisture recuperation. Subsequently, detailed introductions are provided to the mechanisms and materials relevant for the three primary approaches to low-temperature themochemical storage, including: (i) absorption in solids (hydrates, ammoniates, and methanolates); (ii) adsorption in porous hosts (zeolites, metal-organic frameworks); and (iii) dilution in liquids. For each category, advantages and shortcomings of benchmark and emerging materials are discussed. Finally, challenges and opportunities are highlighted for research aimed at developing optimal materials for thermochemical energy storage.

Introduction

Heat is a central component of the world's energy ecosystem. One example of heat's ubiquity is the production of heat in fossil-fuel-based combustion engines. The subsequent conversion of this heat into mechanical work is the basis for many of the transportation devices and industrial machinery in use since the 19th century. In addition, heat from solar energy, geothermal wells, and combustion is used to condition the air and water in homes, offices, and factories.

Given its prevalence in our society, managing the flow and use of heat presents an opportunity for improving energy efficiency. For example, over two thirds of the energy produced in the United States – approximately 62 quadrillion BTUs – does no useful work, and is ultimately lost to the surroundings as heat.1 This fraction of lost energy is typical of countries worldwide.^{2,3} While the second law of thermodynamics limits the conversion of heat into work, the magnitude of these losses suggests that the capture, storage, and/or re-use of only a small fraction of this 'lost' thermal energy would be beneficial. Furthermore, since the production of heat often occurs through the combustion of fossil fuels, strategies that maximize the use of the generated heat have the potential to reduce carbon emissions.

One technology for effective heat management is thermal energy storage (TES), i.e., the storage of heat. Several studies have estimated the potential benefits of TES systems, and the results are promising. For example, in the European Union TES has been projected to achieve a 7.5% overall energy savings.4 Globally, TES is expected to reduce energy costs (by 5-15%) and peak electrical power demand (by 13-33%).5 TES is also one of the few technologies that can provide significant value in decarbonizing multiple use sectors. For example, TES has the projected potential to reduce carbon emissions by ~25% through the decarbonization of the energy grid. 7,8

TES has the potential to be applied in many contexts and for multiple applications:

Buildings. Applications of TES in buildings can improve the performance of heating, ventilation, and air conditioning (HVAC) systems. 9-11 21% of the energy consumed in the U.S. can

^{a.} Mechanical Engineering Department, University of Michigan, Ann Arbor, MI 48109, USA.

^{b.} Iberian Centre for Research in Energy Storage, CIIAE, Polígono 13, Parcela 31, "El Cuartillo", Cáceres, 10004, Spain

^{c.} Eindhoven Institute for Renewable Energy Systems, Eindhoven University of Technology, P.O. Box 513, 5600 MB Eindhoven, the Netherlands.

d. Oden Institute for Computational Engineering and Sciences, University of Texas at Austin, Austin, TX, 78712, USA.

e. Walker Department of Mechanical Engineering and Texas Materials Institute, University of Texas at Austin, Austin, TX, 78712, USA.

[†] These authors contributed equally

^{*} Corresponding authors

Open Access Article. Published on 24 oktober 2025. Downloaded on 02.11.2025 08.53.33.

ARTICLE Journal Name

be traced to residential applications, 12 48% of which is devoted to heating and cooling. 13 Because approximately 75% of all waste heat generated is below 100 °C (a temperature suitable for use in buildings), there is a high reuse potential for this lower-temperature heat in domestic heating applications. Improvements to HVAC made possible by TES will translate to higher efficiencies, lower operating costs, and reduced CO_2 emissions through reduced consumption of the fossil fuels used to generate the electricity that powers HVAC devices.

Preservation of perishables. TES systems offer an increase in thermal inertia, which is measured by the responsiveness of a system's temperature to the supply or withdrawal of heat. As thermal inertia increases, a greater amount of heat is required to change the system's temperature. This feature of thermal energy storage systems has been exploited to preserve food and other perishables by maintaining them at low temperatures. A common example is the use of ice as a phase change material, but containers with even greater thermal inertia have been developed. For example, the Greenbox Thermal Management System has been used to keep vaccines and other temperature-sensitive medical supplies cool during long periods of transportation.¹⁴

Electronics. TES can be deployed to protect sensitive electronics. ^{15,16} As electricity flows through a circuit, the resistance of the circuit results in energy loss through heat. This heat can physically damage fragile components in a circuit. As such, either cooling or a heat sink (a TES system) can aid in maintaining acceptable temperatures.

Vehicles. TES can be used in vehicles to condition the temperature of engines.^{17–19} When a vehicle starts from cold conditions, several minutes of operation are needed before a steady operating temperature is achieved. When cold, the engine operates less efficiently, consumes more fuel, and the exhaust gas from the engine is lower in temperature, resulting in a less effective catalytic converter. A TES system can aid in pre-heating the engine by capturing waste heat from prior operation, thereby reducing the inefficiencies associated with cold-start. Further benefits can be derived by using TES as a thermal sink to reduce overheating under high tractive efforts.²⁰

Thermal batteries. A thermal battery, i.e. a system that captures and stores heat for later use, is a generalization of the cold-start TES application discussed above. Thermal batteries have been proposed to capture waste heat from industrial processes, operating in the range of 100–300 °C.^{21–24} This captured heat is then used for electricity production, thus increasing the overall efficiency of the cogeneration scheme. TES can also be used in conjunction with solar energy generation.^{25,26} The availability of solar energy fluctuates due to weather conditions and according to daily and seasonal cycles. By storing excess solar energy, a TES-enabled solar plant can provide output that is less dependent on the instantaneous solar conditions to meet time-varying energy demand.

The examples mentioned above illustrate that TES systems can take a variety of forms. Nevertheless, at their core all these systems share the common trait of employing a material that stores thermal energy. These materials store heat in one of

three ways: as sensible heat, as latent heat, heat hermochemical heat.

DOI: 10.1039/D5MH01794G

Sensible heat storage. All materials store sensible heat within the kinetic energy of atomic vibrations. The amount of heat stored is indicated macroscopically by the temperature. Materials with higher specific heat capacities store more sensible heat for a given temperature increase; therefore, these materials tend to store heat with higher energy densities. Liquid water, with its high specific heat capacity, is a common medium for sensible heat storage. Other materials such as alcohols, plastics, concretes, molten salts, and metals have also seen use in sensible heat storage systems.⁹

Sensible heat storage is the simplest form of TES. It has the advantage of being reversible, so long as changes to the operating temperature — which can trigger phase transformations — are avoided. However, sensible heat storage is characterized by low energy densities (Figure 1). Thus, it is not suitable for applications where lightweight and/or compact TES systems are required. Furthermore, sensible heat storing materials will lose stored energy if the system is not well insulated. This limits its use in applications that target long-duration storage.

Latent heat storage. Another method of TES exploits the latent heat of a phase transformation. To implement this approach, the so called phase change materials (PCMs) are used. ^{9,27} A common example is an ice cube that keeps a drink cool. Here, heat transferred from the surroundings is absorbed

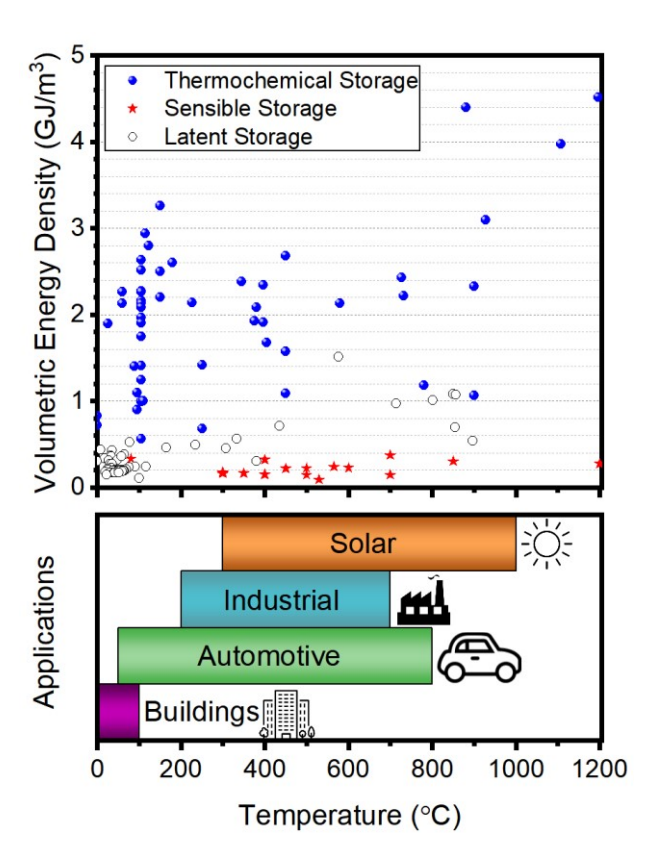


Figure 1. Temperature ladder for thermal energy storage materials and their typical storage densities (top). The general temperature ranges for various thermal energy storage applications are also shown (bottom).

Journal Name ARTICLE

by the ice as the (endothermic) latent heat of melting. These phase changes occur at a specific temperature, which dictates the temperature at which the material will store or release heat. PCMs have 2–6 times greater energy densities than sensible heat-storing materials.²⁸ However, the change in the material during phase change can lead to practical issues, such as melting/solidification temperature hysteresis and volume change.

Thermochemical Energy storage. Lastly, thermochemical materials store heat by undergoing a reversible chemical reaction or sorption process. A typical thermochemical energy storage (TCES) reaction takes the form:

$$Q + A \rightleftharpoons B + C. \tag{1}$$

In the forward endothermic reaction, material A decomposes into material B and working fluid C while simultaneously absorbing heat Q. Unlike PCMs and sensible heat storing materials, thermochemical heat storing materials do not discharge energy over time as the energy is stored in the form of the chemical potential of the products, as long as they remain physically separated. When B and C are recombined and react, the reverse exothermic reaction occurs, re-forming A and releasing the stored heat. In the case of a sorption-based thermochemical process, B represents the sorbent, C is the sorbate, and A is the sorbate-sorbent complex. TCES materials have the largest energy densities of all TES materials, reflecting the large amount of energy that can be stored by a chemical reaction. However, the chemical reaction also poses some complexities. For example, it is common for these materials to experience irreversibility due to side reactions as well as slow kinetics due to limitations in mass and/or heat transfer.^{29,30}

Figure 1 shows a "temperature ladder" for various TES materials,31-40 as well as temperature ranges9,17,21,31,41 for various TES applications. Although they exhibit more practical complexity, thermochemical heat storage materials offer significantly higher energy densities on the material level. Additionally, the temperature ladder shows a general correlation between the operating temperature of TES materials and their energy densities. One reason for this is that higher enthalpies of transformation, ΔH , associated with the relevant chemical reaction or phase change, correlate both with higher thermodynamic equilibrium temperatures and energy densities. This correlation is useful for understanding the limits of energy density for a particular application as materials are generally chosen based on the target operating temperature. In some cases, it is possible to use all three methods in one material, thus boosting energy storage density.⁴²

Although Li-ion batteries have experienced significant cost reductions, the low efficiency of converting heat to electricity suggests that batteries are less efficient options for energy storage when the energy to be stored is in the form of heat. For example, modern thermoelectric devices convert heat to electricity with efficiencies in the range of 5 to 15%. 43,44

The preceding discussion illustrates that the field of TES is broad, encompassing many different applications, materials, and system designs. The present review provides an overview of an important subset of the field, specifically focusing on thermochemical and sorptive heat storage materials that

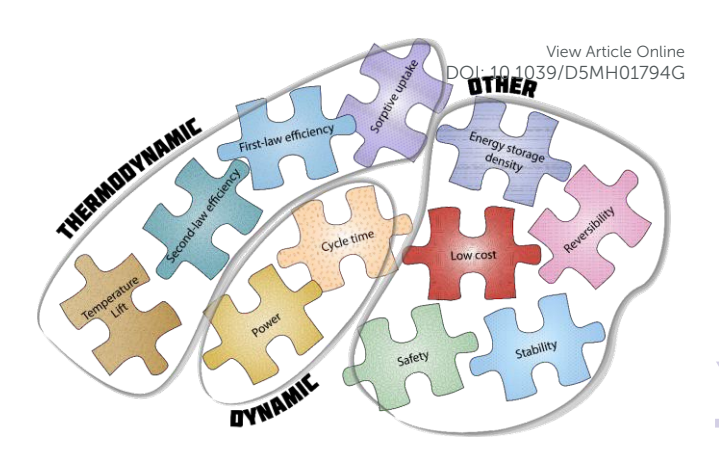


Figure 2. Examples of thermodynamic, dynamic, and other selection criteria relevant for thermochemical heat storage systems.

operate at low temperatures (i.e., below ~100 °C). Additionally, applications that operate in the low temperature region of interest, including TCES systems in buildings, are briefly discussed to illustrate the implications for materials selection and characterization. The materials of interest include salt hydrates, porous media, and liquid absorption of gases. Key properties of these materials are discussed, including thermodynamic operating conditions, energy density, kinetic performance, stability, and several non-technical aspects. The review concludes with a discussion of current challenges and opportunities in the field.

Materials performance criteria and example applications

A. Criteria for materials selection

Several performance criteria exist for TCES systems (Figure 2). These criteria can be loosely divided into those based on thermodynamic, dynamic, and 'other' characteristics. Thermodynamic criteria refer to the capacity and efficiency with which heat is stored (e.g., COP, second-law efficiency). Dynamic criteria refer to the rate at which thermal energy is stored or released (power and cycle time). Other important characteristics include safety, cost, and energy density.

Since the properties of the TCES material strongly influence the performance of the resultant TCES system, the system criteria illustrated in Figure 2 can also be used to guide materials selection. Additional application-specific requirements (e.g. low toxicity for domestic usage) or system design constraints (open/closed, fixed or moving bed) should also be accounted for when selecting suitable TCES materials.^{45–48} This selection task is further complicated by the presence of design trade-offs (e.g. storage density vs. temperature lift^{49,50}) and limited understanding of the relative importance of the various materials attributes in determining system performance.

Table 1 summarizes performance targets associated with several key properties of thermochemical energy storage systems and materials, as proposed by the U.S. Department of Energy (DOE) and the European Technology and Innovation

sen Access Article. Published on 24 oktober 2025. Downloaded on 02.11.2025 08.53.33.

ARTICLE Journal Name

Platform on Renewable Heating and Cooling (RHC-ETIP). 51,52 The target for energy density at the system level, 200 and 220 kWh/m³, respectively, is similar for both the DOE and RHC-ETIP. Translating this system-level target to an energy density at the materials level requires knowledge of the volume occupied by the non-active components of the storage device. These components will vary depending on the system design (open vs.

Table 1: Performance targets for domestic thermochemical energy storage

Property	Target	Comments
System-level energy density	200 kWh/m ^{3 49} 220 kWh/m ^{3 52}	Based on U.S. DOE and RHC-ETIP
Materials-level energy density	400-600 kWh/m ³	Assumes system energy density is 30%-50% of materials energy density ⁵³
Cost of composite storage material	<\$15/kWh ⁴⁹	Includes active material and materials that facilitate heat/mass transport
Thermal conductivity	>1.0 W/m K ⁴⁹	For composite storage material
Capacity retention and cycle life	>90%, 7500 cycles or 20 years ⁴⁹ 25 years ⁵²	
Subcooling / supercooling	<2 °C ⁴⁹	Low temperature hysteresis desired for charging/discharging

closed), and may include heat exchangers, evaporators, storage vessels, etc. Hence, to account for the volumes of the non-active components, a target for the energy density of the storage material should exceed that for the system. N'Tsoukpoe compared the system-level and materials-level energy densities of several prototype thermal storage systems.⁵³ Their analysis found that in most cases the system-level energy densities were significantly smaller than the that of the active material. In the best cases, the system energy density was 30% to 50% of the materials-only value. Assuming that these (best case) systems represent what can be achieved through system design optimizations, then a reasonable target for the materials-level energy density would be two to three times the system-level target, or 400-600 kWh/m3.

Below, important materials selection criteria are described for applications including domestic heating, cooling, heatmoisture recuperation in buildings, and water harvesting.

Thermodynamic criteria. The thermodynamic properties of a TCES system refer to the amount and quality of thermal energy processed.

First-law efficiency: The first-law efficiency or the Coefficient of Performance (COP) of a TCES system is defined as follows:

$$COP = \frac{\left|Q_{useful}\right|}{Q_{input}}, \text{DOI: } 10.1039/\text{D5MH017} \\ 42$$

where Q_{useful} is the amount (or flow) of useful heat from a system, and Qinput is the total amount (or flow) of heat that drives a cycle under consideration. For thermal energy storage, a larger COP implies that a greater amount of useful heat can be recovered upon discharging relative to the lower-grade heat supplied to the system upon charging. A high COP can be achieved by minimizing thermal losses incurred during charging or discharging, for example by minimizing hysteresis and improving the system's kinetics. For water as the working fluid, the COP for TCES systems is usually less than 1.54,55 For thermally-driven TCES applications where the input energy Qinput is available 'for free' from, for instance, a solar concentrator or a PV panel, the COP is often not a highlyrelevant quantity.

Temperature lift: Temperature lift, TL_{eq} , is another parameter that is meaningful for heat storage systems. Thermodynamic temperature lift may be defined as:

$$TL_{eq} = T_{release}(eq) - T_0 (3)$$

Here, $T_{release}(eq)$ is the equilibrium temperature for the heat release process and T_0 is the ambient temperature, which is equal to the temperature of the working fluid.

Second-law efficiency: The second-law efficiency (or exergy efficiency) describes the usefulness of the heat recovered upon charging and discharging a TCES system.56 The exergy, A, of a heat transfer process is defined in terms of the Carnot factor as:

$$A = \left(1 - \frac{T_0}{T}\right)Q,\tag{4}$$

where T_0 is the ambient temperature, T is the temperature at which heat is transferred, and Q is the amount of heat transferred. By analogy with Eq. 2, one can introduce the exergy efficiency, Ψ , of a system:

$$\Psi = \frac{\left| A_{useful} \right|}{A_{input}} \tag{5}$$

where Auseful is the amount (or flow) of useful exergy from a system, and Ainput is the total input amount (or flow) of exergy. Exergy quantifies the usefulness of heat by quantifying how much work could be extracted from 1 J of heat supplied to an ideal machine operating with Carnot efficiency. For instance, a material releasing "useful" heat at 299 K with T_0 = 298 K will not be suitable for TCES as the number of "useful" Joules (exergy) extracted will be low, even if Q_{useful} is large. For a similar reason, low values of temperature lift for TCES systems yield low values of exergy efficiency. For many solid-state transformations, a substantial metastability is observed (discussed below), which results in sluggish kinetics for heat storage and/or release close to equilibrium.⁵⁷ Such metastability lowers the exergy efficiency, thus limiting that material's applicability for TCES. However, we note that despite low exergy efficiency for some TCES cycles they still may be appropriate for certain lowtemperature applications where heat is used directly, e.g. space heating or drying.

Dynamic criteria. Heat must be absorbed or released at sufficient rates for a TCES system to be practically useful.

Journal Name

ARTICLE

Heating power: Heating power, W, is the most straightforward way to quantify the rate of heat or cold storage/release:

$$W = \frac{dQ_{useful}}{dt} \tag{6}$$

The heating power is predominantly determined by the system design and by material properties such as the rate of heat/mass transfer within the material bed. For a bed of TCES particles, thermal conductivity, heat capacity, and the diffusion coefficient are important factors in achieving an optimal bed design.48

Cooling power or SCP: Cooling power or specific cooling power, SCP, is defined as the amount of heat absorbed by a system per unit time divided by either the mass of the material

$$SCP = -\frac{1}{m} \frac{dQ_{useful}}{dt} \tag{7}$$

or by its volume (V):

This article is licensed under a Creative Commons Attribution-NonCommercial 3.0 Unported Licence

pen Access Article. Published on 24 oktober 2025. Downloaded on 02.11.2025 08.53.33

$$SCP = -\frac{1}{V} \frac{dQ_{useful}}{dt}$$
 (8)

Cycle time: Cycle time is another important factor that affects material selection. For short-term cycles (e.g. daily storage) adsorption on a surface or absorption in a liquid is often preferable for TCES. On the other hand, for long-term storage, chemical reactions involving absorption in solid materials are preferable due to their lower tendency for heat losses.

Dynamic temperature lift: An alternative form of temperature lift, termed dynamic temperature lift, TL_{dyn} , is commonly used in studies dedicated to TCES prototypes. In this case the temperature lift is defined as the temperature reached during discharging, Trelease, at the outlet (maximal or average) minus the initial temperature, T_{inlet} , of the heat transfer fluid

$$TL_{dyn} = \max(T_{release}) - T_{inlet}$$
 (9)

Other criteria. Other aspects of TCES materials relevant for domestic applications include:

- · Energy storage density (ESD, energy stored per unit volume of the material, bed, or the device) and specific energy (energy stored per unit mass)
- · Amount of working fluid (or sorbate) exchanged during the cycle Δw , g/g (for cooling, moisture recuperation, water harvesting)
- Presence/absence of side reactions (i.e., chemical degradation)
- · Reversibility of reaction or sorption/desorption
- Mechanical properties (compressibility, volume change, flowability - for moving beds)
- Cost (per unit of processed energy)
- Toxicity (high LD₅₀, mg/kg)
- Flammability

The above criteria point to challenges associated with the use of several materials for domestic applications, for instance, those based on ammonia or methanol (due to toxicity and flammability) or those involving compounds of expensive metals.39,45-47,59 While the costs of new technologies that rely on the sourcing of materials that are not in wide use can initially be high (such as for the TCES systems discussed here), Flaplid Cost reductions have been demonstrated in related technologies by exploiting economies of scale. For example, the cost of Li-ion batteries has decreased by approximately 97% over the past three decades. 60 We anticipate that similar cost reductions can be achieved for the materials relevant for TCES.

B. Example applications for TCES

Domestic heat storage. A thermochemical energy storage system for domestic applications may be considered as a thermally-driven heat pump based on endothermic decomposition (or desorption) and exothermic synthesis (or sorption) reactions.⁴⁷ Figure 3 shows an ideal thermodynamic cycle of a domestic TCES system, which consists of two isobars and two isosteres. During storage or charging (process $3\rightarrow 4$) the material is decomposed at ($T_{storage}$, P_{dec}) while the resultant gas is condensed at $T_{\it cond}$ in the condenser (or ejected to the surroundings for an open system). Once the decomposition is complete (4), the heat is stored in the form of chemical potential which is constant across isosteres (2-3 and 1-4 in Figure 3). In a domestic storage cycle, heat is released at $T_{release} < T_{storage}$ during synthesis by evaporating the working fluid at (P_{syn}, T_{evap}) while bringing it in contact with the charged thermochemical material. The cooling effect in the evaporator is produced simultaneously with useful heating,

The most popular closed TCES systems exchange only heat with the surroundings. These consist of an adsorber-desorber for decomposition/synthesis of the TCES materials and an evaporator-condenser for the evaporation/condensation of a working fluid. In contrast, open systems exchange the working fluid with the environment and do not require a separate vessel for condensation.

For both open and closed systems the adsorber-desorber subsystem often consists of a packed bed of an active storage material with an integrated heat exchanger. 61 Alternatively, one can decouple decomposition-synthesis and storage by allowing them to occur separately in a heat exchanger and a storage tank, respectively. However, this approach requires transport of

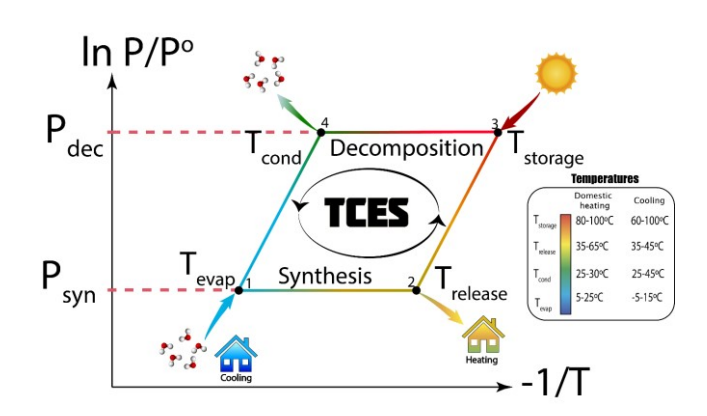


Figure 3. The four-temperature thermodynamic cycle of a thermally-driven chemical heat pump for domestic TCES depicted in In P/Po - (-1/T) coordinates with typical temperature values in the inset

Journal Name

This article is licensed under a Creative Commons Attribution-NonCommercial 3.0 Unported Licence

pen Access Article. Published on 24 oktober 2025. Downloaded on 02.11.2025 08.53.33

Table 2. Examples of lab-scale prototypes of domestic TCES systems and their most relevant characteristics. Only prototypes releasing heat at T_{release} > 30 to make the prototypes releasing heat at T_{release} > 30 to make

Heat release transition	Туре	ESD _{mat} / ESD _{bed} , GJ/m ³	Temperatures Tevap/Trelease/Tstor age, °C	TL _{max} , °C	Power, W/kg	N _{cycles}	Ref.
$MgCl_2 \cdot 2H_2O + 4H_2O \rightleftharpoons MgCl_2 \cdot 6H_2O$	Packed bed, closed	2.0/0.5	10/50/130	54	-	-	339
$K_2CO_3 + 1.5H_2O \rightleftharpoons K_2CO_3 \cdot 1.5H_2O$	Packed bed, closed	1.3/0.8	10/40/90	50	-	14	340
$SrBr_2 \cdot H_2O + 5H_2O \rightleftharpoons SrBr_2 \cdot 6H_2O$	Packed bed, closed	2.6/0.67	15/35/80	-	86.4(avg)	-	341
LiCl+H₂O ⇌ LiCl solution (vermiculite)	Packed bed, closed	-/1.0	10/35/90	12	2100 (peak)	14	342
LiBr+H₂O ⇌ LiBr solution (silica)	Packed bed, closed	1.37/-	10/30/120	17	300 (peak)	10	343
$K_2CO_3+H_2O \rightleftharpoons K_2CO_3$ solution (vermiculite)	Packed bed, closed	-/0.9	25/40/120	15	450 (avg)	47	344
$CaCl_2 \cdot 2H_2O + H_2O \rightleftharpoons CaCl_2$ solution (vermiculite)	Packed bed, open	-/0.36	20/57/80	36	106 (peak)	6	58

the storage material from the storage vessel to the heat exchanger; such systems are referred to as moving bed systems. Each system design has advantages and drawbacks; helpful reviews of these topics can be found elsewhere.^{30,62}

For domestic heat storage, the boundary temperatures and pressures are defined by the available source(s) of heat to be stored and by the heating demand. Ideally, decomposition would be driven by a solar collector/PV panel with typical temperatures $T_{storage}$ = 80–100 °C, while the condensation of the working fluid (water) would occur at near ambient temperature, T_{cond} = 25–30 °C.⁴⁷ The stored heat may be used for space heating ($T_{release} = 30-45$ °C) or for the production of hot water ($T_{release}$ = 60–70 °C) by upgrading low-temperature heat taken from the environment (e.g. from geothermal wells or directly from air) at $T_{evap} = 5-25$ °C. While these boundary conditions are typical for domestic applications (Table 2), more exotic examples include decomposition via an electric heater at $T_{storage} > 300 \, ^{\circ}C^{63}$ or upgrading heat using a temperature difference between air (-40-25 °C) and water (2-3 °C) in colder climates for space heating.⁶⁴ In the latter case, the so-called "heat-from-cold" (HeCol) cycle differs from the one presented in Figure 3 as the sorbent is regenerated via pressure rather than through a temperature difference. 65,66

The criteria for material selection in domestic heating applications arise from space constraints for the TCES system, and from temperature requirements for hot tap water or space heating. Consequently, energy storage density (i.e. the amount of heat stored per cubic meter of the storage bed or device), temperature lift, power, and cyclability are the most relevant parameters. Material toxicity is also a concern as many governments impose restrictions on working fluids for refrigerants used in the domestic environment (e.g. ammonia or methanol). Unsurprisingly, material price per unit of stored energy is also an important criterion.⁶⁷ Additional system-specific requirements on the storage materials may be introduced — e.g. absence of side reactions with air or mechanical strength of the storage particles — for certain system designs (open/closed and fixed/moving bed).

Most existing domestic heat storage prototypes based on salt hydrates are closed systems that contain a packed bed. In these designs a heat exchanger is embedded within the bed, usually by means of metal plates or fins (Table 2). Only a few existing prototypes employ solid-state heat-storing reactions; most are based on solid-solution transitions, followed by dilution of the salt solution held by capillary forces in porous media. The deliquescence of the salt allows for the extraction of more heat in comparison with solid-state transformation, but at the expense of reduced temperature lift.⁴⁹

TCES for domestic heat storage has not been widely adopted because the primary operating requirements are not yet fully met. For example, typical energy storage densities are 0.3-0.9 GJ per m³ of bed, and these values are further lowered by the volume of the condenser, pipes, and other components. Unfortunately, energy storage densities at the system level are reported infrequently. For systems that undergo deliquescence, low temperature lift (< 20 °C) remains a challenge, while low power is a common limitation for systems employing solid-solid heat-storing reactions. At present, there exists no "best" material or system design for TCES in domestic applications. Rather, every prototype strives to meet performance demands through a combination of design trade-offs. The necessity of these compromises reflects the absence of an ideal TCES material. Developing improved material(s) is one of the main challenges for accelerating the adoption of TCES.

Cooling and air conditioning. Sorptive cooling dates to the work of Michael Faraday, who used ammonia as an adsorbate and AgCl as a sorbent.^{68,69} The thermodynamic cycle for cooling is similar to the cycle for domestic heating (Figure 3), with two major differences: the useful effect (i.e. cooling) occurs during evaporation, and the boundary temperatures can vary depending on the purpose of the cooling.

Typical applications include air conditioning in buildings and in transport (cars, marine vessels), cooling of datacenters, and ice making for food preservation. For air conditioning, $T_{evap} = 0-10$ °C, while $T_{evap} = -5-0$ °C is used for ice making and deep

Open Access Article. Published on 24 oktober 2025. Downloaded on 02.11.2025 08.53.33.

ARTICLE

View Article Online DOI: 10.1039/D5MH01794G

Table 3. Examples of working pairs for sorptive cooling by salts, based on prototype studies.

Sorbent	Refrigerant	SCP, W/kg	∆w, g/g	Ref.
CaCl ₂ in silica	H ₂ O	-	0.75	345
CaCl ₂ in zeolite+MWCNT	H ₂ O	1111	0.5	346
MnCl ₂ in expanded graphite	NH ₃	350	0.54	285
BaCl ₂ in vermiculite	NH ₃	300-680	0.25	286,347
LiCl in silica	CH₃OH	210-290	0.6	348

freezing. ⁷⁰ Depending on ambient conditions, the condensation temperature is typically 25–40 °C. $T_{storage}$ and $T_{release}$ are usually within similar ranges as for heat storage: 80–100 °C and 35–50 °C, respectively.

The two main criteria for material selection for a refrigeration cycle are the specific cooling power of a bed, SCP, (i.e., how fast cold can be produced,) and the amount of refrigerant exchanged in a cycle⁷⁰ (i.e., the specific refrigerant uptake, Δw), defined by:

$$\Delta w = w_{rich} - w_{weak} \tag{10}$$

where w_{rich} and w_{weak} are the maximum and minimum mass of sorbate, respectively, ad- or absorbed during a refrigeration cycle per mass of sorbent (Figure 4). Other criteria include cyclability and cost.

The preference for high specific cooling power (SCP) limits the use of water as a refrigerant; the saturated vapor pressure of water at 0–10 °C is too low for fast vapor transport and, therefore, fast heat reallocation. (In principle, water may be used at T < 0 °C in the form of a salt solution. The forthis reason, the most promising refrigerants are ammonia, methanol, ethanol, CO_2 and some fluorocarbons. The need for high SCP implies that the sorption process itself should be rapid. The two main sorption mechanisms employed in the TCES field are physical adsorption and absorption of the refrigerant by a salt solution (often in pores of a matrix). Typical SCPs for existing prototypes fall within 300–1000 W/kg (Table 3). There is a complex and not yet fully understood interplay of power, layer and heat exchanger geometry, and cycle time, leading to heuristic relations for optimization of such systems. The saturated vapor resource of th

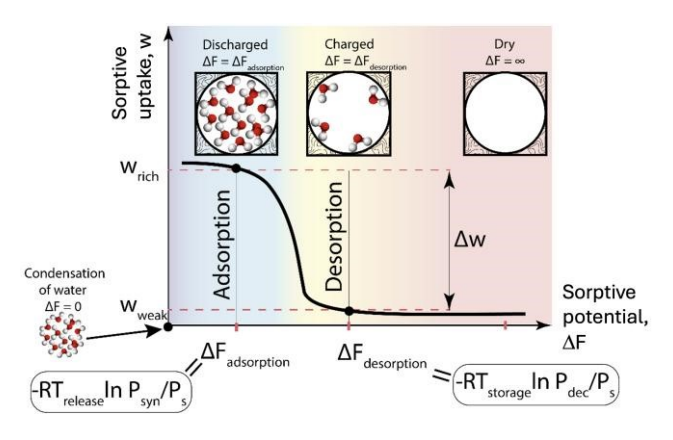


Figure 4. Representation of the four-temperature adsorptive/desorptive cycle for domestic heating and cooling in w, $-\Delta F$ coordinates.

The connections between adsorbate uptake, pressure, and temperature can be described in terms of the Polanyi sorption potential:⁷⁵

$$\Delta F(T, P) = -RT \ln \left(\frac{P}{P_c}\right),\tag{11}$$

where R is the ideal gas constant and P_s is the saturated pressure of the sorbate at temperature T. For most physical adsorbents and composites the sorption uptake curve is invariant of sorption potential (Figure 4). Once the boundary conditions of the cycle are fixed (Figure 3), the Polanyi potentials required to trigger sorption and desorption can be defined (Figure 4). An optimal sorbent will exchange a large amount of refrigerant between the two boundary potentials. Typical Δw values are 0.2–0.7 g/g for adsorbents such as silica gel, zeolites, and salt composites retained within the pores of a host. Recently, several metal-organic frameworks (MOFs) with high water uptake (up to 2 g/g, the highest uptake reported to date) were identified as promising for cooling. $^{76-78}$

Thus, the main challenge for material science in sorptive cooling is the identification of sorbents that can exchange large quantities of adsorbate rapidly and repeatedly under *T,P* conditions appropriate for the cooling cycle.

Heat and moisture recuperation in ventilation systems. In cold climates, the share of heat loss from ventilation systems can reach ~50%. Hence, one promising niche application for TCES is sorptive recuperation of moisture and heat from ventilation. The operating principle for sorptive heat/moisture recuperation involves sorption of water from outgoing air at room temperature and relative humidity (RH) ~40–50%, followed by heat transfer to the ingoing air by means of a heat exchanger (Figure 5). The ingoing air (which is heated in the heat exchanger) is moisturized via the sorbent bed to recuperate humidity. This process minimizes the freezing of air in the heat exchanger and allows for the maintenance of comfortable relative humidity indoors.

Climate conditions and the desired indoor RH set the requirements for the sorbents used for heat and moisture recuperation:

- The water affinity of the sorbent must be large enough to ensure deep drying of the outlet air to the ambient dew point, to prevent ice formation at the bed outlet
- Water affinity must be low enough to ensure release of water to humidify the inlet air to a comfortable RH (40–60%)
- Water uptake, ∆w, must be maximized

Den Access Article. Published on 24 oktober 2025. Downloaded on 02.11.2025 08.53.33

View Article Online

Journal Name

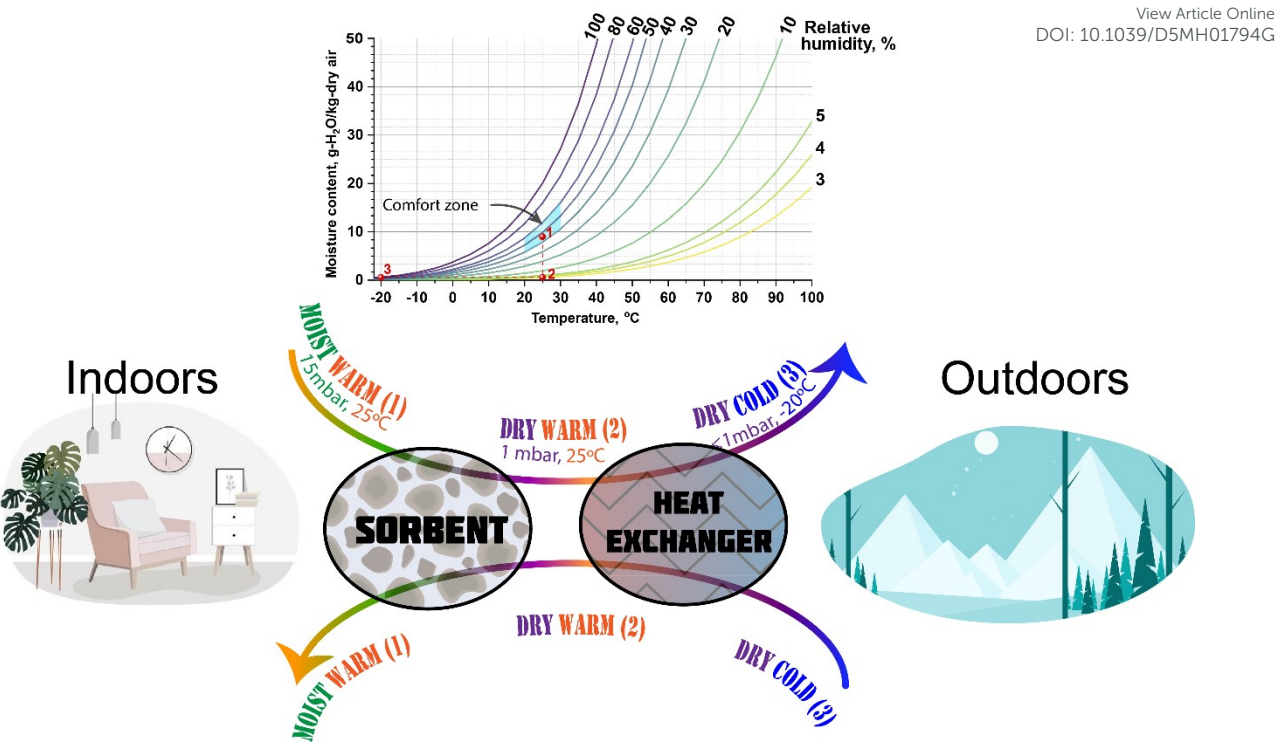


Figure 5, ventilation systems. The moist warm air (point 1 on the psychrometric chart) enters the layer of adsorbent to isothermally dry (point 2), then it exchanges the heat with the cold air at point 3 and is exhausted. Conversely, the outside cold air is heated up and moisturized by the sorbent. The indoor comfort zone is highlighted in blue on the psychrometric chart.

These requirements can be formulated in terms of the sorption potential, as explained above for sorptive cooling. Currently, traditional adsorbents⁷⁹ (e.g. in form of desiccant wheels) and composite sorbents⁸⁰ are considered promising for this application.

Other applications. Other sorptive applications include water desalination81 and water harvesting from air.82 Performance requirements for these cases are typically formulated in terms of the amount of water harvested/produced per unit time. For the materials, this means a large uptake swing Δw between sorptive potentials (Figure 4), which are in turn defined by climatic or ambient conditions such as temperature and relative humidity. Other requirements are low cost and cycling stability. Recent advances in MOF chemistry have led to the design of adsorbents suited for these applications.83 Unlike zeolites or salts in porous matrices, these MOFs allow for milder regeneration temperatures and greater water uptake.84-86

Materials classes and their key attributes

A. Overview of low-temperature thermochemical storage materials

There are three general classes of processes for low temperature thermochemical energy storage. In the first class, a solid chemically reacts with a gas through an absorption process, forming another solid. The most common materials used for this class are salt hydrates, although ammoniates and methanolates operate analogously. The second class consists of the adsorption of a gas within a porous host, such as silica gel, a zeolite, or a MOF. Finally, the third class involves the absorption of a gas by a liquid. The different material families corresponding to these three classes of processes have different properties, which are summarized in Table 4.

In the process, heat is stored in the endothermic decomposition of a more complex solid into another (compositionally simpler) solid and a gas. Heat is released during the reverse synthesis reaction. In the case of salt hydrates (i.e., salts with water molecules incorporated into their crystal structure), the reaction is:

 $Q + S \cdot bH_2O_{(s)} \rightleftharpoons S \cdot aH_2O_{(s)} + (b-a)H_2O_{(a)}$ where Q is the heat of reaction, $S \cdot bH_2O_{(s)}$ is a salt hydrate, $S \cdot bH_2O_{(s)}$ $aH_2O_{(s)}$ is the dehydrated salt or hydrate (with b > a), and $H_2O_{(q)}$ is water vapor. The choice of water as the reactive fluid carries several benefits for low temperature TCES, including safety and abundance, as well as favorable thermodynamic properties that allow the (de)hydration reactions to be reversed at relatively low temperatures.

Of the low temperature TCES materials, hydrates tend to have the highest energy densities on the materials level, both theoretically⁸⁷ and experimentally.⁸⁸ However, many salt hydrates display complexities when implemented in practical systems. For example, some hydrates melt (i.e., form concentrated aqueous salt solutions) rather than dehydrate (i.e., release water vapor) when heated. Others deliquesce when the water vapor pressure is too large, i.e., greater than

Open Access Article. Published on 24 oktober 2025. Downloaded on 02.11.2025 08.53.33.

Journal Name

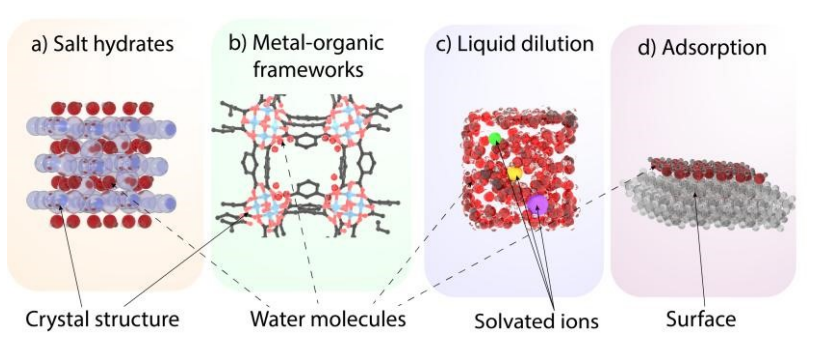
ARTICLE

the deliquescence relative humidity (DRH) of the material. Still others will experience side reactions, such as the well-known hydrolysis of lower hydrates of MgCl₂, which forms gaseous HCl.89 All of these phenomena cause irreversibilities that reduce, upon cycling, the amount of active material that can store heat. Furthermore, the complexities of heat and mass transfer in salt hydrates can result in slow kinetics. In addition to these technical issues, some salts are impractical due to their high cost or toxicity. Despite these practical complications, salt hydrates remain a promising class of TCES materials. Much research is being done to characterize and understand their performance at the materials level, and recently some largescale prototypes using salt hydrates have been built. 63,90

Like hydrates, ammoniates are salts with ammonia molecules present within the crystal structure. Salt ammoniates were originally proposed decades ago for TCES, but only recently have drawn serious attention. 91–93 The ammoniates are analogues of salt hydrates as they are defined by the reaction:

 $Q + S \cdot bNH_{3(s)} \rightleftharpoons S \cdot aNH_{3(s)} + (b - a)NH_{3(g)}$ where the reactive fluid is ammonia rather than water. The use of ammonia poses a practical challenge for many applications as ammonia is toxic. Regardless, these materials may be of interest to a sub-set of applications where the toxicity is sue ean be managed. Recently, Müller et al. characterized many ammoniates according to their energy density.91 The value recorded in Table 4 has been adjusted to maintain consistency with other entries in the table, where energy densities are reported in terms of the volume and/or mass of the more complex (hydrated or ammoniated) material. Here, it can be seen that ammoniates have comparable, although slightly smaller energy densities than hydrates. Similar to hydrates, ammoniates may experience irreversible side reactions, such as the formation of NH₄Cl in chloride salts.⁹¹ They also require the use of pressurized vessels in system designs, which will increase cost and potentially impact energy densities. However, one potential advantage of ammoniates over hydrates is their faster charging/discharging rates due to higher pressures. This is demonstrated by the power value calculated from data reported by Yan et al. for the reaction of MnCl₂ with ammonia.⁹⁴ Finally, since ammoniates have not drawn as much attention as salt hydrates, most ammoniate studies for TCES are on the laboratory scale.

Table 4. Overview of low temperature thermochemical heat storing materials. The illustration shows a few examples of TCES materials, including a) a crystal structure of a salt hydrate (LiCI-H₂O, Class I), b) a crystal structure of a MOF (CAU-10, Class II), c) a cartoon depicting liquid dilution (Class III), and d) surface adsorption (on quartz (001)).



Class	Material	Energy Density	Stability	Power Output	Non-technical Attributes	Technology Readiness Level
I	Salt Hydrates	Up to 3.8 GJ/m³ and 2.3 MJ/kg ⁸⁷	Issues with melting, deliquescence, and hydrolysis	Up to 0.7 MW/m ³ and 0.5 kW/kg ^{136,155}	Rarity and toxicity vary by salt	Laboratory and prototype scale
I	Salt Ammoniates	Up to 2.1 GJ/m³ and 1.6 MJ/kg ^{91,94}	Issues with thermal decomposition	Up to 1.5 kW/kg ⁹⁴	Rarity varies by salt, ammonia is toxic	Laboratory scale
I	Salt Methanolates	Up to 1.3 MJ/kg ⁹⁶	Limited data available	Up to 0.4 kW/kg ⁹⁷	Methanol is flammable and toxic	Laboratory scale
Ш	Silica Gel	Up to 0.8 GJ/m³ and 1.4 MJ/kg ³⁴	Good stability	Up to 0.01 kW/kg (prototype) ¹⁰⁴	Cheaper	Commercial scale
Ш	Zeolites	Up to 0.7 GJ/m³ and 1.1 MJ/kg ³⁴	Good stability	Up to 0.03 kW/kg (prototype) ³⁴⁹	Can be expensive	Commercial scale
Ш	MOFs	Up to 1.3 MJ/kg ¹⁰⁹	Issues with hydrolysis	Up to 2.1 kW/kg ¹⁰⁹	Can be expensive	Laboratory scale
III	Liquid Dilution	Up to 1.4 GJ/m ³ 111	Good stability	Up to 0.03 MW/m³ (prototype) ³⁵⁰	Can be cheaper	Commercial scale

Journal Name

This article is licensed under a Creative Commons Attribution-NonCommercial 3.0 Unported Licence.

Den Access Article. Published on 24 oktober 2025. Downloaded on 02.11.2025 08.53.33

ANTICLE

A smaller family of TCES materials in the first class are salt methanolates, which store methanol molecules in the salt crystal structure. Their reaction is defined as:

 $Q + S \cdot b \operatorname{CH}_3 \operatorname{OH}_{(s)} \leftrightarrow S \cdot a \operatorname{CH}_3 \operatorname{OH}_{(s)} + (b - a) \operatorname{CH}_3 \operatorname{OH}_{(g)}.$ (14)

The literature on m ethanolates for TCES is sparse. Given methanol's favorable properties for refrigeration they are mainly of interest for refrigeration applications. From the data available in the literature, methanolates appear to exhibit similar (perhaps slightly smaller) energy and power densities compared to salt hydrates. Methanolates tend to deliquesce easily, so porous matrices have been used to stabilize and exploit deliquescence. Methanolates to their use is the flammability and toxicity of methanol.

The second class of low temperature TCES materials are porous media. These materials adsorb a reactive gas onto the surfaces of their pores. In most cases, this gas is water, as water has many favorable properties mentioned previously. The different porous media display a range of pore sizes, classified as micropores (pore diameter < 2 nm), mesopores (2-50 nm), or macropores (> 50 nm).102 An example of one of the most mature TCES storage materials is silica gel, which consists of mesoporous amorphous silicon dioxide. These pores readily absorb water from the environment, leading to its common use as a desiccant. Advantages of silica gel include its relatively low cost, widespread availability, and good cyclability. 103 As a result, it has been developed to commercial scale quicker than other thermochemical materials. However, its relatively low energy density in the operational window of low-temperature TCES limits its potential in compact applications. The low power cited in Table 4 for this material is derived from a large-scale prototype involving 350 kg of silica gel. 104

Zeolites represent another category of material that falls within the second class of TCES media. Zeolites are aluminosilicates that can adsorb water into their micropores. Like silica gel, zeolites have been developed to the commercial scale. They are stable but are costlier than silica gel. They possess slightly smaller gravimetric energy densities than silica gels due to their weight, but higher power densities at the prototype scale compared to silica gels. One characteristic of zeolites is their hydrophilicity, resulting in high desorption temperatures for water. ¹⁰³ As such, depending on the maximum charging temperature available, the reversible capacity of zeolites at low temperatures (100 °C) can be limited.

Metal-organic frameworks (MOFs) represent another promising category of porous materials that are of interest for low temperature TCES. MOFs are porous, crystalline materials consisting of metal clusters connected by organic linkers. Well known for their extremely high surface areas, the size of the pores in MOFs can be tuned by substitution of linkers of varying length. ¹⁰⁵ Given the many degrees of freedom in MOF structure and composition, the potential chemical space for MOFs is extremely large, which has attracted the interest of materials designers. ¹⁰⁶ In addition to their cost, the main disadvantage of MOFs is that some MOFs decompose irreversibly in the presence of water, making reversible water capture and release an impossibility for those compositions. ¹⁰⁷ However, several water-stable MOFs are known and show promise for TCES, such

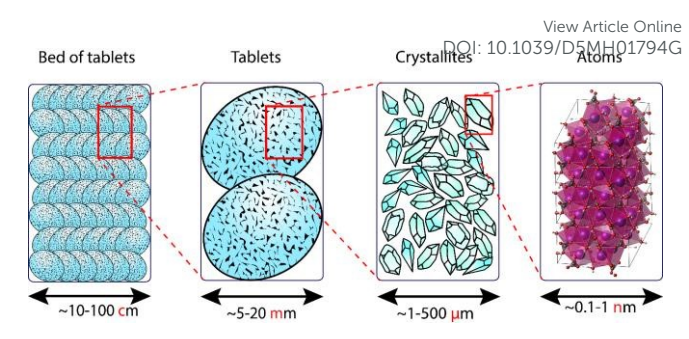


Figure 6. The different length scales associated with the hydration of K_2CO_3 . Reproduced from reference 113 under the terms of the Creative Commons CC-BY license converget 2024.

as MIL-101, CAU-10, NH₂-MIL-125, MOF-801.⁸⁶ Recent efforts have focused on computationally predicting the water stability of MOFs.¹⁰⁸ Ehrenmann et al. characterized the water adsorption of MIL-101, for which energy density and power are reported in Table 4.¹⁰⁹ While the energy density of MOFs is similar to other types of materials, the main advantages are the high power density, which reflects the high degree of regular porosity found in MOFs, and the stepwise adsorption behavior which albeit has only been demonstrated for a few MOFs.¹¹⁰

Finally, the third class of low temperature TCES materials operates via liquid absorption, in which a solute is reversibly evaporated from/absorbed into a solvent. Evaporation, which concentrates the solute (by desorbing the solvent), is endothermic, while the condensation of the solvent back into solution is exothermic. This approach tends to exhibit good stability and thus has reached commercial scale. Also, depending on the solute chosen, the material cost can be relatively inexpensive. Regarding its energy density and prototype-scale power density, its performance is average compared to other types of materials. Yu et al. proposed a three-phase sorption cycle using LiCl/H2O, where the liquid absorption accounted for 57% of the energy stored, translating to an energy storage density of 1.4 GJ/m³ for heat storage. 111 Another remarkable solute is NaOH with potential storage density exceeding 1 GJ/m³ and 20-25 °C temperature lift.50 A trade-off between the energy storage density and the temperature lift is the main reason why absorptive heat storage systems are not yet widespread. 112

B. Class I: Salt hydrates, ammoniates, and methanolates

Materials and scales. Before going into details regarding the properties of salts and their interactions with vapor, it is helpful to have a basic understanding of how these materials will be deployed within a thermal energy storage device. In the core of the device will be a storage bed comprised of small particles of the storage material. Since a powder based on very small crystallites will have a poor permeability for water vapor, use of millimeter-sized particles is foreseen. The particles will be manufactured from a powder and themselves be porous in nature. This introduces several length scales as illustrated in Figure 6, where a cartoon of a hydrating K_2CO_3 particle is shown. The structure and processes occurring at these

pen Access Article. Published on 24 oktober 2025. Downloaded on 02.11.2025 08.53.33

Journal Name ARTICLE

length scales have distinct contributions to properties like energy density, power, stability, etc.

Phase equilibria. Consider a salt that can change its loading with vapor according to the following reaction equilibrium.

$$Q + S \cdot bL_{(s)} \rightleftharpoons S \cdot aL_{(s)} + (b - a)L_{(q)} \tag{14}$$

Here, S represents a neutral ion pair in the salt. L is the gaseous compound that reacts with the salt: i.e. H₂O (hydrates), ^{46,47,114} NH₃ (ammoniates),^{115–117} CH₃OH (methanolates),¹¹⁸ C₂H₅OH (ethanolates), 118 etc. Q is the heat associated with the reaction. During reaction, the salt switches between two states of loading (the number of molecules L per neutral ion pair) a and b with b> a. Bonding of the gas to the salt is accompanied by a release of heat. Therefore, increasing the loading of L within the salt $(a \rightarrow b)$ takes place with the discharge of heat, while reducing the loading $(b \rightarrow a)$ charges the medium. Since the reaction involves a structural change of the crystalline lattice, the process behaves as a phase change. According to the Gibbs phase rule, such a transition occurs at a well-defined set of temperatures T and vapor pressures p, with p = f(T). From here forward we will focus the discussion on salt hydrates, $L = H_2O$, but similar considerations apply to ammoniates, methanolates, etc. As needed, considerations unique to the ammoniates and methanolates will be discussed separately.

When the reaction shown in Equation 14 is in equilibrium, $\Delta G_{rxn}=0$. It follows from this equilibrium condition that the equilibrium vapor pressure p_{eq} and T are related via the van't Hoff equation.

$$p_{eq} = p^0 \exp\left[\frac{\Delta H_{ab}^0 - T\Delta S_{ab}^0}{RT}\right] \tag{15}$$

where p^0 , ΔH^0_{ab} and ΔS^0_{ab} are the standard pressure (1 bar), the standard molar enthalpy of absorption (per mole vapor), and the standard molar entropy of absorption (per mole vapor), respectively. Further, R is the gas constant and T [K] the absolute temperature. In the case of hydration reactions, the enthalpy and entropy are the molar enthalpy and entropy of hydration, respectively. Typical values for the enthalpy ΔH^0_{ab} and entropy S^0_{ab} are 40 - 80 kJ/mol and 140 – 160 J/mol K, respectively.^{87,119}

To illustrate the phase behavior of hydrates a water vapor pressure diagram for MgCl₂ is shown in Figure 7. MgCl₂ can form multiple hydrate phases (n=0, 1, 2, 4, 6, 8, 10, 12)^{120–124} that are stable at different combinations of temperature and water vapor pressure. The most important of these are for n=2, 4 and 6, which are shown in Figure 7, with data taken from Derby et al.¹²⁵ and Carling.¹²⁶ The higher hydrates (n > 6) are not stable at the given conditions. The lines for the lower hydrates n=0 and 1 (not shown) are below the line for the 2-4 transition. At high vapor pressures the salt deliquesces: i.e. it absorbs water and liquifies (turns into solution). It is important to stress that a pressure-temperature diagram like Figure 7 is an intrinsic property of the selected salt.

A driving force for the hydration reaction exists when the chemical potential for water in the vapor phase and water in the solid is unequal.

$$\Delta \mu = RT \ln(p/p_{eq}) \neq 0 \tag{16}$$

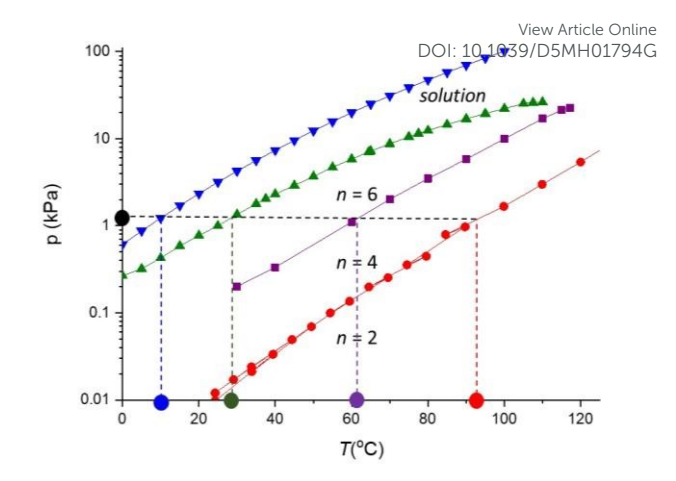


Figure 7. Water vapor pressure-temperature lines for phase transitions of MgCl₂ hydrates MgCl₂•nH₂O: deliquescence (green), n = 4 \rightarrow 6 transition (purple), and n = 2 \rightarrow 4 transition (red). The blue line/points refer to the P-T combinations for saturated water vapor. The coloured dots on the abscissa indicate the theoretical output temperatures of the different phase transitions at water vapor generated at 10 °C (12 mbar). Data adapted from Derby et al. ¹²⁵ and Carling. ¹²⁶

Specifically, the salt is hydrated (discharged) when $\,p/p_{eq}>1\,$ and dehydrated (charged) when $\,p/p_{eq}<1.$

Diagrams like the one shown for MgCl₂ in Figure 7 are helpful because they demonstrate important aspects of the operation of salt hydrates. First, a strong coupling exists between the use conditions of a heat storage device and the optimal salt. As the phase lines are intrinsic features of the crystalline structure and composition of the salt, they cannot be easily adapted to accommodate the prescribed conditions. For discharge (heat generation) it is extremely important to know the conditions of the water vapor source that comes into contact with the salt. For example, Figure 7 shows that when MgCl₂ is reacted with saturated water vapor at 12 mbar / 10°C, the resulting reactions can theoretically deliver heat at several temperatures, corresponding to one deliquescence reaction and two distinct hydration reactions. When the $2 \rightarrow 4$ transition occurs, heat at a temperature slightly above 90 °C is released. However, the temperature of the discharge will drop to lower values of $^{\sim}60$ °C at the 4 \rightarrow 6 transition. In cases where multiple hydration reactions occur for a given salt (i.e., several hydrated phases are stable), the temperature of the generated heat will decrease as one progresses through transitions corresponding to the formation of phases with larger water content. Hence, the use conditions not only determine the kinetics, but also the available heat and thus the effective energy storage density.

The hydration reaction involves risks. At low temperatures, a salt may undergo deliquescence, which can harm the operation of the heat storage device. This complication can be circumvented by avoiding the low temperatures with a system control, or by stabilizing the material to minimize the impact of deliquescence. Despite these stabilization options, extremely deliquescent salts, like LiCl•H₂O (DRH = 11.2%),¹²⁷ LiBr•2H₂O (DRH = 7.75%),¹²⁷ and CaCl₂•2H₂O (DRH = 12.9%),¹²⁸ are not suitable candidates for heat storage based on salt hydration, as decreases in temperature will immediately lead to

pen Access Article. Published on 24 oktober 2025. Downloaded on 02.11.2025 08.53.33.

ARTICLE Journal Name

View Article Online

Table 5. Overview of crystal-level properties of a selection of salts reported as promising TCES materials. The range of possible hydration states (n), energy density for an open TCES system, decrease in molar volume upon dehydration, temperature delivered during hydration (T_{release}), and deliquescence relative humidity are presented for each material. All values are calculated based on water vapor pressures of 12 and 20 mbar for hydration and dehydration, respectively. Data obtained from ref 47.

Salt	n in Salt•n H₂O	Energy density [GJ/m³]	Volume decrease (%)	T _{release} [°C]	DRH (%)
CaCl ₂	0-2	1.54	35	63	13
K ₂ CO ₃	0 – 1.5	1.30	22	59	43
MgCl ₂	2-6	1.93	47	61	33
MgSO ₄	1-7	2.27	63	24	90
Na ₂ S	0.5 – 5	2.79	60	66	>34
SrBr ₂	0-6	2.49	61	48	61
SrCl ₂	0-6	2.99	62	28	73

deliquescence. It should be noted though that exploiting deliquescence is one of the routes to mitigate these risks. 111,344 While it is possible to boost storage density by exploiting deliquescence, such systems operating with salt solutions require a porous media to stabilize and, as noted earlier, often suffer from a poor trade-off between storage density and temperature lift.

Temperature lift. While equilibrium temperature lift (Equation 3) is determined by the transition on the phase diagram dictated by the boundary conditions (T, P(H2O)) for heat storage and release, dynamic temperature lift (Equation 9) is determined by the balance between mass transport and heat transport in a TCES material. 129 The rate of heat release is determined by the rate at which the sorbate reaches the reaction front and the reaction rate, while the rate of heat transport away from the reaction front is determined by diffusive and advective processes. The dynamic temperature lift is closely related to the power density. Mass transport, reaction kinetics, and heat transport are discussed in more detail below.

Energy density. Energy storage density (ESD) is a key property of an energy storage device. Of course, the system ESD is limited by the intrinsic ESD of the material itself: by embedding the storage material in a system the resulting system ESD will be less than that of the material alone, due to the volume occupied by the system components. Similar arguments hold for specific energy. Given that system-related penalties are unavoidable, it is desirable to maximize the intrinsic ESD of the material. Since the molar enthalpy of hydration H^0_{ab} of an a o b transition is a fixed number, the energy density on the crystal level $oldsymbol{u}_c$ equals

$$u_c = \frac{N(b-a)H_{ab}^0}{V_{\rm max}} = \frac{(b-a)H_{ab}^0}{v_b} \eqno(17)$$
 where N [moles], $V_{max} = V_b$ [m³], and v_b [m³/mole] are the

moles of neutral ionic pairs, the maximal molar volume of the material (mostly V_b), and the molar volume of neutral ion pair in phase b, respectively. Note this formula assumes that in the device only a single hydration reaction is accessible. Equation 17 demonstrates that materials with large energy densities should exhibit an efficient packing of water molecules in combination with a large hydration enthalpy.

In cases where multiple reactions (involving different degrees of hydration of the salt) can be accessed the energy density may be expressed as:

$$u_c = \frac{N \sum_{ij} \Delta n_{ij} \Delta H_{ij}^0}{V_{\text{max}}}$$
 (18)

The summation ij runs over all possible hydration transitions and V_{max} is the maximal molar volume, usually for the highest hydrate considered. H_{ij}^0 and Δn_{ij} are the molar enthalpy and change in degree of hydration during the transition ij. The total change in hydration state is given $\Delta n = \sum_{ij} \Delta n_{ij}$.

Although Equations 17-18 provide an upper limit to the ESD, taking into consideration the discussion about the accessibility of phase lines and the use conditions, the system ESD is strongly dependent on the use conditions of the foreseen application. To illustrate this, Table 5 lists the values for the energy densities and output temperatures for use conditions relevant for the built environment (i.e., assuming hydration at 12 mbar and 10 °C, and dehydration at 20 mbar).47

When the ambient temperature or relative humidity are not sufficient to deliver water vapor to the storage system at the required vapor pressure, energy may be required to generate additional vapor from liquid water.³⁰ Accounting for this energy reduces the effective ESD, assuming that this energy cannot be recovered upon discharging. Ideally, all the energy required to generate water vapor should be freely extracted from the environment. However, in some applications, such as in environments near 0 °C, this may not be possible.

There are many system-related factors influencing the system-level ESD.130 These include bed porosity, internal storage of water, piping, auxiliary equipment, sensible heat losses during operation, etc. Here we limit the discussion to the impact of bed porosity and the internal storage of water.

Regarding porosity, the storage system should allow for easy access of water vapor to the salt. For that reason, the storage medium will likely be filled with discrete particles rather than with a salt monolith. Incomplete particle packing introduces porosity (typically 30-50%) into the storage bed, reducing the energy density proportionally.⁴⁷ Furthermore, the particles themselves may exhibit internal porosity which further reduces the ESD.131 Regarding the internal storage of water,47,130 in a closed system the water involved in the hydration reaction is not extracted from the environment and must be stored. As the amount of water to hydrate a salt can be

Journal Name ARTICLE

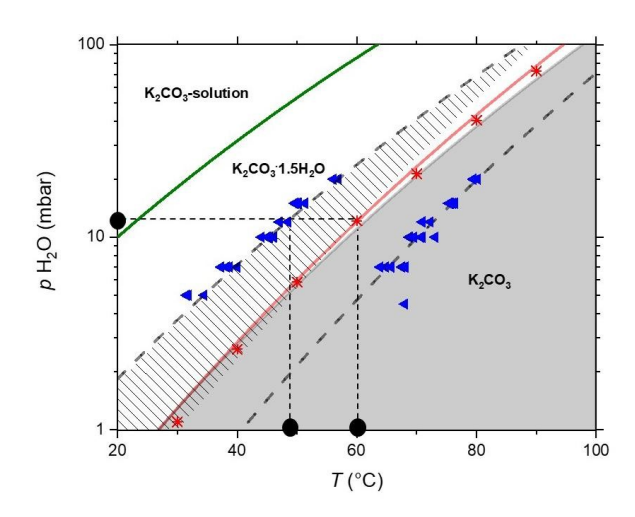


Figure 8. Phase diagram of K_2CO_3 illustrating its metastable zone. The red and green lines refer to the hydration transition and deliquescence line, respectively. The red and blue data points refer to measurements of the hydration-dehydration equilibrium and the metastable zone boundaries. Data adapted from Ref. 57.

large, the volume of the water storage vessel should be accounted for and can significantly reduce the ESD on the system level.

Metastability. Although the thermodynamics of a hydration reaction imply that hydration will occur when $p/p_{eq}>1$ and dehydration at $p/p_{eq} < 1$, there can exist a zone around the equilibrium pressure-temperature line where the kinetics of the reaction are slow: this is referred to as the metastable zone.⁵⁷ Some reactions suffer from large metastable zones, while others with narrow metastable zones demonstrate fast kinetics close to equilibrium. Metastable zones have been observed for many salts, including LiOH, 132 BaCl₂, 133 K₂CO₃, 57,134 Na₂S, 135 MgCl₂, ¹³⁶ CuCl₂, ⁵⁷ SrBr₂ ¹³⁷ and certain minerals. ¹³⁸ In Figure 8 the implications of a metastable zone for discharge are shown with the help of the phase diagram of K₂CO₃.⁵⁷ Upon discharge, when water vapor at 12 mbar is supplied the maximum temperature is about 10 °C lower (50 °C) than what is expected in equilibrium (60 °C). Sufficient power is extracted only outside of the metastable zone. Despite numerous reports of metastable behavior,^{57,88} this phenomenon is still poorly understood.

The existence of a metastable zone with poor kinetics has been hypothesized to result from two rate-limiting mechanisms: deliquescence-recrystallization and nucleation. Deliquescence-recrystallization has been introduced to explain poor hydration kinetics of certain salts in regions of the phase diagram where the thermodynamics favor hydration. For example, the hydration rates of Na_2SO_4 and $Mg(ClO_4)_2$ dramatically increase when the water vapor pressure exceeds the point where the original (lower hydrate phase) deliquesceses. 139,140 The idea is that an $a \rightarrow b$ hydration process follows two steps: deliquescence of the lower hydrate phase, a, followed by crystallization of the higher hydrate phase, b.

However, predictions for the deliquescence points of anhydrous K_2CO_3 and $CuCl_2$ demonstrated that this hydration mechanism could not explain metastability for these two salts.⁵⁷

In the same study it was shown that the hydration rate of these salts was slowed due to sluggish nucleation of the hydrate phase. This explanation was proposed decades ago 141 for the dehydration of salts. When metastability is explained using classical nucleation theory (CNT), the boundaries of the metastable zones are the points where the critical nucleus size becomes on the order of a neutral ion pair and/or the free energy barrier for nucleation is comparable to the thermal energy: 57 $\Delta G^{\#}/k_BT \sim 1$.

As hydration-dehydration processes are solid-solid transitions involving significant modifications to the crystalline lattice, mobile intermediate phases could play a role in controlling the rate of the reaction. Therefore, CNT alone is likely insufficient to explain the origins of metastability. In the case of the hydration transition $a \rightarrow b$ a natural source for ionic mobility could be the surfaces of the relevant crystalline phases. Studies on NaCl have reported the presence of water layers on the crystalline surface far below the deliquescence point of NaCl (DRH = 75%).142,143 Furthermore, in these layers there is significant ionic mobility, implying local dissolution processes. 144,145 Some reports indicate that similar processes might occur on the surfaces of salt hydrates, 146,147 potentially facilitating the hydration process. It may be expected that the ion mobility on the surface of an ionic crystal will strongly increase with the applied water vapor pressure. In recent studies the existence of such a mobile layer has been proven with the help of electrical impedance spectroscopy. 148 Related to this, extreme deliquescent salts have successfully been used to decrease the metastable zone and/or increase the reaction rate.149-151 These surface processes, in combination with a nucleation barrier, could contribute to the metastable zone. Hence, the metastable boundary for hydration might not only be determined by the disappearance of a nucleation barrier, but also by the presence of sufficient water molecules at the surface allowing for increased ion mobility.

Kinetics and power. The power delivered by a salt hydrate-based storage system relies upon the rate of the underlying hydration-dehydration reaction. In the previous section metastability due to sluggish nucleation and surface effects were introduced as factors influencing these rates. Here, the kinetics of the material outside of the metastable zone are discussed. Although many kinetic studies have been published, ^{29,152,153} the complexity of these reactions has limited the development of mechanistic insight: crystalline lattices must be restructured, water molecules must be incorporated (hydration) or extracted (dehydration) from the lattice, water molecules must migrate through solids, etc.

Based on Figure 6 the hydration reaction can be thought of as consisting of two steps: a) diffusion of water vapor through the particle's pore space to the reaction zone, and, b) transformation of the crystal lattice during simultaneous insertion of water. While the first process occurs at length scales comparable to the particle diameter, the second process occurs at nanometer length scales. Below we briefly summarize the current understanding of these processes.

ARTICLE Journal Name

As an example of a solid-gas reaction, 154 the rate of a hydration-dehydration reaction X can be expressed as:

$$\frac{dX}{dt} = k(T)f(X)h(p/p_{eq})$$
 (19)

Here, k(T), f(X) and $h(p/p_{eq})$ are, respectively: a temperature dependent reaction constant that can be coupled with an energy barrier, a function describing the reaction pathway, and a driving force term related to the water vapor pressure. Examples of studies using this model to fit the hydration kinetics of salts and salt composites abundant. 137,153,155,156 What most studies overlook is that the equation is an attempt to decouple the reaction pathway f(X)from the driving force $h(p/p_{eq})$ and the intrinsic rate k(T). However, in the case of salt hydration, one might expect that the water vapor pressure can influence both the rate and the reaction pathway. For example, (and as discussed above,) with increasing water vapor pressure the amount of adsorbed water at the surface of an ionic solid increases 142,143,157 and can enhance surface (reaction) mobility.¹⁵⁸ Transition State Theory¹⁵⁹ gives the best justification for using Equation 20 for local hydration/dehydration processes and the most rigorous derivation of the functional relationship of $h(p/p_{eq})$, 156 but fails in describing many kinetic aspects of salt hydration. 160 Presently, the model is mainly useful for parameterizing the kinetics of salt hydration on a powder level as input for models to describe the kinetics of porous salt particles.

This article is licensed under a Creative Commons Attribution-NonCommercial 3.0 Unported Licence.

Open Access Article. Published on 24 oktober 2025. Downloaded on 02.11.2025 08.53.33.

In larger salt particles, the diffusion of water vapor to the reaction zones can impact the reaction rate. The relative importance of this diffusion process can be estimated with the second Dahmköhler number, $Da_{II}=k_RL^2/D$, where k_R , L, and D are the reaction rate, size of the particle, and the diffusion constant in the particle, respectively. For millimeter size $\rm K_2CO_3$ particles $Da_{II}>1$ and diffusion thus limits the reaction rate and power output of the particle, 131 allowing modelling with the Shrinking Core Model. 161 The following equation holds for the conversion rate in $1\rm D.^{131}$

$$\frac{dX}{dt} = \frac{M_a D}{(b-a)\rho_a (1-\phi_a)L^2 RT} \left(\frac{1}{X}\right) \left(p - p_{\text{eq}}\right) \tag{20}$$

In this model $\rho_{\rm a}$, ϕ_a , and M_a are the density, porosity, and molar mass of the starting phase. Note that Equation 20 can be mapped onto Equation 21 with the substitution $h=p-p_{\rm eq}$ and $f=X^{-1}$. Equation 21 demonstrates the key factors for understanding and improving the power of TCES particles. Firstly, the power decreases with the extent of the reaction: $dX/dt \propto X^{-1}$. Secondly, the power can be increased by reducing the particle dimensions: $dX/dt \propto L^{-2}$. Based on these findings, models for the hydration of particle beds have been developed. 162,163

Degradation. Robustness with respect to degradation of the storage material is also important for the (long-term) performance of a storage device. Three considerations related to degradation are important: First, side reactions during materials manufacturing and use are generally undesirable and should be avoided, as they can compromise energy density and can lead to safety concerns. Second, humid conditions should be avoided during production as deliquescence can hinder the

performance of the salt. Third, volume expansion of the salt should not block access of water vapor a ਜ਼ਿੰਪੀ ਵਿਚੰਦ ਸਿੰਘੀ ਅੰਗਰੀ power output. These three aspects are described in more detail below.

First, in selecting salt hydrates, assessing chemical stability under use conditions is a necessary step. Several examples can be found in the literature that emphasize this point. Na₂S has been considered as a storage material due to its high energy density. 164,165 Unfortunately, it readily reacts with CO_2 and forms Na₂CO₃ with emission of H₂S.^{136,166} These reactions make Na₂S particle manufacturing a cumbersome process, restricts its use to pure water vapor conditions, and involves a safety risk due to the toxicity of H₂S. Similarly, MgCl₂ is still a widely studied material in the field of thermochemical energy storage, 153,167–169 despite the fact it is prone to hydrolysis reactions leading to HCl formation^{170–172} even at relatively low temperatures.¹³⁶ Similar hydrolysis reactions are known for other halides like CuCl₂, ^{173,174} MgBr₂,¹⁷⁵ and carnallite KMgCl₃.^{176,177} Further, metal ions that are prone to oxidation by air (e.g., Fe²⁺, Cr²⁺, Mn²⁺, I⁻) should be avoided.⁴⁷ Less stable anions (i.e., ClO₄-, NO₃-) should also be treated with care.46,47

Second, deliquescence presents a challenge for hygroscopic salt hydrates. A salt or salt hydrate's tendency to deliquesce is characterized by the deliquescence relative humidity (DRH). When the RH of the environment exceeds the material's DRH, the material will deliquesce, i.e., it will spontaneously absorb water from the atmosphere and dissolve within it, forming a liquid solution. Hygroscopic salts/hydrates are characterized by a low DRH. Generally, deliquescence results in reduced cyclability and reaction kinetics due to agglomeration when liquified. 178 While this tends to hold true for many salt hydrates, some mixed salt hydrates have demonstrated good cyclability when deliquesced. 179 Furthermore, while hygroscopic salts require more care regarding their stability with respect to deliquescence, these salts also tend to have faster hydration kinetics (below the DRH of the hydrated phase) due to the mobility of the resulting wetting layer.⁵⁷

Third, the volume expansion of the heat storage material is a source of performance degradation in TCES systems. When a salt hydrates and dehydrates, it undergoes considerable volume expansion and contraction. According to the Thermodynamic Difference Rules, the relative volume expansion during hydration from $a \rightarrow b$ can be approximated as:

$$\frac{\Delta V}{V_0} \approx (b-a)\frac{v_w}{v_a},\tag{21}$$

where ΔV is the volume change, V_0 is the volume of the dehydrated phase, v_w is the average specific volume of water in a salt hydrate (similar to the specific volume of ice), and v_a is the specific volume of the dehydrated phase.

Figure 9 presents the relative volume expansion for selected salt hydration reactions.⁴⁷ A trade-off exists with respect to volume expansion. When a salt undergoes a large volume expansion, many water molecules are typically absorbed in the hydrate (Equation 21). As shown in Equations 17 and 18, a large difference (b-a) results in a larger energy storage density. However, a large volume expansion poses greater risk to the

View Article Online

Journal Name ARTICLE

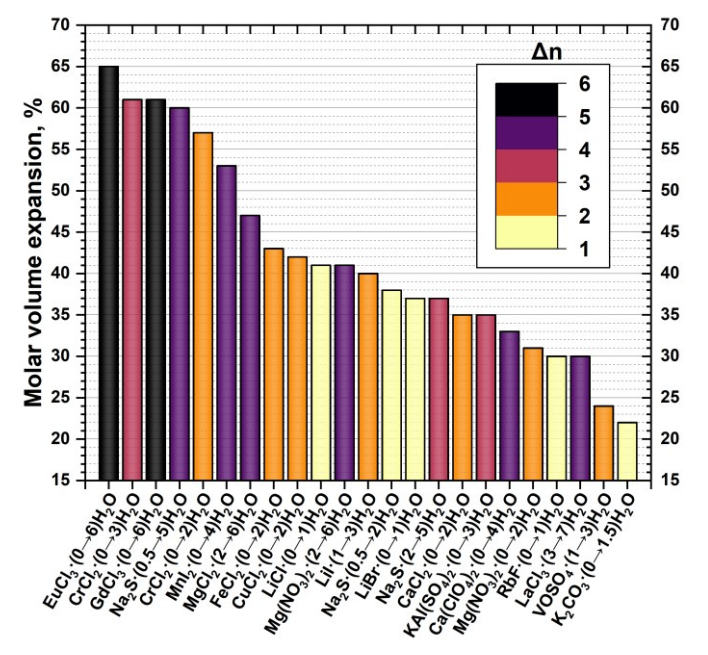


Figure 9. Relative volume expansion during hydration for representative salt hydrates. The numbers in parentheses indicate the range of hydration states (n in Salt•n H₂O) accessed during the hydration reaction. Δn is the number of water molecules absorbed. Data adapted from ref 47.

mechanical stability of the salt hydrate. Large volume expansion/contraction can create voids and cracks in the material as it is repeatedly hydrated and dehydrated, resulting in mechanical wear on the system. The material in a TCES reactor will expand over cycling, leading to a porosity reduction of the bed. 182 This leads to a reduction of the permeability of the bed, which compromises the working of the TCES reactor. 183 Furthermore, these voids can affect the kinetics of reaction. Negatively, the voids reduce the contact area with heat exchanging elements, resulting in lower heat transfer. Positively, the voids increase the porosity of the material, increasing local mass transfer on a particle scale.

One of the major challenges with salt hydrates is to make them stable upon cycling. There are several approaches reported in the literature: encapsulation, matrix stabilization and impregnation of porous media. A review of this topic is beyond the scope of this paper and for this we refer to recent literature. Prolonging the cyclability of salt hydrate particles is of utmost importance to make salt hydrates viable for the application. It is the opinion of the authors that a breakthrough at this point has not been achieved so far.

Synthetic salts. In recent years there have been several attempts to synthesize new salt hydrates. Especially the sulphate based Tutton salts seem to be a versatile class of materials as the composition of these materials can be changed, which allows for targeted design of the phase diagram of these salts. $^{185-187}$ Sulphate based Tutton salts have a chemical formula $\rm M_2M'(SO_4)_2(H_2O)_6$, where $\rm M^+$ and $\rm M'^{2+}$ are to different cations. Just like with the regular sulphate and phosphate salts, the major challenge with these salts is in the reversibility of the hydration/dehydration reaction.

Thermal properties. The power output : 64.183970ESHOEVite depends on the rates of mass and heat transfer during the chemical reaction. Thus, high thermal conductivity is desirable within the heat storage medium to allow for rapid heat transfer. Unfortunately, many TCES materials exhibit low thermal conductivities. Thermal conductivities for salt hydrates fall within the range of 0.3-1.3 W/(m·K). 188-191 This is much smaller than that of metallic conductors such as Al and Cu, whose values are roughly 200-400 W/(m·K). Thermal conductivity tends to increase with the hydrate number, 191 indicating a greater thermal limitation in the dehydrated phase. The use of composite materials, such as a salt hydrate embedded in expanded graphite, has been used to increase the thermal conductivity of the material. 192,193 This approach incurs a tradeoff between thermal conductivity and energy storage density, as the energy storage density of the overall material decreases as more of the thermal conductivity enhancing material is used. Thus, TCES system designs must strike a balance between energy storage density and power density.

Scarcity, cost, and toxicity. Non-technical aspects such as scarcity, cost, and toxicity can impact the practicality of a TCES material. The importance of these factors can be illustrated with a simple calculation focusing on the built environment in Europe. In 2019 the population of the EU was 513 million 194 people living in 223 million households. 195 Let us assume that each of these households owns a 2 GJ thermal storage unit, and that the typical energy density at the materials level is $m{u}_c = 1$ GJ/m³, with a materials density of 1000 kg/m³. For this scenario approximately 400 million metric tons of storage material is required. Although this is a simple estimate, it demonstrates that significant demand for TCES materials may be expected. This increase in demand mimics the dramatic increase in the supply of raw materials required for widespread adoption of more mature energy technologies (PV, wind turbines, and batteries).196

Although the price of a given salt on the bulk market serves as one indicator of scarcity,47 this approach is not predictive of future demand and associated costs.196 An analysis that accounts for known resources, mining capacities, and production capacities for synthetic salts would be more useful in assessing scarcity. Although elements such as K, Na, and Ca are abundant, limiting factors for using salts containing these elements are the mining capacities for specific minerals or the production capacities in the case of synthetic salts (i.e. K₂CO₃ and Na₂S). Furthermore, many salts under investigation contain minerals that should be treated with care in view of resources and mining production. Figure 10 illustrates resource and mining data from the U.S. Geological Survey for elements frequently considered in studies of TCES materials.197 These materials quantities are compared to the 400 million ton estimate for widespread use of thermal energy storage in Europe.

First, let us consider the data presented in Figure 10 for lithium. Although lithium salts are promising for thermochemical energy storage, 198 lithium already plays a key

ARTICLE Journal Name

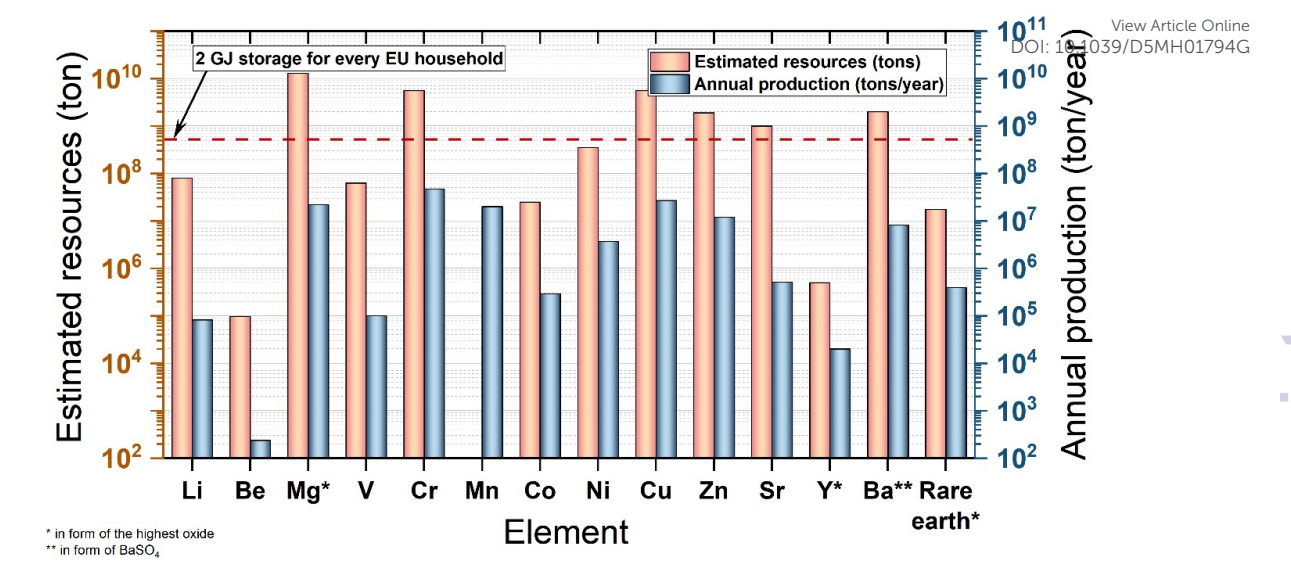


Figure 10. Estimated resources (left axis) and global annual mining production (right axis) in 2023-2024 for elements that frequently appear in studies of thermochemical energy storage. The dashed red lines mark the 400 million tons of material needed for a use scenario in which all EU-households operate a 2 GJ thermal storage unit. Data is from the U.S. Geological Survey.¹⁹⁷

role in the electrification of energy systems due to its use in Liion batteries. While the abundance of lithium is high (estimated mining resources in 2020 were 86 million tons¹⁹⁷), its use as a key ingredient for both electrical and thermal energy storage devices presents challenges. Considering the production capabilities of Li, Figure 10 shows that in 2020 the global annual mining production was about 82000 tons.¹⁹⁷ This is orders of magnitude below what is expected to be needed for global implementation of Li-based thermal energy storage systems. In view of the growing demand for Li-ion batteries (which is expected to cause a 40-fold increase in Li supply by 2040¹⁹⁹) and the emerging strain this has induced on the global market, it is fair to ask whether TCES should also employ Li-based media.

Salts based on rare earth metals should also be treated with care. In light of the available resources and the present mining production volumes, Figure 10, the use of Lanthanum (i.e. $LaCl_3^{39}$ and $La_2(SO_4)_3)$, 200 Yttrium (i.e. $Y_2(SO_4)_3)^{201}$ and Vanadium containing salts are of questionable viability. Similar reasoning can be applied to sulphate salts based on elements such as Sc, Yb, Y, Dy, Ga and In. 201 On the other hand, strontium-containing salts deserve attention in view of their substantial annual mining production. $SrBr_2$ and $SrCl_2$ are considered promising as they have suitable thermodynamic properties. 39,137,202 However, mining and production capacities will need to be increased for these salts to become practical ingredients in future heat storage systems.

As discussed above, costs can be high to source materials that are not in wide use. One may expect these higher costs to apply to materials needed for new technologies such as the TCES materials discussed here. Nevertheless, rapid cost reductions have been demonstrated in related technologies by exploiting economies of scale. For example, the cost of Li-ion batteries has decreased by approximately 97% over the past three decades. ⁶⁰ We anticipate that similar cost reductions can be achieved for the materials relevant for TCES.

Toxicity is another important factor for salt hydrates. ^{39,47,203} A screening study of 125 salts focusing on safety issues highlighted that 80 salts exhibit challenges due to toxicity. ³⁹ For similar reasons, an assessment of medium-temperature heat storage applications urged caution in the use of compounds containing ions like Cr⁶⁺, Co^{2+/3+} and Ni^{2+/4+}. ²⁰³ An assessment of 563 hydration reactions (later extended to 1073 reactions ⁴⁸) for the built environment (hot tap water and space heating) generated a list of 25 candidates with suitable thermodynamic properties (energy density and discharge temperatures). In this case salts such as GdCl₃, NiCl₂, Na₂S, Mnl₂, VOSO₄ and CuCl₂ were excluded due to toxicity considerations. ⁴⁷ Hence, substances such as CrF₃ and CuBr₂, identified as promising based on their hydration enthalpies, ⁸⁷ warrant additional care in their manufacture and use due to toxicity considerations.

The above considerations suggest two conclusions: First, investments in mining and production capabilities are needed to facilitate global adoption of salt hydrate heat batteries. Secondly, more detailed knowledge of the non-technical features of these materials will be helpful to material scientists in the selection of appropriate materials.

Computational Discovery of Salt Hydrates. Computational modelling has also been employed to investigate materials for TCES. In a trio of studies, 87,204,205 Kiyabu et al. used Density Functional Theory calculations to predict the energy densities and turning temperatures of salt hydrates and hydroxides. In the first study, 87 265 hydration reactions were examined for all the halide hydrates and hydroxides present within the Inorganic Crystal Structure Database (ICSD). Promising reactions having high gravimetric and volumetric energy densities were identified and categorized according to their operating temperatures. Of these, $CrF_3 \bullet 9H_2O$ was highlighted as a promising under-explored material for moderate-temperature TCES applications (T ~ 200 °C). Using this database of calculated

Open Access Article. Published on 24 oktober 2025. Downloaded on 02.11.2025 08.53.33

Journal Name ARTICLE

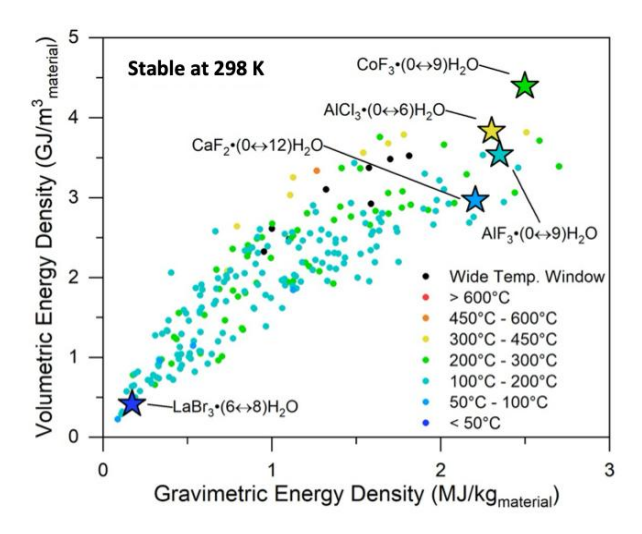


Figure 11. Volumetric energy density, gravimetric energy density, and temperature category for 238 TCES reactions involving new hypothetical salt hydrates. Promising reactions in distinct temperature categories are shown as stars. All of these hydrates, as well as all intermediate phases present during (de)hydration, are predicted to sit on the convex hull, and thus to be stable with respect to the formation of other phases at 298 K. Adapted from reference 204 with permission from the American Chemical Society, copyright 2022.

properties, property-performance relationships were examined across the hydrates and hydroxides using a Pearson correlation matrix. In the hydroxides these analyses identified the ionicity of the cation-hydroxide bond as a good predictor of the enthalpy of reaction. However, similar (linear) correlations did not emerge in the hydrates, suggesting that more flexible models were needed to predict the thermodynamics in this class of materials.

Kiyabu et al. subsequently expanded their screening of TCES materials to include a larger collection of hypothetical salt hydrates, including 5292 metal halides²⁰⁴ and 7012 salts containing chalcogenides and complex anions.²⁰⁵ From these datasets, the hydrates of several salts, including CaF₂, VF₂, CoF₃, Li₂S, Ca(OH)₂, and Li₂CO₃ were identified as potentially-new TES

materials with class-leading energy densities and operating temperatures suitable for use in domestic 1/2 Meating 17240 intermediate-temperature applications. Figure 11 illustrates energy densities for the subset of the screened metal halides that were predicted to stable with respect to competing phases at all stages of their respective hydration/dehydration reactions. The performance of these materials was projected to the system level by parameterizing an operating model 90,165,206 of a solar thermal TES system with data from the new hydrates. Finally, machine learning models were developed to predict salt hydrate thermodynamics and identify design guidelines for maximizing energy density. These models demonstrate that salts composed of cations that exhibit small electronegativities and molar masses (e.g., Na+ and K+) yield increased energy densities via increased ΔH of hydration. For complex anion hydrates, the identity of the anion was also found to be a significant predictor of ΔH : a greater elemental fraction of nonmetals was found to correlate with a greater ΔH .

C) Class II: Porous media/sorption

Porous solid adsorbents constitute a well-established class of thermal energy storage materials that have been considered for use in heat pumps and chillers. Prominent examples of this class include activated carbon, silica gel, zeolites, activated alumina oxide, covalent organic frameworks (COFs), and metal organic frameworks (MOFs). These materials store heat by exploiting the heat of adsorption of the working fluid vapor. Recent developments have demonstrated remarkable performance improvements, with advanced COF materials achieving thermal conductivities exceeding 15 W/(m·K),207 while novel MOF-salt composites have reached ammonia storage capacities of 48.3 mmol g⁻¹.²⁰⁸ The working fluid can be condensed during the storage/release cycle (e.g. water, ethanol, methanol, ammonia); alternatively, non-condensable gases are used, the most common of which are CO₂ and H₂.

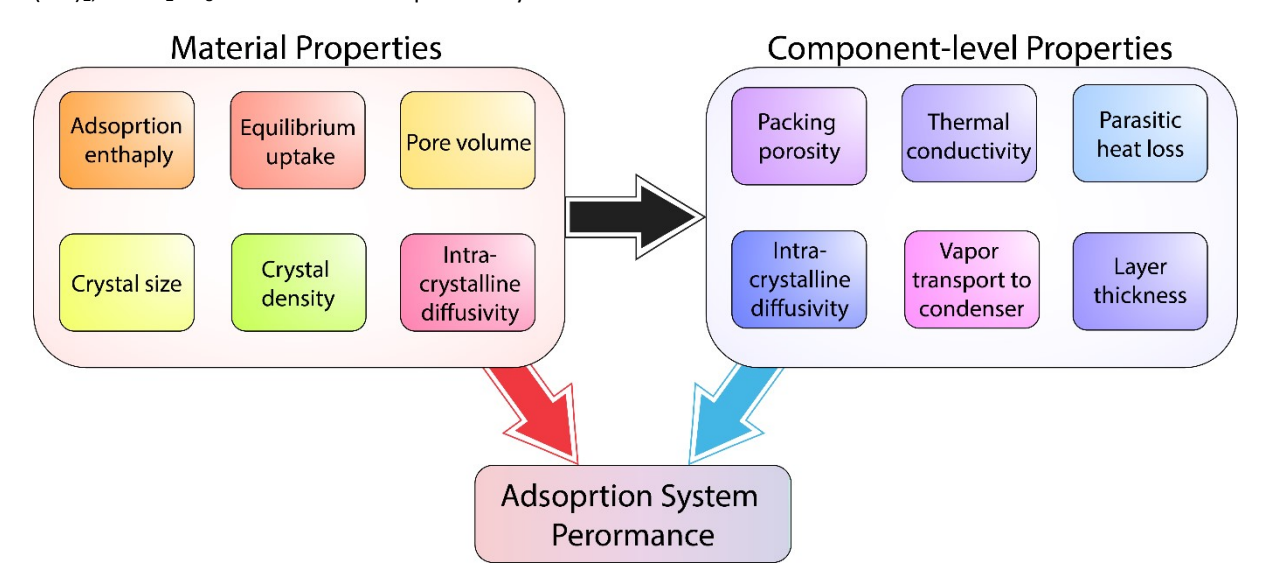


Figure 12. Performance and efficiency of porous materials-based TCES systems depends on both material-level and system-level property optimizations. Reproduced from reference 229 with permission from the American Chemical Society, copyright 2019.

ARTICLE Journal Name

combination of materials-level (i.e., chemical composition, textural/crystallographic, thermodynamic, and kinetic) and system-level (i.e., packing density, vapor transport, thermal conductivity, etc.) properties determine the performance of an adsorption-based TCES system (Figure 12). In general, textural/crystallographic properties such as specific surface area, pore volume, pore size and distribution, and single crystal density determine the amount of working fluid adsorbed by the porous host at a certain sorption potential (Figure 4). Hence, the structure of the adsorbent strongly influences the capacity of stored heat. On the other hand, the operating temperature window is partly determined by the enthalpy of adsorption and its dependency on sorption uptake, which itself strongly influenced by the composition of the adsorbent/adsorbate pair through the nature of the bonds formed between the host atoms and those of the guest.

Criteria for selecting adsorbents. The selection of porous adsorbents for TCES is guided by the operating conditions of the intended application. As described below, the application places constraints upon the adsorbent's operating temperature range, storage capacity, and its kinetics.

Adsorbent-adsorbate working pair: The selection of the working fluid is a critical component of an adsorbent-based TCES system. The selection criteria for a suitable working fluid include: a high enthalpy of evaporation, condensable under operating conditions, moderate vapor pressure, pollution free, non-toxic, and non-corrosive to the system components.²⁰⁹ Water is a popular choice of working fluid due to its abundance, low cost, and non-toxic nature. Water is currently used commercially with zeolites and silica gel adsorbents.^{209,210} However, water is not suitable for subzero temperature applications due to ice formation/freezing. Ethanol and methanol have been adopted as alternatives in MOF-based systems to overcome this limitation. Recent simulations and experiments demonstrated high working capacities and COPs in ethanol/MAF-6 systems.²¹¹ Advanced composite working pairs

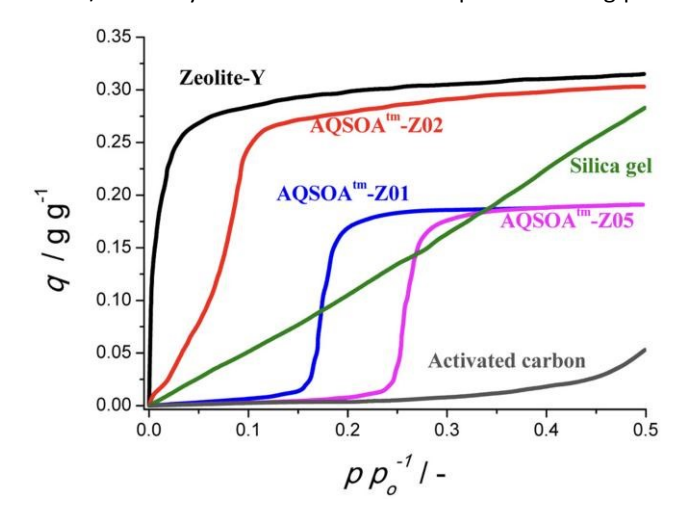


Figure 13. Adsorption isotherms for water in common commercially available adsorbents. Reproduced from reference 209 with permission from the American Chemical Society, copyright 2015.

have emerged that significantly outperform traditional systems. For instance, vermiculite/LiCl systems demonstrate superfor thermal performance with COPs of 0.75 for cooling and 1.51 for heating, alongside specific cooling performance of 5,760.7 kJ/kg.²¹² Zeolite-based composites, 13X/MgSO₄-LiCl, have also shown substantial improvements, exhibiting higher energy density than pure zeolite 13X and achieving heat storage capacities of 458.3 kJ/kg.²¹³ Hydrogen²¹⁴ and classical freons²¹⁵ are also popular choices.

The selection criteria for adsorbents are goverened by thermodynamic boundary temperatures and pressures for adsorption and desorption.

Adsorption isotherms: The adsorption isotherm quantifies the capacity of a given adsorbent for the uptake of a working fluid as a function of pressure at a constant temperature, Figure 13. So-called "S-shaped" or stepwise isotherms are desirable for achieving high working capacity and second-law efficiency.⁷⁰ The International Union of Pure and Applied Chemistry (IUPAC) classifies this family of isotherms as Type V.216 The stepwise adsorption typical of a Type V isotherm facilitates the storage of a large quantity of energy within a relatively small change in pressure. 209,217,218 Recent experiments comparing water adsorption isotherms across Zeolite-Y, activated carbon, silica gel, and AQSOA™ variants confirm the significance of isotherm steepness and step pressure. AQSOA-Z01 and -Z02, for example, demonstrate sharper S-shaped isotherms at P/P_o ≈ 0.15–0.35, enabling better utilization of low-temperature driving heat.²¹⁹ New MOFs such as KMF-1 and KMF-2 are engineered to produce Type V water isotherms centered at relative pressures ~0.13-0.2, with corresponding volumetric energy densities up to 330 kWh·m⁻³.²²⁰ Recent data show MOFs like MIL-125(Ti)-NH₂ exhibit Type V isotherms with high water uptake at relative pressures of 0.1-0.4, ideal for cooling and heating applications.²²¹ For water-based TCES systems, the hydrophilicity or hydrophobicity of the adsorbent governs the shape of the adsorption isotherm: hydrophobic adsorbents often exhibit Type V isotherms. In addition, the volumetric capacity (i.e., the mass of working fluid adsorbed per unit volume of adsorbent), is related to the crystal density and influences the size of the TCES system.

Heat of adsorption: The isosteric heat of adsorption (IHA) is a measure of the strength of interaction between molecules of the working fluid and the adsorbent at a fixed adsorption uptake.^{222,223} In computational studies, this quantity is commonly referred to as the differential enthalpy of adsorption, and is typically derived from Monte Carlo simulations. This interaction determines the hydrophilicity or hydrophobicity of the adsorbent and the regeneration temperature. Recent work suggests that the ideal IHA range for water adsorbents lies between 45-60 kJ·mol⁻¹, balancing high working capacity with low-temperature desorption.²²⁴ For example, KMF-2 achieves an IHA of 40.7 kJ·mol⁻¹ and can be regenerated at 70 °C, enabling integration with solar or waste heat sources. A more exothermic IHA leads to a greater amount of energy stored per adsorbate molecule and to a higher regeneration temperature. In addition to the composition of the working fluid and adsorbent, the IHA depends on the size,

Open Access Article. Published on 24 oktober 2025. Downloaded on 02.11.2025 08.53.33.

ARTICLE

Journal Name

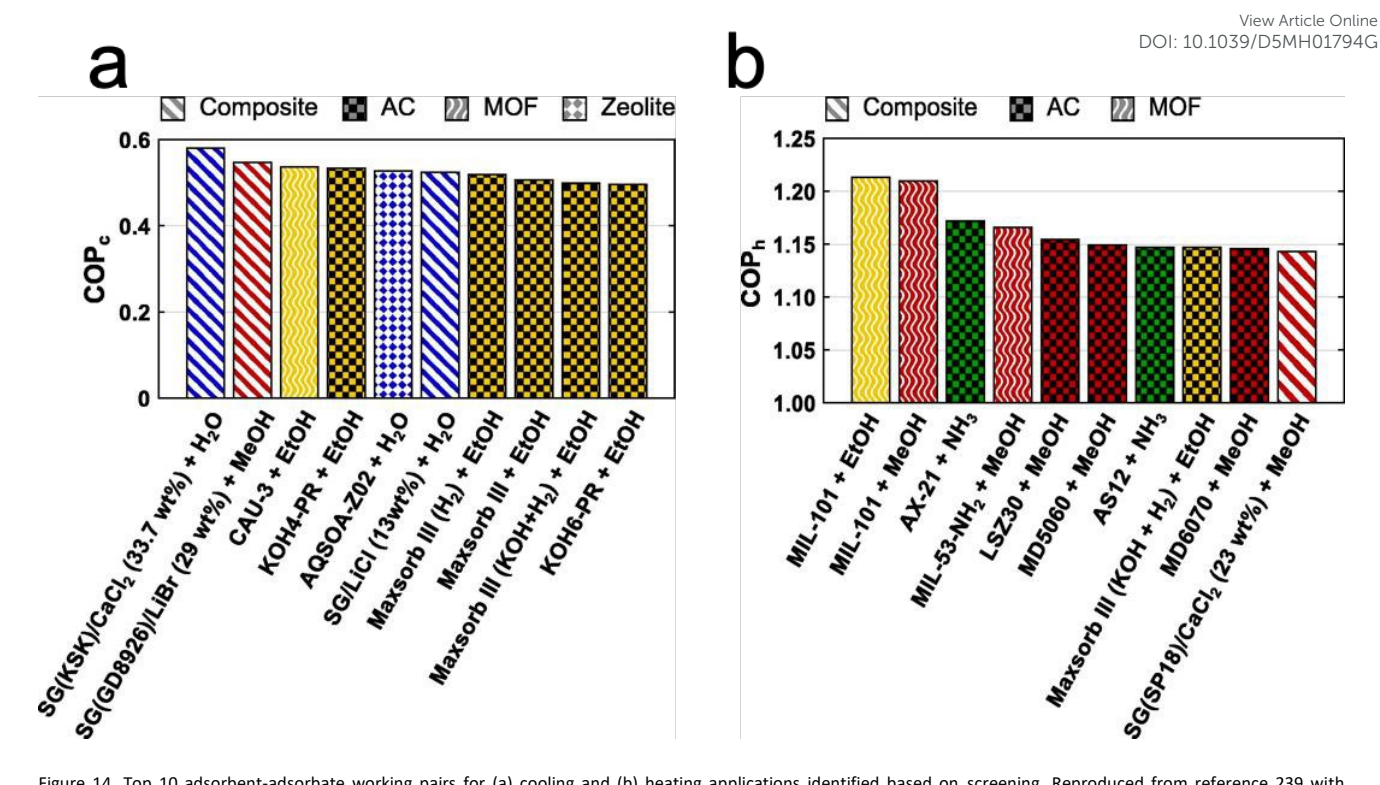


Figure 14. Top 10 adsorbent-adsorbate working pairs for (a) cooling and (b) heating applications identified based on screening. Reproduced from reference 239 with permission from Elsevier, copyright 2017.

shape, and polarity of the adsorbate molecules, and on the amount of the working fluid adsorbed (i.e., uptake). IHAs are known to be more exothermic for the adsorption of polar working fluids (e.g., water, ethanol, ammonia) at coordinatively unsaturated metal sites in MOFs. For example, MIL-100(Fe) and MIL-125-NH₂ achieve IHAs supporting energy densities of ~875 MJ/m³ and ~1100 MJ/m³, respectively,²²¹ making them promising candidates for compact thermal storage systems. Thus, the IHA defines the first-law efficiency and the COP. The optimal IHA depends on the application and operating conditions of the TCES system. It should also be noted that, due to the di-variancy of the adsorption equilibrium, the IHA is often presented as a function of the adsorption uptake.

Regeneration temperature: The temperature at which the adsorbed working fluid molecules are desorbed from the porous host determines the second-law efficiency and cyclability of a TCES system. Ideally, a low (<100 °C) regeneration temperature is preferable for domestic, solar, and industrial waste heat-based TCES systems.²²⁵

Heat and mass transport: The performance of an adsorbent-based TCES system also depends on the rates at which heat and mass can be transported through the sorbent bed. These properties depend upon intra-crystalline and inter-crystalline diffusivities (Figure 12).85,209,226 Fick's law85,227 is often used to estimate intracrystalline diffusion – i.e., vapor diffusion within single crystals of porous materials – of the working fluid vapor, which in turn allows for modelling of sorption kinetics within porous media employing the linear driving force model.85,226,228 Due to their crystallinity (and thus lower tortuosity), MOFs are anticipated to exhibit advantages in mass transport compared

to non-crystalline hosts such as activated carbons and zeolites. In contrast, intercrystalline diffusion – i.e., vapor diffusion through the interstitial regions between crystallites or particles of the adsorbent – depends on the size, shape, and packing densities of the adsorbent crystals/particles.^{229,230}

One transport-related challenge associated with the use of porous TCES materials such as MOFs is their low thermal conductivity.^{231–233} Hence improving the rate of heat transport through the storage bed may require the addition of thermallyconductive additives, 234-236 which will degrade the effective energy density and possibly slow mass transport. However, recent progress in materials design have demonstrated progress in overcoming this limitation. For example, threedimensional COFs have demonstrated thermal conductivities exceeding 15 W/(m·K), which is unique performance for 3D polymers.237 These improvements stem from optimized structural parameters, particularly small pore sizes around 0.63 nm, four-connected nodes, and material densities above 1.0 g cm⁻³.²³⁸ In addition, interpenetrated COFs performance through phonon hardening mechanisms, achieving up to 6-fold thermal conductivity improvements.²⁰⁷ Achieving optimal performance in an adsorption-based TCES system thus depends on both materials-level and system-level design considerations.

Discovery of promising adsorbents. In 2017, Boman et al.²³⁹ assessed 110 and 81 adsorbent/adsorbate working pairs for cooling and heating applications, respectively. They identified several MOF-ethanol pairs that outperformed other pairs for heating applications, and additional activated carbon-ethanol pairs suitable for cooling

ARTICLE

This article is licensed under a Creative Commons Attribution-NonCommercial 3.0 Unported Licence

Open Access Article. Published on 24 oktober 2025. Downloaded on 02.11.2025 08.53.33.

Journal Name

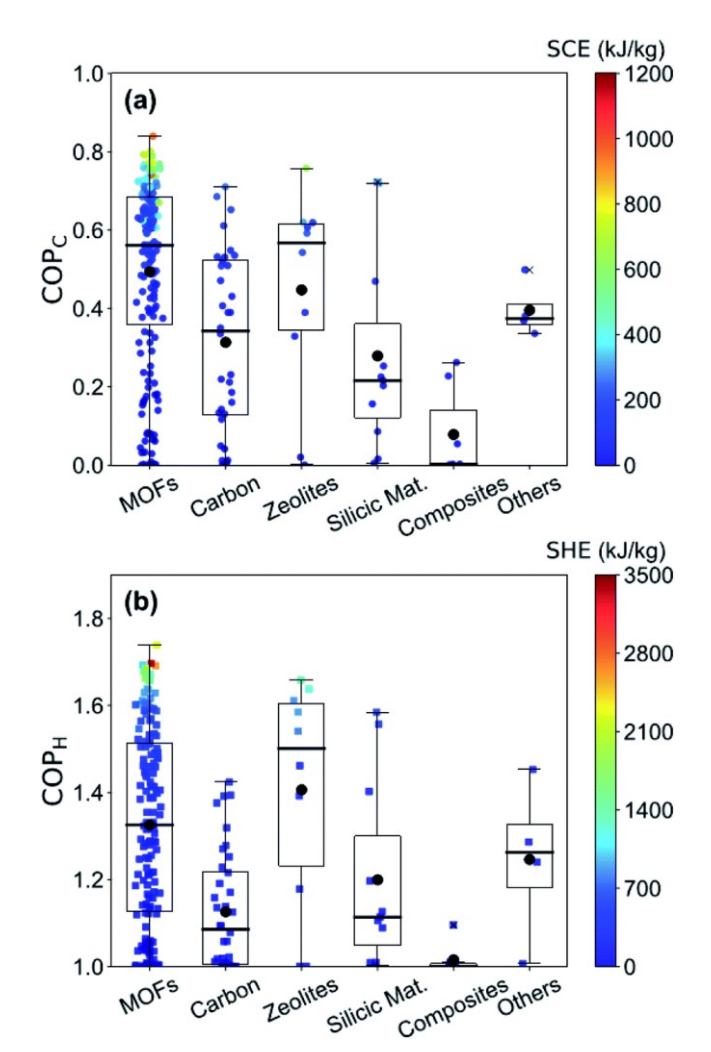


Figure 15. Coefficients of performance (COP) for cooling (a) and heating (b) for different classes of adsorbent materials. Specific cooling/heating effects (SCE/SHE) indicate the amount of useful energy for cooling/heating, corresponding to Q_{useful} in Equation 2. COP_C and SCE were obtained at T_{evap} = 283 K, T_{con} = T_{ads} = 303 K, T_{des} = 368 K, and COP_H and SHE were obtained at $T_{\rm ev}$ = 288 K, $T_{\rm con}$ = $T_{\rm ads}$ = 318 K, $T_{\rm des}$ = 413 K. Reproduced from reference 241 with permission from the Royal Society of Chemistry, copyright 2021.

applications (Figure 14).²³⁹ MOF-water-alcohol pairs were identified as strong candidates for both cooling and heating applications (Figure 14).^{239,240} In 2021, Liu et al.²⁴¹ reported a screening study of 231 experimentally measured water adsorption isotherms for 6 different classes of porous adsorbents. These included MOFs, carbons, zeolites, silicic materials, composites, and other adsorbents. Isotherm data were collected from the NIST/ARPA-E Database of Novel and Emerging Adsorbent Materials, 242 The 231 systems were assessed according to two metricles the coefficient of performance for cooling/heating (COP_C/COP_H) and the specific cooling/heating effects (SCE/SHE). Figure 15 shows the distribution of different classes of porous materials according to their COP_C/SCE (Figure 15a) and COP_H/SHE (Figure 15b). Liu et al. ²⁴¹ found that MOFs and zeolites outperform other porous adsorbents based on the COP_C/COP_H and SCE/SHE metrics. The best adsorbents were found to exhibit Type V isotherms with step positions at relative pressures of 0.1-0.4 and 0-0.2 for cooling and heating applications,

Computational screening for porous materials for water adsorption remains an area ripe for development. The absence of validated interatomic potentials for adsorbent-water interactions²⁴³ and a lack of consensus regarding atomic charges for adsorbent atoms^{244,245} have both contributed to the limited application of simulation in accelerating materials discovery. Nevertheless, significant computational advances have emerged through large-scale screening studies. Highthroughput molecular dynamics investigations have evaluated over 10,000 hypothetical MOFs for thermal conductivity, revealing that optimal performance requires material densities above 1.0 g/cm³, pore sizes below 10 Å, and four-connected metal nodes.²⁴⁶ These computational capabilities are supported by expanded databases, with the CoRE MOF Database containing over 40,000 experimentally reported structures,²⁴⁷ a nearly three-fold increase from the previous version which contained ~14,000 structures.248

Moreover, grand canonical Monte Carlo (GCMC) simulations of water adsorption in hydrophobic adsorbents are computationally challenging due to the long simulation times required to successfully sample configuration space.²⁴⁹ The use of flat histogram sampling methods have been proposed as a potential route towards reducing simulation time.²⁵⁰ Furthermore, the hydrophilic/hydrophobic nature of porous materials reported in various databases is either unreported or unknown. To overcome this, Monte Carlo calculations of Henry's law constants (HLC) for water adsorption in MOFs have been proposed to distinguish between hydrophilic and hydrophobic MOFs. 251,252 HLC calculations are several orders of magnitude faster than those needed to predict the adsorption isotherm.^{251,252} Despite these challenges, GCMC has been applied in a few high-throughput computational screening studies of MOFs for water adsorption, particularly in tandem machine learning approaches for predictions. 239,253-255

Table 6. Ranges of properties for MOFs from the CoRE 2019 database, i.e. volumetric surface area (VSA), isosteric heat of adsorption (IHA) largest cavity diameter (LCD), density, and void fraction, with a coefficient of performance (COP) and working capacity greater than the specified targets for each application. Adapted from reference 259 with permission from the Royal Society of Chemistry, copyright 2021.

Application	СОР	Working capacity (mg/g)	VSA (m²/cm³)	IHA (kJ/mol)	LCD (Å)	Density (kg/m³)	Void fraction
Heat pump	>1.75	>350	1550-3000	35–50	7.1-21.7	435-880	0.67-0.89
Ice making	>0.70	>170	1585-2947	34-54	7.1-21.7	434-1582	0.65-0.89
Refrigeration	>0.80	>400	1600-3000	34–52	7.4–20.0	484–1165	0.68-0.89

Den Access Article. Published on 24 oktober 2025. Downloaded on 02.11.2025 08.53.33

ARTICLE Journal Name

Computational screening for porous adsorbents using alcohol as the working fluid is less challenging than for water, as intermolecular interactions involving alcohols are simpler and therefore more accurately described by interatomic potentials.²⁵⁶ Nevertheless, only a few studies on these systems have been reported.^{257–259} Li et al.²⁵⁸ predicted the COP_C for 1527 MOFs compiled from the CoRE 2014 database²⁶⁰ for ethanol adsorption. Guidelines were provided for selecting optimal MOF-alcohol pairs based on crystallographic (pore size and specific surface area) and thermodynamic properties (HLCs and heat of adsorption).²⁵⁸ Shi et al.²⁵⁹ evaluated methanol adsorption capacities of 6013 MOFs from the CoRE 2019 database²⁶¹ and 137,953 hypothetical MOFs from the Northwestern database²⁶² for heating/cooling TCES systems, including heat pumps, ice making, and refrigeration applications. They identified optimal ranges for COP working capacity, volumetric surface area (VSA), isosteric heat of adsorption (IHA), largest cavity diameter (LCD), single crystal density (ρ) , and void fraction (ϕ) (Table 6). 275 COFs from the CoRE-COF 2.0 database²⁶³ were evaluated using GCMC simulations by Li et al. 264 Ethanol was adopted as the working fluid and assessments were performed with respect to COP_C and COPH. They found that COFs are more suitable for cooling applications compared to MOFs because COFs have weaker interactions with methanol at low temperatures. Liang et al.²⁶⁵ calculated the adsorption and transport properties of 1072 MOFs from the CoRE MOF Database to evaluate their COPc and SCP. The best-performing MOF exhibited a SCP of 1359 W/kg and a COP_C of 0.64.

Design of adsorbents for TCES: Among the various categories adsorbents of interest for TCES systems, MOFs stand out due to their highly tunable properties. This tunability presents opportunities for tailoring the design of MOFs to optimize performance. For example, based on computational and experimental input, Cho et al.²⁶⁶ designed the MOF KMF-1, and demonstrated its promising heat storage capacity. The design involved tuning of pore channels and hydrophilicity by selecting and functionalizing the 2,5-pyrroledicarboxylate (PyDC) linker. These design choices were informed by analyzing the structure and performance of two well-known MOFs:²⁶⁷ CAU-10 and MIL-160. Similarly, Rieth et al.²⁶⁸ designed two isoreticular triazolate MOFs with record-setting values for COP (1.63). They demonstrated how to control the relative humidity at which water uptake occurs by modulating the pore size. Finally, Rieth et al.,269 demonstrated an increase in the reversible water uptake of two MOFs (Ni₂Cl₂BTDD & Ni_2Br_2BTDD , where BTDD = bis(1,2,3-triazolo-[4,5-b],[4',5'i])dibenzo-[1,4]-dioxin) by systematic anion exchange. Recent work has also demonstrated the use of mixed-linker MOFs for TCES, enabling tuning of hydrophilicity and volumetric energy density. A notable example is KMF-2, a mixed-linker Al-MOF incorporating isophthalate and pyridinedicarboxylate linkers, which exhibits a COP for cooling of 0.75 with a volumetric heat capacity of ~330 kWh·m⁻³ at regeneration temperatures < 70 °C.220

Techno-economic analysis of adsorbents: Shi et al.259 conducted a techno-economic analysis of real and hypothetical MOFs for use in adsorption heat pumps/chillers with methanol as the working fluid. Their analysis considered the equipment cost, cycle cost, and materials cost. The materials cost was identified as the most significant. They identified 12 MOFs with a low system-level cost of ~1 USD/kJ in heat-pump/chiller applications. Shi et al. validated their analysis by synthesizing a variant of Cu₃BTC₂,²⁷⁰ measuring its methanol capacity and estimating costs. Emerging techno-economic analyses for porous adsorbents now consider lifecycle emissions, regeneration energy requirements, and material scalability. While most existing models focus on general adsorbents, similar scoring frameworks are being adapted to MOFs and COFs for solar-driven TCES applications.²⁷¹

Characterization and system integration of porous adsorbents: Water adsorption/desorption characterization at multiple temperatures enables the optimization of working capacity and COP for heat pump applications, with experimental studies demonstrating that MOFs like MIL-100(Fe) achieve COP values of 0.80 and specific cooling of 569.42 kJ/kg.272 Thermal cycling stability measurements reveal that zeolite-based composites maintain performance over hundreds of cycles, with zeolite 13X/MgCl₂ systems showing heat storage capacities of 686.86 kJ/kg.²⁷³ System integration approaches address thermal transport limitations of porous materials through composite design. For example, zeolite-graphene nanoplatelet composites demonstrate thermal conductivity improvements up to 127 times over pure zeolite while maintaining 43% improvement in volumetric water uptake.274 These approaches leverage the high energy density of porous adsorbents while incorporating enhanced heat transfer capabilities needed for practical applications.²⁷⁵

Commercial deployment and market outlook for porous adsorbents: Zeolite-water systems have achieved commercial deployment in residential applications, with demonstrated energy densities of 150-200 kWh/m3 and capabilities for seasonal heat storage with limited heat loss.²⁷⁶ Pilot-scale demonstrations include household-scale systems with 250 L zeolite-based system achieving storage capacities of 52 kWh and maximum delivered power of 4.4 kW.²⁷⁷ MOF-based systems continue to be researched, with MOF-ammonia working pairs showing promise due to their performance under extreme climates compared to conventional sorbent-ammonia pairs.²⁷⁸ Improvements for industrial heat pumps have been demonstrated in MOF-water systems like aluminum fumarate, can operate at desorption temperatures as low as 65°C.279

D) Class III: Sorption in liquids

Liquid sorptive TCES operates by reversibly concentrating and diluting a solute (e.g. LiBr) by exchanging the solvent (e.g., H₂O) between vapor and liquid phases.^{280–283} Spontaneous absorption of the vapor into the liquid solution releases heat, while solute desorption/vaporization is the mechanism by which heat is stored. The solute-solvent and solvent-solvent binding interactions are primarily van der Waals in nature; they can be supplemented by hydrogen bonding for solvents such as water, alcohols, and ammonia. In the solution, the chemical

ARTICLE Journal Name

Table 7. Salt-solvent working pairs for heating and cooling absorptive cycles and their characteristics. "Crystallization" indicates whether the solvates are crystalline. Article Online

				DO1. 10.10	,,,
Working pair	Crystallization	$T_{evap}/T_{release}/T_{storage}$ (°C)	ESD _{ab} , GJ/m ³	Ref.	
LiBr-H₂O	no	7/43/80	0.40	350	
LiBr-H ₂ O	yes	10/20/93	1.4	111	
CaCl ₂ -H ₂ O	no	10/20/45	0.43	351	
CaCl ₂ -H ₂ O	yes	10/20/54	0.95	111	
LiCl-H ₂ O	yes	10/20/66	1.4	111	
LiBr-CH₃OH	yes	5/35/75	0.2	352	
LiCl- CH ₃ OH	yes	10/35/75	0.8	352	
LiBr-C ₂ H ₅ OH	yes	10/30/95	0.2	353	

potential of the solvent is reduced due to interactions with the solute. According to the Gibbs-Duhem equations, the chemical potential μ of the solvent (e.g. water) decreases as the concentration of the solute increases. Thus, the vapor pressure over water solutions is lower than for pure water: 284

$$\mu(T) = \mu^{0}(T) + RT \ln a = \mu^{0}(T) + RT \ln \frac{P}{P^{0}}$$

$$\mu(T) = \mu^{0}(T) + RT \ln \frac{RH}{100\%}$$
(22)

$$\mu(T) = \mu^{0}(T) + RT \ln \frac{RH}{100\%}$$
 (23)

where standard state refers to pure water, a is water activity (a= 1 for pure solvent), P⁰ is saturated vapor pressure at temperature T, and RH is the relative humidity at temperature T for the case of water. The activity of salts in water solutions may be estimated from Debye-Hückel theory at low ionic strength of solution on the order of 10⁻³ M. For higher concentrations, including brines, semi-empirical models such as the Pitzer-Simonson-Clegg model can succeed in predicting the activity of water.²⁸² However, the availability of parameters for such models remain limited mainly due to their experimental origin, which makes the targeted design of solutions for absorptive applications challenging.

This article is licensed under a Creative Commons Attribution-NonCommercial 3.0 Unported Licence

Open Access Article. Published on 24 oktober 2025. Downloaded on 02.11.2025 08.53.33.

While there is no general theory on calculating activities for very high concentration solutions used for sorptive applications, qualitative considerations for ionic salts suggest that a higher dissolution enthalpy and a lower activity for water is observed for the case of hard ions (more polarizing, smaller radii) that form crystallohydrates with low lattice energy. The activity of water in saturated solutions corresponds to the deliquescence relative humidity and can be found in the literature. 127

A typical P-T phase diagram for salt-H₂O systems (Figure 16) consists of the solution region, the region corresponding to the highest hydrate Salt•nH₂O, and the area of the lower hydrates and/or the anhydrous salt. Accordingly, there are three types of sorptive cycles with various technical implementations, namely, cycles with only absorption/desorption within a (liquid) solution (cycle identified with green lines in Figure 16), cycles involving crystallization of the highest hydrate (blue cycle) and cycles involving decomposition of the highest hydrate into lower hydrates and/or the anhydrous salt (red). Below, the energy storage densities and temperature lifts for the most popular working pairs for all three cycle types are described.

Absorption and crystallization cycles. Absorptive heat storage or cooling cycles typically consist of two isobars corresponding to sorption/desorption and two isosteres corresponding to strong (concentrated) and weak (diluted) solutions. The energy storage density ESDab on the materials level can be calculated from the enthalpy difference between strong and weak solutions, or from the specific absorption enthalpy:

$$ESD_{ab} = \frac{1}{V_M} \int_{c_c}^{c_W} \overline{\Delta_{ab} H}(c) dc$$
 (24)

where c_s and c_w are concentrations of the strong and weak solution, and V_M is the molar volume of weak solution.

Due to low temperatures and concentration span, systems based on liquid sorption have relatively low temperature lift. For domestic heating, the most popular solutes are NaOH, KOH, CaCl₂, LiBr, HCOOK, glycerol and ammonia.^{60,62} For cooling applications, non-water solvents are preferred, and the list is supplemented by alcohol-based pairs such as LiBr-CH₃OH and LiBr-C₂H₅OH.^{285,286} Ionic liquids represent a novel alternative for which crystallization is not reached.287,288

A trade-off between energy storage density and temperature lift exists for absorptive cycles: higher energy storage densities are achieved at the expense of lower temperature lift, and vice versa. This approach to absorptive storage allows for low charging temperatures (<80 °C); the largest energy storage densities for heat storage in buildings may reach 1 GJ/m³ (Table 7), however the temperature lift is modest, 10-15°C. The temperature lift can be boosted by increasing the charging temperature to access the crystalline

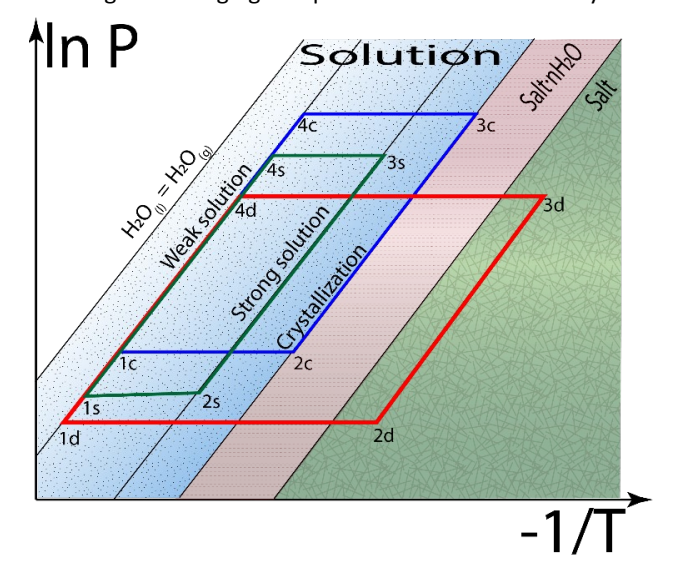


Figure 16. Generic phase diagram for a water-salt system in van 't Hoff coordinates illustrating three types of absorptive heat storage cycles: (green) sorption in a liquid phase, 1s-2s-3s-4s; (blue) three-phase storage, 1c-2c-3c-4c; (red) storage with full decomposition, 1d-2d-3d-4d.

pen Access Article. Published on 24 oktober 2025. Downloaded on 02.11.2025 08.53.33.

Journal Name ARTICLE

Table 8. Examples of "Salt in porous matrix" composites, with their corresponding specific energy, ESD per unit bed volume, Teval/Trelease for the heating cycle and the result of t storage density (ExSD).

Salt	Matrix	Specific	ESD,	$T_{evap}/T_{release}$, $^{\circ}C$	ExSD	Ref.
		energy,	GJ m⁻³		MJ m ^{−3}	
		MJ kg ^{−1}				
CaCl ₂	Hollow silica	1.1	0.86	13/45	96	49
CaCl ₂	Ethylcellulose	2.1	0.4	10/20	14	354
CaCl ₂	SiO ₂ (Grace Davisil™)	1.1	0.76	10/30	54	355
CaCl ₂	Silica-alumina	0.9	0.65	3/20	40	356
CaCl ₂	PHTS*	1.2	-	10/30	-	357
CaCl ₂	MIL-101(Cr)	1.6	1.0	10/30	71	358
LiCl	UiO-66	0.9	-	10/40	-	291
LiCl	Hollow silica	0.75	0.65	13/45	73	49
LiCl	Hollow silica	0.63	0.52	13/60	85	49
LiCl	MWCNT+PVA**	1.6	0.65	10/35	57	359
LiCl	Expanded vermiculite	>1.8	0.8	10/35	70	360
LiCl	SiO ₂ (Fuji Type A)	1.1	0.6	15/40	52	361
MgCl ₂	Zeolite 13x	1.2	-	25/62	-	362
SrBr ₂	Hollow silica	0.69	0.63	18/45	59	49
SrBr ₂	Expanded vermiculite	1.6	0.38	20/30	13	339
SrBr ₂	MIL-101(Cr)	1.35	0.84	10/30	59	363
K ₂ CO ₃	Expanded vermiculite	-	0.9	20/30	31	344

^{*}Plugged hexagonal templated silicate

hydrate, thus allowing access to the crystallization energy ESD_{cr}. One drawback of this approach is that the complexity of the system design must increase to account for these 'three-phase cycles' that permit melting and solidification/crystallization of the storage medium. Three phase thermal energy storage systems have been commercialized by ClimateWell.

Decomposition cycles. A further increase of energy storage density (compared to a three-phase cycle with crystallization) can be achieved by increasing the charging temperature to dehydrate the crystalline salt (red cycle in Figure 16). In this case the energy storage density is given by:

$$ESD_d = ESD_{cr} + ESD_{ab} + \frac{1}{V_M} \Delta_{dec} H^0$$
 (25)

where $\Delta_{dec}H^o$ is the specific decomposition enthalpy for the transition (or series of transitions) associated with the lower hydrates and/or complete dehydration. The most promising materials for thermal energy storage in this usage mode involve salts capable of forming hydrates with appropriate DRH = 10-40% such as LiCl, CaCl₂, MgCl₂, MgSO₄, K₂CO₃ (Table 8).

The practical realization of these decomposition cycles is difficult without the aid of porous media that provide efficient heat/mass transfer within the sorbent bed during cycling.²⁸⁹ While such composites should allow high charging temperatures and high relative volume change of the active storage component, the skeletal volume of the porous matrix and void space in pores necessary to accommodate for the resultant solution (to avoid leakage) decreases the effective energy storage density of the composite relative to that of the pure salt (Table 8). For this reason, the most popular porous matrices are formed from mechanically stable particles with large porosity and sub-micrometer pores capable of containing

the salt solution via capillary forces. Popular and inexpensive options include vermiculite, attapulgite, and silica gel.290 Recently, MOFs are being considered as promising matrices due to their high porosity, which yields a potentially high fraction of "useful" space to be occupied by a salt. 291-293 Finding a balance between energy storage density on the bed level, temperature lift, and heat/mass transfer is one important remaining challenge.49

Suggested directions for future research

The preceding sections have introduced the primary classes of materials for low-temperature thermochemical storage and summarized their respective attributes and performance limitations. Based on those limitations, this section suggests high-priority research directions aimed at overcoming performance gaps and accelerating the adoption of TCES devices.

Computational materials discovery. A comprehensive materials discovery effort has not been performed in the field of thermal energy storage. The absence of such an effort differs from that of related applications - e.g., electrochemical energy storage, photovoltaics, CO₂ capture, etc. - in which the properties of an active material largely determine the performance of its respective device. Recent materials discovery efforts targeting these other applications have taken advantage of accurate and efficient computational methods coupled to high-performance computing.^{294–305} These efforts have demonstrated the capability to screen large databases of materials containing as many as 106 distinct compositions.306-

^{**}MultiWall Carbon NanoTubes with polyvinyl alcohol binder

Journal Name

ARTICLE

This article is licensed under a Creative Commons Attribution-NonCommercial 3.0 Unported Licence.

Open Access Article. Published on 24 oktober 2025. Downloaded on 02.11.2025 08.53.33.

Two of the most widely used computational methods for materials discovery are Density Functional Theory (DFT) and classical Grand Canonical Monte Carlo (GCMC). Although both techniques simulate matter at the atomic scale, they differ in their approach to describing atomic interactions (i.e., bonding) and therefore exhibit distinct capabilities with respect to the size of systems that can be simulated and the properties that can be predicted. DFT is a quantum-mechanical technique that solves for the ground state electron density and total energy of a material. These quantities allow for the accurate prediction of energy densities and other macroscopic thermodynamic quantities such as enthalpies and free energies, both of which are relevant for predicting the equilibrium properties of TCES materials, such as the turning temperature.309 The high accuracy of DFT calculations comes at the cost of high computational expense: if the goal is to screen thousands of compounds in a reasonable time-frame (several months), then the size of the simulation cells generally cannot exceed ~100 atoms. Fortunately, this size limitation allows calculations on a sizeable sub-set of the materials classes of interest to TCES, such as salt hydrates.87,203,205

In contrast to DFT, classical GCMC can simulate large systems. This feature makes it useful for simulating adsorption in porous hosts, such as MOFs and zeolites, where the simulation cell ranges from hundreds to thousands of atoms.^{249,255,310-312} The greater computational efficiency of classical GCMC reflects its use of a predefined interatomic potential, which can be evaluated with low computational cost. GCMC is a statistical sampling method that predicts equilibrium properties within the grand canonical (μVT) ensemble.³¹³ In the context of an adsorption process, the simulation consists of a fictitious gas reservoir at constant chemical potential, $\mu(P,T)$, and a porous host into which the gas molecules may adsorb. The output of the simulation is the equilibrium number of molecules adsorbed within the host at the prescribed chemical potential of the gas (which corresponds to a constant pressure and temperature). An adsorption isotherm can be predicted by calculating the number of molecules adsorbed as a function of pressure at constant temperature.313 The adsorption enthalpy can also be calculated from such simulations.314 As adsorption isotherms and enthalpies are also routinely measured experimentally, 315,316 a direct comparison between theory and experiment is possible.

The primary shortcoming of classical GCMC derives from inaccuracies in the interatomic potential. If the potential does not accurately capture the nature and strength of bonding, then the quantities derived from it — uptake capacity, shape of the isotherm — will reflect these inaccuracies. 311 These inaccuracies arise partly from the fact that most classical GCMC simulations assume a rigid $\rm H_2O$ geometry. In reality, however, the H–O–H bond angle and O–H bond lengths of water molecules depend on their local environment within the MOF, which can affect the nature of their interatomic interactions. 249 This effect is neglected.

At present, DFT and GCMC screening have been applied only to a limited set of potential TCES materials. This includes known salt hydrates, hypothetical salt-hydrates based on halogen

anions, and a small number of studies on adsorption in pocous materials. 87,203,205,249,250,259,317 The largest study to date in that of the tal., 259 who examined methanol adsorption in more than 140,000 real and hypothetical MOFs. An even larger space exists for hydrates of 'mixed metal' salts, where the cation sites are occupied by two or more distinct cations. In all these cases computation can be used to assess the thermodynamic stability of various hypothetical hydrate compositions, predict capacities, and estimate equilibrium turning temperatures. Subsequently, experiments should be performed to validate the synthesizability and performance of the most promising materials.

Similar discovery opportunities exist for adsorption in porous hosts. Here, the most promise arguably lies with MOFs. This promise reflects the compositional and structural tunability of MOFs — approximately a million MOF variants have been proposed^{318–321} — but is also inspired by their crystallinity: the regularity of the pore structure in MOFs implies low tortuosity for mass transport, potentially enhancing the power density of a MOF-based thermal storage device. As with absorption in salts, care must be taken in the screening to assess stability of any new MOF composition. This is especially important in the case where water is the adsorbate, as some MOFs will undergo (irreversible) hydrolysis in humid environments¹⁰⁷. For this reason, extending the screening to adsorbates other than water is an area also worth exploring.

Enhancing power density. As discussed in the preceding sections, a practical thermal storage device must store and release heat at rates that are fast enough to meet the requirements of the desired application. In turn, this system-level requirement places constraints on the underlying properties of the storage material(s), such as their thermal conductivity. In the case of TCES materials, where a chemical reaction is responsible for the uptake/release of heat, several factors beyond thermal conductivity contribute to the achievable power density. These include intrinsic kinetic phenomena within the active storage material and larger-scale microstructural features that influence long-range heat and mass transport. 131,140,322

Regarding the intrinsic kinetics of the storage material, let us consider the discharge of a salt-hydrate-based TCES device. During discharge, the anhydrous salt and water vapor react to form a salt-hydrate through absorption of the water into the solid salt. As the salt-hydrate is a distinct crystalline phase, the rate of its formation (and the accompanying rate of heat release) is governed by nucleation and growth processes, either of which may be rate-limiting.³²³ The rate of nucleation of the hydrate is governed by a nucleation energy barrier associated with the formation of nanoscopic nuclei of the nascent hydrate phase.⁵⁷ Subsequent growth of these nuclei requires rearrangement of the salt's crystalline lattice to adopt the new structure of the hydrate, and transport of water to the salt/hydrate two-phase interface.131 To achieve high power density, one must ensure that both of these processes are sufficiently fast.

Journal Name ARTICLE

Similar kinetic limitations exist in hydrogen storage materials. Known strategies from the hydrogen literature for overcoming these limitations may be relevant to TCES materials that operate via absorption and should be investigated. One important strategy is doping. Bogdanovic et al.³²⁴ were the first to demonstrate that doping sodium alanate, NaAlH₄, with titanium significantly enhances the hydrogenation kinetics. This effect has been reported in other complex hydrides and with other dopants.^{323,325–328} Although the exact mechanism responsible for the kinetic enhancements remains a matter of debate, it is reasonable to hypothesize that similar beneficial effects may be realized for absorption reactions of interest for TCES. Some progress in this regard has already been achieved.^{149,327}

A second strategy that could be adopted from the field of hydrogen storage is impregnation of the active TCES material within a porous host. This approach has been used to improve the kinetics of complex hydrides, 329–331 and in some cases have resulted in dramatic changes to reaction behavior. 332–333 These improvements are hypothesized to result from reductions in particle size (which is constrained by the pore diameter) and associated diffusion lengths, and by phenomena associated with the guest/host interface. The downside to this approach is that the mass and volume of the (inactive) host decreases the system's specific energy and ESD.

Finally, we note that the limitations associated with nucleation and growth during absorption in solids are much less severe in materials that operate via adsorption. 334–336 This behaviour provides further motivation for developing materials such as MOFs for TCES. In the field of hydrogen storage, the kinetic performance of MOFs is well-known to surpass that of materials that operate via absorption, such as complex hydrides. 337,338

Conclusions

Heat is a primary component of the world's energy ecosystem. Its prevalence implies that its use and manipulation have major implications for energy efficiency and carbon emissions. The development of systems that can store and manage heat would have a positive impact upon numerous processes throughout multiple sectors of the global economy.

This review has focused on the materials that underlie systems that store and manipulate heat, with an emphasis on those that operate via thermochemical reactions. Starting from an overview of general concepts, a detailed discussion of relevant for low-temperature properties applications is subsequently presented. These applications include domestic heat storage/amplification (hot water heating), adsorptive cooling (air conditioning), and heatmoisture recuperation. Although these systems remain in an early stage of development, their commercialization will be accelerated by improving the performance of their respective thermal storage materials. This goal motivates a deep-dive into three main classes of low-temperature thermochemical storage materials: (i) absorption in solids (hydrates, ammoniates, and methanolates); (ii) sorption in porous hosts (metal-organic

frameworks); and (iii) dilution in liquids. For each class the underlying storage mechanisms are introduced?/benchimark materials are discussed, and a summary of advantages and limitations is provided. Although not widely discussed, the implementation of thermal energy storage also needs to consider the potential limited availability of raw materials and production constraints.

Finally, opportunities are described for research aimed at developing optimal thermochemical energy storage materials. Discovery of new storage materials and the development of strategies for increasing the rate of the heat-storing reaction — thus improving power density — are proposed as two important areas that are ripe for research and development.

List of Abbreviations

ARPA-E	Advanced Research Projects Agency - Energy
BTU	British Thermal Units
CAU	Christian-Albrechts-Universität
CNT	Carbon Nanotube
COP	Coeffiicient of Performance
CoRE	Computation-Ready, Experimental
DFT	Density Functional Theory
DOE	Department of Energy
DRH	Deliquescence Relative Humidity
ESD	Energy Storage Density
ETIP	European Technology and Innovation Platform
EU	European Union
GCMC	Grand Cannonical Monte Carlo
GJ	Giga-Joules
HLC	Henry's Law Constant
HTF	Heat Transfer Fluid
HVAC	Heating, Ventilation, and Air Conditioning
ICSD	Inorganic Crystal Structure Database
IHA	Isosteric Heat of Adsorption
IUPAC	International Union of Pure and Applied Chemistry
LCD	Largest Cavity Diameter
LD50	Lethal Dose 50
MIL	Materials of Institute Lavoisier
MJ	Mega-Joules
MOF	Metal-organic Framework
NIST	National Institutes of Standards and Technology
PCM	Phase Change Material
PV	Photovoltaic
RH	Relative Humidity
RHC	Renewable Heating and Cooling
SCE	Specific Cooling Effect
SCP	Specific Cooling Power
SHE	Specific Heating Effect

Thermochemical Energy Storage

Thermal Energy Storage

Volumetric Surface Area

Author Contributions

TCES

TES

VSA

pen Access Article. Published on 24 oktober 2025. Downloaded on 02.11.2025 08.53.33.

ARTICLE Journal Name

All authors made significant contributions to the drafting of this

Conflicts of interest

There are no conflicts to declare.

Acknowledgements

S.K. acknowledges support from the J. Robert Beyster Computational Innovation Graduate Fellows program. D.J.S. acknowledges the support of the Automotive Research Center (ARC), Cooperative Agreement W56HZV-19-2-0001 U.S. Army DEVCOM GVSC, the University of Michigan Graham Sustainability Institute's Carbon Neutrality Acceleration Program, and Welch Foundation grant F-2213-20240404. A.A. acknowledges support from the University of Michigan's Graham Sustainability Institute through the Carbon Neutrality Acceleration Program. H.H. and A.S. acknowledge support from the EIC Pathfinder project 4TunaTES - For Tunable Thermochemical Energy Storage (grant agreement 101130021).

Notes and references

- Lawrence Livermore National Laboratory. Estimated U.S. Energy Consumption in 2023: 93.6 Quads; Livermore, CA. https://flowcharts.llnl.gov/commodities/energy (Accessed on 16 April 2025), 2024.
- Forman, C.; Muritala, I. K.; Pardemann, R.; Meyer, B. Estimating the Global Waste Heat Potential. Renew. Sustain. Energy Rev. 2016, 57, 1568-1579.
- Firth, A.; Zhang, B.; Yang, A. Quantification of Global Waste Heat and Its Environmental Effects. Appl. Energy 2019, 235, 1314-1334.
- Arce, P.; Medrano, M.; Gil, A.; Oró, E.; Cabeza, L. F. Overview of Thermal Energy Storage (TES) Potential Energy Savings and Climate Change Mitigation in Spain and Europe. Appl. Energy **2011**, *88*, 2764–2774.
- DeForest, N.; Mendes, G.; Stadler, M.; Feng, W.; Lai, J.; Marnay, C. Optimal Deployment of Thermal Energy Storage under Diverse Economic and Climate Conditions. Appl. Energy 2014, 119, 488-496.
- Henry, A.; Prasher, R.; Majumdar, A. Five Thermal Energy Grand Challenges for Decarbonization. Nature Energy. Nature Research September 2020, pp 635–637.
- US Environmental Protection Agency (EPA). Inventory of US Greenhouse Gas Emissions and Sinks: 1990-2009; Washington, 2011.
- IPCC. Climate Change 2014: Synthesis Report. Contribution of Working Groups I, II and III to the Fifth Assessment Report of the Intergovernmental Panel on Climate Change; Core Writing Team, Pachauri, R. K., Meyer, L., Eds.; Geneva, Switzerland, 2014.
- Tatsidjodoung, P.; Le Pierrès, N.; Luo, L. A Review of Potential Materials for Thermal Energy Storage in Building Applications. Renew. Sustain. Energy Rev. 2013, 18, 327-349.
- 10. Sun, Y.; Wang, S.; Xiao, F.; Gao, D. Peak Load Shifting Control Using Different Cold Thermal Energy Storage Facilities in Commercial Buildings: A Review. Energy Convers. Manag. **2013**, *71*, 101–114.
- 11. Wang, Q.; Wu, R.; Wu, Y.; Zhao, C. Y. Parametric Analysis of Using PCM Walls for Heating Loads Reduction. Energy Build. **2018**, 172, 328-336.

- 12. U.S. Energy Information Administration. Annual Energy DOI: 10.1039/D5MH02947 https://www.eia.gov/pressroom/presentations/sieminski_0 1052017.pdf, 2017.
- 13. U.S. Energy Information Administration. Residential Energy Consumption https://www.eia.gov/consumption/residential/methodolog y/2009/pdf/techdoc-summary010413.pdf, 2009.
- 14. Sonoco Thermosafe. Greenbox® Pre Qualified Shipping Box https://www.thermosafe.com/products/pre-qualifiedsolutions/parcel-solutions/greenbox/ (Accessed on 16 April
- 15. Sharma, R. K.; Ganesan, P.; Tyagi, V. V.; Metselaar, H. S. C.; Sandaran, S. C. Developments in Organic Solid-Liquid Phase Change Materials and Their Applications in Thermal Energy Storage. Energy Convers. Manag. 2015, 95, 193–228.
- 16. Krishnan, S.; Garimella, S. V. Thermal Management of Transient Power Spikes in Electronics - Phase Change Energy Storage or Copper Heat Sinks? In International Electronic Packaging Technical Conference and Exhibition; Maui, Hawaii, 2003; pp 1-12.
- 17. Jankowski, N. R.; McCluskey, F. P. A Review of Phase Change Materials for Vehicle Component Thermal Buffering. Appl. Energy 2014, 113, 1525-1561.
- 18. Gumus, M. Reducing Cold-Start Emission from Internal Combustion Engines by Means of Thermal Energy Storage System. *Appl. Therm. Eng.* **2009**, *29*, 652–660.
- 19. Gao, J.; Tian, G.; Sorniotti, A.; Karci, A. E.; Di Palo, R. Review of Thermal Management of Catalytic Converters to Decrease Engine Emissions during Cold Start and Warm Up. Appl. Therm. Eng. **2019**, 147, 177–187.
- 20. Putrus, J. P.; Jones, S. T.; Jawad, B. A.; Kfoury, G.; Arslan, S.; Schihl, P. Solving Military Vehicle Transient Heat Load Issues Using Phase Change Materials. In Proceedings of the ASME 2015 International Mechanical Engineering Congress and Exposition; Houston, Texas, 2015; pp 1-7.
- 21. Kato, Y.; Takahashi, R.; Sekiguchi, T.; Ryu, J. Study on Medium-Temperature Chemical Heat Storage Using Mixed Hydroxides. Int. J. Refrig. 2009, 32, 661-666.
- 22. Myagmarjav, O.; Ryu, J.; Kato, Y. Waste Heat Recovery from Iron Production by Using Magnesium Oxide / Water Chemical Heat Pump as Thermal Energy Storage. ISIJ Int. 2015, 55, 464-472.
- 23. Brückner, S.; Liu, S.; Miró, L.; Radspieler, M.; Cabeza, L. F.; Lävemann, E. Industrial Waste Heat Recovery Technologies: An Economic Analysis of Heat Transformation Technologies. Appl. Energy 2015, 151, 157-167.
- 24. Ishitobi, H.; Ryu, J.; Kato, Y. Combination of Thermochemical Energy Storage and Small Pressurized Water Reactor for Cogeneration System. Energy Procedia 2015, 71, 90-96.
- Carrillo, A. J.; González-Aguilar, J.; Romero, M.; Coronado, J. M. Solar Energy on Demand: A Review on High Temperature Thermochemical Heat Storage Systems and Materials. Chem. Rev. **2019**, 119, 4777–4816.
- 26. Teng, L.; Xuan, Y.; Da, Y.; Liu, X.; Ding, Y. Modified Ca-Looping Materials for Directly Capturing Solar Energy and High-Temperature Storage. Energy Storage Mater. 2020, 25, 836-
- 27. Sharma, A.; Tyagi, V. V.; Chen, C. R.; Buddhi, D. Review on Thermal Energy Storage with Phase Change Materials and Applications. Renew. Sustain. Energy Rev. 2009, 13, 318–345.
- 28. Faraj, K.; Khaled, M.; Faraj, J.; Hachem, F.; Castelain, C. Phase Change Material Thermal Energy Storage Systems for Cooling Applications in Buildings: A Review. Renew. Sustain. Energy Rev. 2020, 119, 109579.
- 29. Rammelberg, H. U.; Schmidt, T.; Ruck, W. Hydration and Dehydration of Salt Hydrates and Hydroxides for Thermal

Open Access Article. Published on 24 oktober 2025. Downloaded on 02.11.2025 08.53.33

Journal Name ARTICLE

- Energy Storage Kinetics and Energy Release. Energy Procedia 2012, 30, 362-369.
- 30. N'Tsoukpoe, K. E.; Kuznik, F. A Reality Check on Long-Term Thermochemical Heat Storage for Household Applications. Renew. Sustain. Energy Rev. 2021, 139, 110683.
- 31. Pardo, P.; Deydier, A.; Anxionnaz-Minvielle, Z.; Rougé, S.; Cabassud, M.; Cognet, P. A Review on High Temperature Thermochemical Heat Energy Storage. Renew. Sustain. Energy Rev. 2014, 32, 591-610.
- 32. Zalba, B.; Marín, J. M.; Cabeza, L. F.; Mehling, H. Review on Thermal Energy Storage with Phase Change: Materials, Heat Transfer Analysis and Applications. Appl. Therm. Eng. 2003, 23. 251-283.
- 33. Pielichowska, K.; Pielichowski, K. Phase Change Materials for Thermal Energy Storage. Prog. Mater. Sci. 2014, 65, 67–123.
- 34. Aydin, D.; Casey, S. P.; Riffat, S. The Latest Advancements on Thermochemical Heat Storage Systems. Renew. Sustain. Energy Rev. 2015, 41, 356-367.
- 35. Herrmann, U.; Kearney, D. W. Survey of Thermal Energy Storage for Parabolic Trough Power Plants. J. Sol. Energy Eng. **2002**, 124, 145-152.
- 36. Tian, Y.; Zhao, C. Y. A Review of Solar Collectors and Thermal Energy Storage in Solar Thermal Applications. Appl. Energy **2013**, 104, 538-553.
- 37. N'Tsoukpoe, K. E.; Liu, H.; Le Pierrès, N.; Luo, L. A Review on Long-Term Sorption Solar Energy Storage. Renew. Sustain. Energy Rev. 2009, 13, 2385-2396.
- 38. van Essen, V. M.; Cot Gores, J.; Bleijendaal, L. P. J.; Zondag, H. a.; Schuitema, R.; Bakker, M.; van Helden, W. G. J. Characterization of Salt Hydrates for Compact Seasonal Thermochemical Storage. ASME 2009 3rd Int. Conf. Energy Sustain. Vol. 2 2009, 2, 825-830.
- 39. N'Tsoukpoe, K. E.; Schmidt, T.; Rammelberg, H. U.; Watts, B. A.; Ruck, W. K. L. A Systematic Multi-Step Screening of Numerous Salt Hydrates for Low Temperature Thermochemical Energy Storage. Appl. Energy 2014, 124, 1-
- 40. Wentworth, W. E.; Chen, E. Simple Thermal Decomposition Reactions for Storage of Solar Thermal Energy. Sol. Energy **1976**, *18*, 205–214.
- 41. Jiang, Z.; Jiang, F.; Li, C.; Leng, G.; Zhao, X.; Li, Y.; Zhang, T.; Xu, G.; Jin, Y.; Yang, C.; et al. A Form Stable Composite Phase Change Material for Thermal Energy Storage Applications over 700 °C. Appl. Sci. 2019, 9.
- 42. Saher, S.; Johnston, S.; Esther-Kelvin, R.; Pringle, J. M.; MacFarlane, D. R.; Matuszek, K. Trimodal Thermal Energy Storage Material for Renewable Energy Applications. Nature **2024**, 636, 622-626.
- 43. Jaziri, N.; Boughamoura, A.; Müller, J.; Mezghani, B.; Tounsi, F.; Ismail, M. A Comprehensive Review of Thermoelectric Generators: Technologies and Common Applications. Energy Reports **2020**, *6*, 264–287.
- 44. Enescu, D. Thermoelectric Energy Harvesting: Basic Principles and Applications. In Green Energy Advances; Enescu, D., Ed.; 2019; pp 1-37.
- 45. Deutsch, M.; Müller, D.; Aumeyr, C.; Jordan, C.; Gierl-mayer, C.; Weinberger, P.; Winter, F.; Werner, A. Systematic Search Algorithm for Potential Thermochemical Energy Storage Systems. Appl. Energy 2016, 183, 113-120.
- Richter, M.; Habermann, E.-M.; Siebecke, E.; Linder, M. A Systematic Screening of Salt Hydrates as Materials for a Thermochemical Heat Transformer. Thermochim. Acta 2018, 659. 136-150.
- 47. Donkers, P. A. J.; Sögütoglu, L. C.; Huinink, H. P.; Fischer, H. R.; Adan, O. C. G. A Review of Salt Hydrates for Seasonal Heat Storage in Domestic Applications. Appl. Energy 2017, 199, 45-68.

- 48. Mazur, N.; Blijlevens, M. A. R.; Ruliaman, R.; Fischer, H.; Donkers, P.; Meekes, H.; Vlieg, E.; Adan 103/Huininko4t Revisiting Salt Hydrate Selection for Domestic Heat Storage Applications. Renewable Energy 2023, 218, 119331.
- Shkatulov, A.; Joosten, R.; Fischer, H.; Huinink, H. Core-Shell Encapsulation of Salt Hydrates into Mesoporous Silica Shells for Thermochemical Energy Storage. ACS Appl. Energy Mater. 2020, 3, 6860-6869.
- 50. Fumey, B.; Weber, R.; Gantenbein, P.; Daguenet-Frick, X.; Hughes, I.; Dorer, V. Limitations Imposed on Energy Density of Sorption Materials in Seasonal Thermal Storage Systems. Energy Procedia 2015, 70, 203-208.
- 51. Nemtzow, D.; Sawyer, K.; Mumme, S.; James, N. Novel Materials in Thermal Energy Storage for Buildings. Thermal Energy Storage Webinar Series; U.S. Department of Energy Office of Energy Efficiency & Renewable Energy, 2020.
- 52. The European Technology and Innovation Platform on Renewable Heating and Cooling (RHC-ETIP), Strategic Research and Innovation Agenda for Climate-Neutral Heating and Cooling in Europe, 2022. https://www.rhcplatform.org/content/uploads/2020/10/EUREC-Brochure-RHC-SRI-06-2022-WEB.pdf (Accessed on 21 April 2025).
- N'Tsoukpoe, K. E.; Kuznik, F. A reality check on long-term thermochemical heat storage for household applications. Renewable Sustainable Energy Rev. 2021, 139, 110683.
- 54. Crespo, A.; Fernández, C.; de Gracia, A.; Frazzica, A. Solar-Driven Sorption System for Seasonal Heat Storage under Optimal Control: Study for Different Climatic Zones. Energies 2022, 15, 5604,
- 55. Liu, H.; Wang, W.; Zhang, Y. Performance gap between thermochemical energy storage systems based on salt hydrates and materials. J. Cleaner Prod. 2021, 313, 127908.
- 56. Bejan, A. Fundamentals of exergy analysis, entropy generation minimization, and the generation of flow architecture. Int. J. Energy Res. 2002, 26, 545-565.
- 57. Sögütoglu, L.-C.; Steiger, M.; Houben, J.; Biemans, D.; Fischer, H. R.; Donkers, P.; Huinink, H.; Adan, O. C. G. Understanding the Hydration Process of Salts: The Impact of a Nucleation Barrier. Cryst. Growth Des. 2019, 19, 2279-2288.
- 58. Aydin, D.; Casey, S. P.; Chen, X.; Riffat, S. Novel "Open-Sorption Pipe" Reactor for Solar Thermal Energy Storage. Energy Convers. Manag. 2016, 121, 321-334.
- 59. Afflerbach, S.; Trettin, R. A Systematic Screening Approach for New Materials for Thermochemical Energy Storage and Conversion Based on the Strunz Mineral Classification System. Thermochim. Acta 2019, 674, 82-94.
- 60. Ziegler, M. S.; Trancik, J. E. Re-examining rates of lithium-ion battery technology improvement and cost decline. Energy Environ. Sci. 2021, 14, 1635-1651.
- 61. Gordeeva, L. G.; Shkatulov, A. I.; Aristov, Y. I. Closed Sorption Systems. In Reference Module in Earth Systems and Sciences; Environmental Elsevier. 2020: B9780128197233000000.
- 62. Fumey, B.; Weber, R.; Baldini, L. Sorption Based Long-Term Thermal Energy Storage – Process Classification and Analysis of Performance Limitations: A Review. Renew. Sustain. Energy Rev. 2019, 111, 57-74.
- 63. Stengler, J.; Linder, M. Thermal Energy Storage Combined with a Temperature Boost: An Underestimated Feature of Thermochemical Systems. Appl. Energy 2020, 262, 114530.
- Tokarev, M. M.; Gordeeva, L. G.; Grekova, A. D.; Aristov, Y. I. Adsorption Cycle "Heat from Cold" for Upgrading the Ambient Heat: The Testing a Lab-Scale Prototype with the Composite Sorbent CaClBr/Silica. Appl. Energy 2018, 211, 136-145.
- 65. Aristov, Y. I. "Heat from Cold" A New Cycle for Upgrading the Ambient Heat: Adsorbent Optimal from the Dynamic Point of View. Appl. Therm. Eng. 2017, 124, 1189-1193.

ARTICLE Journal Name

- 66. Aristov, Y. I. Adsorptive Transformation of Ambient Heat: A New Cycle. Appl. Therm. Eng. 2017, 124, 521-524.
- 67. Rathgeber, C.; Lävemann, E.; Hauer, A. Economic Top-down Evaluation of the Costs of Energy Storages—A Simple Economic Truth in Two Equations. J. Energy Storage 2015, 2, 43-46
- 68. Critoph, R. E. Solid Sorption Cycles: A Short History. Int. J. Refrig. 2012, 35, 490-493.
- 69. Cabeza, L. F.; Solé, A.; Barreneche, C. Review on Sorption Materials and Technologies for Heat Pumps and Thermal Energy Storage. Renew. Energy 2017, 110, 3-39.
- 70. Aristov, Y. I. Challenging Offers of Material Science for Adsorption Heat Transformation: A Review. Appl. Therm. Eng. 2013, 50, 1610-1618.
- 71. Girnik, I. S.; Aristov, Y. I. Water as an Adsorptive for Adsorption Cycles Operating at a Temperature below 0 °C. Energy 2020, 211.
- 72. Younes, M. M.; El-Sharkawy, I. I.; Kabeel, A. E.; Saha, B. A. Review on Adsorbent-Adsorbate Pairs for Applications. Appl. Therm. Eng. 2017, 114, 394–414.
- 73. Aristov, Yu. I. Finned-Flat-Tube Heat Exchangers for Adsorptive Cooling: Review of the Current Studies. Energy 2025, 316, 134305.
- 74. Aristov, Y. I.; Sapienza, A.; Ovoshchnikov, D. S.; Freni, A.; Restuccia, G. Reallocation of Adsorption and Desorption Times for Optimisation of Cooling Cycles. Int. J. Refrig. 2012, *35*, 525-531.
- 75. Polanyi, M. Section III.—Theories of the adsorption of gases. A general survey and some additional remarks. Introductory paper to section III. Trans. Faraday Soc. 1932, 28, 316–333.
- 76. Towsif Abtab, S. M.; Alezi, D.; Bhatt, P. M.; Shkurenko, A.; Belmabkhout, Y.; Aggarwal, H.; Weseliński, Ł. J.; Alsadun, N.; Samin, U.; Hedhili, M. N.; et al. Reticular Chemistry in Action: A Hydrolytically Stable MOF Capturing Twice Its Weight in Adsorbed Water. Chem 2018, 4, 94-105.
- 77. Lenzen, D.; Bendix, P.; Reinsch, H.; Fröhlich, D.; Kummer, H.; Möllers, M.; Hügenell, P. P. C.; Gläser, R.; Henninger, S.; Stock, N. Scalable Green Synthesis and Full-Scale Test of the Metal-Organic Framework CAU-10-H for Use in Adsorption-Driven Chillers. Adv. Mater. 2018, 30.
- 78. Elsayed, E.; AL-Dadah, R.; Mahmoud, S.; Anderson, P. A.; Elsayed, A.; Youssef, P. G. CPO-27(Ni), Aluminium Fumarate and MIL-101(Cr) MOF Materials for Adsorption Water Desalination. Desalination 2017, 406, 25-36.
- 79. Fu, H.-X.; Zhang, L.-Z.; Xu, J.-C.; Cai, R.-R. A Dual-Scale Analysis of a Desiccant Wheel with a Novel Organic-Inorganic Hybrid Adsorbent for Energy Recovery. Appl. Energy 2016, 163, 167-179.
- 80. Shkatulov, A.; Gordeeva, L. G.; Girnik, I. S.; Huinink, H.; Aristov, Y. I. Novel Adsorption Method for Moisture and Heat Recuperation in Ventilation: Composites "LiCl/Matrix" Tailored for Cold Climate. Energy 2020, 201, 117595.
- 81. Wang, Z.; Horseman, T.; Straub, A. P.; Yip, N. Y.; Li, D.; Elimelech, M.; Lin, S. Pathways and Challenges for Efficient Solar-Thermal Desalination. Sci. Adv. 2019, 5, eaax0763.
- 82. Tu, Y.; Wang, R.; Zhang, Y.; Wang, J. Progress and Expectation of Atmospheric Water Harvesting. Joule 2018, 2, 1452-1475.
- 83. Cai, J.; Zheng, X.; Pan, Q.; Li, D.; Wang, W. Advances in Hygroscopic Metal-Organic Frameworks for Air, Water & Energy Applications. Appl. Energy 2025, 377, 124362.
- 84. Elsayed, E.; AL-Dadah, R.; Mahmoud, S.; Anderson, P.; Elsayed, A. Experimental Testing of Aluminium Fumarate MOF for Adsorption Desalination. Desalination 2020, 475, 114170.
- 85. Kim, H.; Yang, S.; Rao, S. R.; Narayanan, S.; Kapustin, E. A.; Furukawa, H.; Umans, A. S.; Yaghi, O. M.; Wang, E. N. Water Harvesting from Air with Metal-Organic Frameworks

- Powered by Natural Sunlight. Science (80-.). 2017, 356, 430-DOI: 10.1039/D5MH01794G
- 86. Gordeeva, L. G.; Tu, Y. D.; Pan, Q.; Palash, M. L.; Saha, B. B.; Aristov, Y. I.; Wang, R. Z. Metal-Organic Frameworks for Energy Conversion and Water Harvesting: A Bridge between Thermal Engineering and Material Science. Nano Energy 2021, 84, 105946.
- 87. Kiyabu, S.; Lowe, J. S.; Ahmed, A.; Siegel, D. J. Computational Screening of Hydration Reactions for Thermal Energy Storage: New Materials and Design Rules. Chem. Mater. **2018**. 30. 2006-2017.
- 88. Blijlevens, M. A. R.; Mazur, N.; Kooijman, W.; Fischer, H. R.; Huinink, H. P.; Meekes, H.; Vlieg, E. A Study of the Hydration and Dehydration Transitions of SrCl2 Hydrates for Use in Heat Storage. Sol. Energy Mater. Sol. Cells 2022, 242, 111770.
- Smeets, B.; Iype, E.; Nedea, S. V.; Zondag, H. a.; Rindt, C. C. M. A DFT Based Equilibrium Study on the Hydrolysis and the Dehydration Reactions of MgCl₂ Hydrates. J. Chem. Phys. 2013, 139, 124312.
- 90. Cuypers, R.; Anastasopol, A.; De Jong, A.-J.; Oversloot, H.; Van Vliet, L.; Bodis, P.; Hoegaerts, C. A Novel Heat Battery to Save Energy & Reduce CO₂ Production. In International Solar Energy Society; Palma de Mallorca, Spain, 2016; pp 1-7.
- Müller, D.; Knoll, C.; Gravogl, G.; Jordan, C.; Eitenberger, E.; Friedbacher, G.; Artner, W.; Welch, J. M.; Werner, A.; Harasek, M.; et al. Medium-Temperature Thermochemical Energy Storage with Transition Metal Ammoniates - A Systematic Material Comparison. Appl. Energy 2021, 285, 116470.
- 92. Sharma, R.; Anil Kumar, E.; Dutta, P.; Srinivasa Murthy, S.; Aristov, Y. I.; Tokrev, M. M.; Li, T. X.; Wang, R. Z. Ammoniated Salt Based Solid Sorption Thermal Batteries: A Comparative Study. Appl. Therm. Eng. 2021, 191, 116875.
- 93. Zhang, W. Y.; Mehari, A.; Zhang, X. J.; Roskilly, A. P.; Jiang, L. Ammonia-Based Sorption Thermal Battery: Concepts, Thermal Cycles, Applications, and Perspectives. Energy Storage Mater. 2023, 62, 102930.
- 94. Yan, T.; Wang, R. Z.; Li, T. X. Experimental Investigation on Thermochemical Heat Storage Using Manganese Chloride/Ammonia. Energy 2018, 143, 562-574.
- Critoph, R. E. Performance Limitations of Adsorption Cycles for Solar Cooling. Sol. Energy 1988, 41, 21–31.
- 96. Neumann, K.; Wiegand, M.; Opel, O.; Korhammer, K. Solid Sorption Refrigeration With Calcium Chloride Methanolates on Technical Scale. Proc. 14th Int. Renew. Energy Storage Conf. 2020 (IRES 2020) 2021, 6, 142-149.
- 97. Korhammer, K.; Neumann, K.; Opel, O.; Ruck, W. K. L. Thermodynamic and Kinetic Study of CaCl₂-CH₃OH Adducts for Solid Sorption Refrigeration by TGA/DSC. Appl. Energy **2018**, 230, 1255-1278.
- Aristov, Y. I.; Gordeeva, L. G.; Pankratiev, Y. D.; Plyasova, L. M.; Bikova, I. V.; Freni, A.; Restuccia, G. Sorption Equilibrium of Methanol on New Composite Sorbents "CaCl2/Silica Gel." Adsorption 2007, 13, 121-127.
- 99. Grekova, A.; Strelova, S.; Gordeeva, L.; Aristov, Y. "LiCl/Vermiculite Methanol" as Working Pair for Adsorption Heat Storage: Adsorption Equilibrium and Dynamics. Energy **2019**, 186, 115775.
- 100. Grekova, A. D.; Girnik, I. S.; Nikulin, V. V.; Tokarev, M. M.; Gordeeva, L. G.; Aristov, Y. I. New Composite Sorbents of Water and Methanol "Salt in Anodic Alumina": Evaluation for Adsorption Heat Transformation. Energy 2016, 106, 231-239
- 101. Strelova, S. V.; Gordeeva, L. G.; Grekova, A. D.; Salanov, A. N.; Aristov, Y. I. Composites "Lithium Chloride/Vermiculite" for Adsorption Thermal Batteries: Giant Acceleration of Sorption Dynamics. Energy 2023, 263, 125733.

Journal Name ARTICLE

- 102. Rouquerol, J.; Avnir, D.; Fairbridge, C. W.; Everett, D. H.; Haynes, J. M.; Pernicone, N.; Ramsay, J. D. F.; Sing, K. S. W.; Unger, K. K. Recommendations for the Characterization of Porous Solids (Technical Report); 1994; Vol. 66.
- 103. Vasta, S.; Brancato, V.; La Rosa, D.; Palomba, V.; Restuccia, G.; Sapienza, A.; Frazzica, A. Adsorption Heat Storage: State-of-the-Art and Future Perspectives. *Nanomater. (Basel, Switzerland)* **2018**, *8*, 522.
- 104. Deshmukh, H.; Maiya, M. P.; Srinivasa Murthy, S. Study of Sorption Based Energy Storage System with Silica Gel for Heating Application. *Appl. Therm. Eng.* **2017**, *111*, 1640–1646.
- 105. Henninger, S. K.; Jeremias, F.; Kummer, H.; Janiak, C. MOFs for Use in Adsorption Heat Pump Processes. *Eur. J. Inorg. Chem.* **2012**, *2012*, 2625–2634.
- 106. Yaghi, O. M.; O'Keeffe, M.; Ockwig, N. W.; Chae, H. K.; Eddaoudi, M.; Kim, J. Reticular Synthesis and the Design of New Materials. *Nature* **2003**, *423* (6941), 705–714.
- 107. Burtch, N. C.; Jasuja, H.; Walton, K. S. Water Stability and Adsorption in Metal–Organic Frameworks. *Chem. Rev.* **2014**, *114*, 10575–10612.
- 108. Batra, R.; Chen, C.; Evans, T. G.; Walton, K. S.; Ramprasad, R. Prediction of water stability of metal-organic frameworks using machine learning. *Nat. Mach. Intell.* **2020**, *2*, 704–710.
- 109. Ehrenmann, J.; Henninger, S. K.; Janiak, C. Water Adsorption Characteristics of MIL-101 for Heat-Transformation Applications of MOFs. *Eur. J. Inorg. Chem.* **2011**, No. 4, 471–474
- 110. Manyimo, T. L.; Ren, J.; Wang, H.; Peng, S. Perspective on Metal-Organic Frameworks-Based Atmospheric Water Harvesting Systems towards Universal Adoption. Coord. Chem. Rev. 2025, 537, 216717.
- 111. Yu, N.; Wang, R. Z.; Lu, Z. S.; Wang, L. W.; Ishugah, T. F. Evaluation of a Three-Phase Sorption Cycle for Thermal Energy Storage. *Energy* **2014**, *67*, 468–478.
- 112. Ding, Z.; Wu, W.; Type II absorption thermal battery for temperature upgrading: Energy storage heat transformer. *Appl. Energy* **2022**, *324*, 119748.
- 113. Shkatulov, A.; Averina, E.; Raemaekers, T.; Fischer, H.; Adan, O. C. G.; Huinink, H. Stabilization of reactive bed particles for thermochemical energy storage with fiber reinforcement. *J. Energy Storage*, **2024**, *101*, 113764.
- 114. N'Tsoukpoe, K. E.; Schmidt, T.; Rammelberg, H. U.; Watts, B. A.; Ruck, W. K. L. A Systematic Multi-Step Screening of Numerous Salt Hydrates for Low Temperature Thermochemical Energy Storage. *Appl. Energy* **2014**, *124*, 1–16
- 115. Donkers, P.; Pel, L.; Steiger, M.; Adan, O. Deammoniation and Ammoniation Processes with Ammonia Complexes. *AIMS Energy* **2016**, *4*, 936–950.
- 116. Zhang, T.; Miyaoka, H.; Miyaoka, H.; Ichikawa, T.; Kojima, Y. Review on Ammonia Absorption Materials: Metal Hydrides, Halides, and Borohydrides. *ACS Appl. Energy Mater.* **2018**, *1*, 232–242.
- 117. Jenkins, H. D. B. The Thermodynamic Difference Rule (TDR) for Non-Aqueous Solvates. Part 2. Review of Methodology, Investigation and Prediction of Thermodynamic Data for Ammoniate Solvates, M_pX_q•nNH₃, Routes to Expand the Database. *J. Chem. Thermodyn.* **2019**, *135*, 316–329.
- 118. Korhammer, K.; Mihály, J.; Bálint, S.; Trif, L.; Vass, Á.; Tompos, A.; Tálas, E. Reversible Formation of Alcohol Solvates and Their Potential Use for Heat Storage. *J. Therm. Anal. Calorim.* **2019**, *138*, 11–33.
- 119. Glasser, L. Thermodynamics of Inorganic Hydration and of Humidity Control, with an Extensive Database of Salt Hydrate Pairs. *J. Chem. Eng. Data* **2014**, *59*, 526–530.
- 120. Sugimoto, K.; Dinnebier, R. E.; Hanson, J. C. Structures of Three Dehydration Products of Bischofite from in Situ

- Synchrotron Powder Diffraction Data (MgCl₂•nH₂O; n = 1, 2, 4). Acta. Cryst. 2007, B63, 235–242. DOI: 10.1039/D5MH01794G
- 121. Schmidt, H.; Hennings, E.; Voigt, W. Magnesium Chloride Tetra-Hydrate, MgCl₂•4H₂O. *Acta Crystallogr. Sect. C Cryst. Struct. Commun.* **2012**, *68*, i4−i6.
- 122. Agron, P. A.; Busing, W. R. Magnesium Dichloride Hexahydrate, MgCl₂•6H₂O, by Neutron Diffraction. *Acta Crystallogr. Sect. C Struct. Chem.* 1985, 41, 8–10.
- 123. Hennings, E.; Schmidt, H.; Voigt, W. Crystal Structures of Hydrates of Simple Inorganic Salts. I. Water-Rich Magnesium Halide Hydrates MgCl₂•8H₂O, MgCl₂•12H₂O, MgBr₂•6H₂O, MgBr₂•9H₂O, Mgl₂•8H₂O and Mgl₂•9H₂O. Acta Crystallogr. Sect. C Cryst. Struct. Commun. 2013, 69, 1292–1300.
- 124. Komatsu, K.; Shinozaki, A.; Machida, S.; Matsubayashi, T.; Watanabe, M.; Kagi, H.; Sano-Furukawa, A.; Hattori, T. Crystal Structure of Magnesium Dichloride Decahydrate Determined by X-Ray and Neutron Diffraction under High Pressure. *Acta Crystallogr. Sect. B Struct. Sci. Cryst. Eng. Mater.* 2015, 71, 74–80.
- 125. Derby, I. H.; Yngve, V. The Dissociation Tensions of Certain Hydrated Chlorides and the Vapor Pressures of Their Saturated Solutions. J. Am. Chem. Soc. 1916, 38, 1439–1451.
- 126. Carling, R. W. Dissociation Pressures and Enthalpies of Reaction in MgCl₂•nH₂O and CaCl₂•nNH₃. *J. Chem. Thermodyn.* **1981**, *13*, 503–512.
- 127. Greenspan, L. Humidity Fixed Points of Binary Saturated Aqueous Solutions. J. Res. Natl. Bur. Stand. Sect. A Phys. Chem. 1977, 81A, 89.
- 128. Gough, R. V.; Chevrier, V. F.; Tolbert, M. A. Formation of liquid water at low temperatures via the deliquescence of calcium chloride: Implications for Antarctica and Mars. *Planet. Space Sci.* **2016**, *131*, 79–87.
- 129. Huinink, H.; de Jong, S.; Houben, V. Hydration fronts in packed particle beds of salt hydrates: Implications for heat storage. *Journal of Energy Storage*, **2023**, *71*, 108158.
- 130. Romaní, J.; Gasia, J.; Solé, A.; Takasu, H.; Kato, Y.; Cabeza, L. F. Evaluation of Energy Density as Performance Indicator for Thermal Energy Storage at Material and System Levels. *Appl. Energy* **2019**, *235*, 954–962.
- 131. Aarts, J.; de Jong, S.; Cotti, M. L.; Donkers, P. A. J.; Fischer, H. R.; Adan, O. C. G.; Huinink, H. P. Diffusion Limited Hydration Kinetics of Millimeter Sized Salt Hydrate Particles for Thermochemical Heat Storage, J. Energy Storage, 2022, 47, 103554.
- 132. Pablo, J. De; Andersson, J.; Azoulay, M. Kinetic Investigation of the Sorption of Water by Lithium Hydroxide. *Thermochim. Acta* **1987**, *113*, 87–94.
- 133. Andersson, J.; Azoulay, M.; Pablo, J. De. Kinetic Investigation of the Sorption of Water by Barium Chloride Monohydrate. *Thermochim. Acta* **1983**, *70*, 291–302.
- 134. Stanish, M. A.; Perlmutter, D. D. Kinetics of Hydrationdehydration Reactions Considered as Solid Transformations. AIChE J. 1984, 30, 557–563.
- 135. Andersson, J. Y.; Pablo, J. De; Azoulay, M. Kinetics of the Rehydration of Sodium Sulphide Dehydrated in Situ, Under Formation of its Pentahydrate. *Thermochim. Acta* **1985**, *91*, 223–234.
- 136. Sögütoglu, L. C.; Donkers, P. A. J.; Fischer, H. R.; Huinink, H. P.; Adan, O. C. G. In-Depth Investigation of Thermochemical Performance in a Heat Battery: Cyclic Analysis of K₂CO₃, MgCl₂ and Na₂S. *Appl. Energy* **2018**, *215*, 159–173.
- 137. Stengler, J.; Bürger, I.; Linder, M. Thermodynamic and Kinetic Investigations of the SrBr₂ Hydration and Dehydration Reactions for Thermochemical Energy Storage and Heat Transformation. *Appl. Energy* **2020**, *277*, 115432.
- 138. Afflerbach, S.; Trettin, R. A Systematic Screening Approach for New Materials for Thermochemical Energy Storage and

ARTICLE Journal Name

- Conversion Based on the Strunz Mineral Classification System. *Thermochim. Acta* **2019**, *674*, 82–94.
- 139. Gough, R. V.; Chevrier, V. F.; Baustian, K. J.; Wise, M. E.; Tolbert, M. A. Laboratory Studies of Perchlorate Phase Transitions: Support for Metastable Aqueous Perchlorate Solutions on Mars. *Earth Planet. Sci. Lett.* **2011**, *312*, 371–377.
- 140. Linnow, K.; Niermann, M.; Bonatz, D.; Posern, K.; Steiger, M. Experimental Studies of the Mechanism and Kinetics of Hydration Reactions. *Energy Procedia* **2014**, *48*, 394–404.
- 141. Dunning, W. J. Nucleation and Growth Processes in the Dehydration of Salt Crystals. In *Kinetics of reactions in ionic systems*; Gray, T. J., Fréchette, V. D., Eds.; Springer: New York, 1969; pp 132–155.
- 142. Dai, Q.; Hu, J.; Salmeron, M. Adsorption of Water on NaCl (100) Surfaces: Role of Atomic Steps. J. Phys. Chem. B 1997, 101, 1994–1998.
- 143. Peters, S. J.; Ewing, G. E. Water on Salt: An Infrared Study of Adsorbed H₂O on NaCl(100) under Ambient Conditions. *J. Phys. Chem. B* **1997**, *101*, 10880–10886.
- 144. Luna, M.; Rieutord, F.; Melman, N. A.; Dai, Q.; Salmeron, M. Adsorption of Water on Alkali Halide Surfaces Studied by Scanning Polarization Force Microscopy. *J. Phys. Chem. A* **1998**, *102*, 6793–6800.
- 145. Koelemeijer, P. J.; Peach, C. J.; Spiers, C. J. Surface Diffusivity of Cleaved NaCl Crystals as a Function of Humidity: Impedance Spectroscopy Measurements and Implications for Crack Healing in Rock Salt. *J. Geophys. Res. Solid Earth* **2012**, *117*, 1–15.
- 146. Chakraborty, S. The Humidity Dependent Conductance of Al₂(SO₄)₃•16H₂O. *Smart Mater. Struct.* **1995**, *4*, 368–369.
- 147. Barboux, P.; Livage, J. Ionic Conductivity in Fibrous Ce(HPO₄)₂• (3+x)H₂O. *Solid State Ionics* **1989**, *34*, 47–52.
- 148. Houben, J.; van Biesen, J.; Huinink, H.; Fischer, H. R.; Adan, O. C. G. Accelerating the hydration reaction of potassium carbonate using organic dopants. *Sol. Energy Mater. Sol. Cells* **2023**, *259*, 112410.
- 149. Houben, J.; Shkatulov, A.; Huinink, H.; Fischer, H.; Adan, O. Caesium doping accelerates the hydration rate of potassium carbonate in thermal energy storage. *Sol. Energy Mater. Sol. Cells* **2023**, *251*, 112116.
- 150. Li, Y.; Shkatulov, A.; Linder, M.; Schaefer, M.; Li, B.; Thess, A. Enhancing Reactivity of Na₂Zn(SO₄)₂ Hydrates by Doping for Thermochemical Energy Storage. *Sol. Energy Mater. Sol. Cells* **2025**, *292*, 113753.
- 151. Mazur, N.; Huinink, H.; Fischer, H.; Donkers, P.; Adan, O. Accelerating the reaction kinetics of K_2CO_3 through the addition of CsF in the view of thermochemical heat storage. Sol. Energy **2022**, 242, 256–266.
- 152. Linnow, K.; Niermann, M.; Bonatz, D.; Posern, K.; Steiger, M. Experimental Studies of the Mechanism and Kinetics of Hydration Reactions. *Energy Procedia* **2014**, *48*, 394–404.
- 153. Fisher, R.; Ding, Y.; Sciacovelli, A. Hydration Kinetics of K₂CO₃, MgCl₂ and Vermiculite-Based Composites in View of Low-Temperature Thermochemical Energy Storage. *J. Energy Storage* **2021**, *38*, 102561.
- 154. Vyazovkin, S.; Burnham, A. K.; Criado, J. M.; Pérez-Maqueda, L. A.; Popescu, C.; Sbirrazzuoli, N. ICTAC Kinetics Committee Recommendations for Performing Kinetic Computations on Thermal Analysis Data. *Thermochim. Acta* **2011**, *520*, 1–19.
- 155. Gaeini, M.; Shaik, S. A.; Rindt, C. C. M. Characterization of Potassium Carbonate Salt Hydrate for Thermochemical Energy Storage in Buildings. *Energy Build.* 2019, 196, 178– 193.
- 156. Birkelbach, F.; Deutsch, M.; Werner, A. The Effect of the Reaction Equilibrium on the Kinetics of Gas-Solid Reactions — A Non-Parametric Modeling Study. *Renew. Energy* 2020, 152, 300–307.

- 157. Foster, M. C.; Ewing, G. E. Adsorption of Water on the NaCl(001) Surface. II. An Infrared 154 April 154 April 154 April 155 April 1
- 158. Verdaguer, A.; Segura, J. J.; Fraxedas, J.; Bluhm, H.; Salmeron, M. Correlation between Charge State of Insulating NaCl Surfaces and Ionic Mobility Induced by Water Adsorption: A Combined Ambient Pressure X-Ray Photoelectron Spectroscopy and Scanning Force Microscopy Study. J. Phys. Chem. C 2008, 112, 16898–16901.
- 159. Reading, M.; Dollimore, D.; Whitehead, R. The Measurement of Meaningful Kinetic Parameters for Solid State Decomposition Reactions. *J. Therm. Anal.* **1991**, *37*, 2165–2188.
- 160. Sögütoglu, L.-C.; Birkelbach, F.; Werner, A.; Fischer, H.; Huinink, H.; Adan, O. Hydration of Salts as a Two-Step Process: Water Adsorption and Hydrate Formation. *Thermochim. Acta* **2021**, *695*, 178819.
- 161. Szekely, J.; Evans, J. W.; Sohn, H. Y. Reactions of Porous Solids. In *Gas-Solid Reactions*; Elsevier, 1976; pp 108–175.
- 162. Huinink, H.; de Jong, S.; Houben, V. Hydration fronts in packed particle beds of salt hydrates: Implications for heat storage. *J. Energy Storage*, **2023**, *71*, 108158.
- 163. Huinink, H.; de Jong, S.; Adan, O. Hydration Fronts in Packed Particle Beds of Salt Hydrates II: The Role of Temperature Gradients and Implications for Heat Storage. In review.
- 164. Trausel, F.; De Jong, A. J.; Cuypers, R. A Review on the Properties of Salt Hydrates for Thermochemical Storage. In *Energy Procedia*; Elsevier BV, 2014; Vol. 48, pp 447–452.
- 165. De Jong, A.-J.; Van Vliet, L.; Hoegaerts, C.; Roelands, M.; Cuypers, R. Thermochemical Heat Storage From Reaction Storage Density to System Storage Density. *Energy Procedia* **2016**, *91*, 128–137.
- 166. Nash, D. B. Infrared Reflectance Spectra of Na₂S with Contaminant Na₂CO₃: Effects of Adsorbed H₂O and CO₂ and Relation to Studies of Io. *Icarus* **1988**, *74*, 365–368.
- 167. Kohler, T.; Biedermann, T.; Müller, K. Experimental Study of MgCl₂•6 H₂O as Thermochemical Energy Storage Material. Energy Technol. **2018**, *6*, 1935–1940.
- 168. Xu, J.; Li, T.; Yan, T.; Chao, J.; Wang, R. Dehydration Kinetics and Thermodynamics of Magnesium Chloride Hexahydrate for Thermal Energy Storage. *Sol. Energy Mater. Sol. Cells* **2021**, *219*, 110819.
- 169. Zhou, H.; Zhang, D. Effect of Graphene Oxide Aerogel on Dehydration Temperature of Graphene Oxide Aerogel Stabilized MgCl₂•6H₂O Composites. *Sol. Energy* **2019**, *184*, 202–208.
- 170. Kipouros, G. J.; Sadoway, D. R. A Thermochemical Analysis of the Production of Anhydrous MgCl₂. *J. Light Met.* **2001**, *1*, 111, 117
- 171. Zhang, Z.; Lu, X.; Yan, Y.; Wang, T. The Dehydration of MgCl₂•6H₂O by Inhibition of Hydrolysis and Conversion of Hydrolysate. *J. Anal. Appl. Pyrolysis* **2019**, *138*, 114−119.
- 172. Galwey, A. K.; Laverty, G. M. The Thermal Decomposition of Magnesium Chloride Dihydrate. *Thermochim. Acta* **1989**, 138, 115–127.
- 173. Ferrandon, M. S.; Lewis, M. A.; Tatterson, D. F.; Gross, A.; Doizi, D.; Croizé, L.; Dauvois, V.; Roujou, J. L.; Zanella, Y.; Carles, P. Hydrogen Production by the Cu-Cl Thermochemical Cycle: Investigation of the Key Step of Hydrolysing CuCl₂ to Cu₂OCl₂ and HCl Using a Spray Reactor. *Int. J. Hydrogen Energy* **2010**, *35*, 992–1000.
- 174. Farsi, A.; Dincer, I.; Naterer, G. F. Second Law Analysis of CuCl₂ Hydrolysis Reaction in the Cu–Cl Thermochemical Cycle of Hydrogen Production. *Energy* **2020**, *202*, 117721.
- 175. Shoval, S.; Yariv, S.; Kirsh, Y. The Study of Thermal Dehydration and Hydrolysis of MgBr₂•6HoH by DTA and TG. *Thermochim. Acta* **1988**, *133*, 263–273.

Open Access Article. Published on 24 oktober 2025. Downloaded on 02.11.2025 08.53.33.

ARTICLE

- 176. Hamze, R.; Nevoigt, I.; Sazama, U.; Fröba, M.; Steiger, M. Carnallite Double Salt for Thermochemical Heat Storage. *J.*
 - Energy Storage **2024**, 86, 111404.
- 177. Gutierrez, A.; Ushak, S.; Linder, M. High Carnallite-Bearing Material for Thermochemical Energy Storage: Thermophysical Characterization. *ACS Sustainable Chem. Eng.* **2018**, *6*, 6135–6145.
- 178. Korhammer, K.; Druske, M.-M.; Fopah-Lele, A.; Rammelberg, H. U.; Wegscheider, N.; Opel, O.; Osterland, T.; Ruck, W. Sorption and Thermal Characterization of Composite Materials Based on Chlorides for Thermal Energy Storage. *Appl. Energy* **2016**, *162*, 1462–1472.
- 179. Rammelberg, H. U.; Myrau, M.; Schmidt, T.; Ruck, W. K. L. An Optimization of Salt Hydrates for Thermochemical Heat Storage. In *International Symposium on Innovative Materials for Processes in Energy Systems 2013 Fukuoka, Japan*; 2013; pp IMPRES2013-117.
- 180. Beving, M. A. J. M.; Frijns, A. J. H.; Rindt, C. C. M.; Smeulders, D. M. J. Effect of cycle-induced crack formation on the hydration behaviour of K_2CO_3 particles: Experiments and modelling. *Thermochim. Acta* **2020**, *692*, 178752.
- 181. Jenkins, H. D. B.; Glasser, L. Difference Rule A New Thermodynamic Principle: Prediction of Standard Thermodynamic Data for Inorganic SoWates. *J. Am. Chem. Soc.* **2004**, *126*, 15809–15817.
- 182. Aarts, J.; Fischer, H.; Adan, O.; Huinink, H. Impact of cycling on the performance of mm-sized salt hydrate particles. *J. Energy Storage*, **2024**, *76*, 109806.
- 183. Arya, A.; Beving, M.; Mahmoudi, A.; Donkers, P. A. J.; Brem, G.; Shahi, M. Quantifying volume variation and agglomeration in thermochemical materials: An in-situ measurement methodology. J. Energy Storage, 2025, 124, 116877.
- 184. Aarts, J.; Fischer, H.; Adan, O.; Huinink, H. Towards stable performance of salt hydrates in thermochemical energy storage: A review. *J. Energy Storage*, **2025**, *114*, 115726.
- 185. Kooijman, W.; Kok, D. J.; Blijlevens, M. A. R.; Meekes, H.; Vlieg, E. Screening double salt sulfate hydrates for application in thermochemical heat storage. *J. Energy Storage*, **2022**, *55*, 105459.
- 186. Smith, J.; Weinberger, P.; Werner, A. Dehydration performance of a novel solid solution library of mixed Tutton salts as thermochemical heat storage materials. *J. Energy Storage*, **2024**, *78*, 110003.
- 187. de Oliveira Neto, J. G.; da Silva, L. F. L.; Alves, T. K. C.; Neumann, A.; de Sousa, F. F.; Ayala, A. P.; dos Santos, A. O. Mixed tutton salts K₂Mn_{0.15}Co_{0.85}(SO₄)₂(H₂O)₆ and K₂Mn_{0.16}Zn_{0.84}(SO₄)₂(H₂O)₆ for applications in thermochemical devices: experimental physicochemical properties combined with first-principles calculations. *J. Mater. Sci.*, **2024**, *59*, 14445–14464.
- 188. Fopah Lele, A.; N'Tsoukpoe, K. E.; Osterland, T.; Kuznik, F.; Ruck, W. K. L. Thermal Conductivity Measurement of Thermochemical Storage Materials. *Appl. Therm. Eng.* **2015**, *89*, 916–926.
- 189. Kleiner, F.; Posern, K.; Osburg, A. Thermal Conductivity of Selected Salt Hydrates for Thermochemical Solar Heat Storage Applications Measured by the Light Flash Method. *Appl. Therm. Eng.* **2017**, *113*, 1189–1193.
- 190. Purohit, B. K.; Sistla, V. S. Inorganic Salt Hydrate for Thermal Energy Storage Application: A Review. *Energy Storage* **2021**, 3, e212.
- 191. Pathak, A. D.; Heijmans, K.; Nedea, S.; van Duin, A. C. T.; Zondag, H.; Rindt, C.; Smeulders, D. Mass Diffusivity and Thermal Conductivity Estimation of Chloride-Based Salt Hydrates for Thermo-Chemical Heat Storage: A Molecular Dynamics Study Using the Reactive Force Field. *Int. J. Heat Mass Transf.* 2020, 149, 119090.

- 192. Li, W.; Klemeš, J. J.; Wang, Q.; Zeng, M. Development and Characteristics Analysis of Salt-Hydrate Based Sommostic Sorbent for Low-Grade Thermochemical Energy Storage. Renew. Energy 2020, 157, 920–940.
- 193. Miao, Q.; Zhang, Y.; Jia, X.; Li, Z.; Tan, L.; Ding, Y. MgSO4-Expanded Graphite Composites for Mass and Heat Transfer Enhancement of Thermochemical Energy Storage. *Sol. Energy* **2021**, *220*, 432–439.
- 194. Eurostat. First Population Estimates EU Population up to Nearly 513 Million on 1 January 2019 - More Deaths than Births; 2019.
- 195. Eurostat. Housing in Europe Statistics Visualized | 2020 Edition: 2020.
- 196. International Energy Agency (IEA). The Role of Critical Minerals in Clean Energy Transitions; 2021.
- 197. U.S. Geological Survey. *Mineral Commodity Summaries 2025*; **2025**,
 - https://pubs.usgs.gov/periodicals/mcs2025/mcs2025.pdf.
- 198. Marín, P. E.; Milian, Y.; Ushak, S.; Cabeza, L. F.; Grágeda, M.; Shire, G. S. F. Lithium Compounds for Thermochemical Energy Storage: A State-of-the-Art Review and Future Trends. *Renew. Sustain. Energy Rev.* **2021**, *149*, 111381.
- 199. Xiao, J.; Cao, X.; Gridley, B.; Golden, W.; Ji, Y.; Johnson, S.; Lu, D.; Lin, F.; Liu, J.; Liu, Y.; Liu, Z.; Ramesh, H. N.; Shi, F.; Schrooten, J.; Sims, M. J.; Sun, S.; Shao, Y.; Vaisman, A.; Yang, J.; Whittingham, M. S. From Mining to Manufacturing: Scientific Challenges and Opportunities behind Battery Production. *Chem. Rev.* **2025**, doi.org/ 10.1021/acs.chemrev.4c00980.
- 200. Shizume, K.; Hatada, N.; Toyoura, K.; Uda, T. Characteristic Microstructure Underlying the Fast Hydration-Dehydration Reaction of β-La₂(SO₄)₃: "Fine Platy Joints" with "Loose Grain Boundaries." *J. Mater. Chem. A* **2018**, *6*, 24956–24964.
- 201. Shizume, K.; Hatada, N.; Uda, T. Experimental Study of Hydration/Dehydration Behaviors of Metal Sulfates M₂(SO₄)₃ (M = Sc, Yb, Y, Dy, Al, Ga, Fe, In) in Search of New Low-Temperature Thermochemical Heat Storage Materials. *ACS Omega* **2020**, *5*, 13521–13527.
- 202. Li, W.; Guo, H.; Zeng, M.; Wang, Q. Performance of SrBr₂•6H₂O Based Seasonal Thermochemical Heat Storage in a Novel Multilayered Sieve Reactor. *Energy Convers. Manag.* **2019**, *198*, 111843.
- 203. Richter, M.; Habermann, E.-M.; Siebecke, E.; Linder, M. A Systematic Screening of Salt Hydrates as Materials for a Thermochemical Heat Transformer. *Thermochim. Acta* **2018**, *659*, 136–150.
- 204. Kiyabu, S.; Girard, P.; Siegel, D. J. Discovery of Salt Hydrates for Thermal Energy Storage. *J. Am. Chem. Soc* **2022**, *144*, 21617.
- 205. Kiyabu, S.; Siegel, D. J.; Computational Discovery of Thermochemical Heat Storage Materials Based on Chalcogenide and Complex Anion Salt Hydrates. ACS Appl. Eng. Mater., 2023, 1, 2614–2625.
- 206. De Jong, A.-J.; Trausel, F.; Finck, C.; Van Vliet, L.; Cuypers, R. Thermochemical Heat Storage System Design Issues. *Energy Procedia* **2014**, *48*, 309–319.
- 207. Thakur, S.; Giri, A. Supramolecular reinforcement drastically enhances thermal conductivity of interpenetrated covalent organic frameworks. J. Mater. Chem. A 2023, 11, 18660-18667.
- 208. Kim, H.; Choe, J. H.; Yun, H.; Kurisigal, J. F.; Yu, S.; Lee, Y. H.; Hong, C. S. High ammonia storage capacity in LiCl nanoparticle-embedded metal-organic framework composites. *Chem. Eng. J.* **2024**, *489*, 151319.
- 209. De Lange, M. F.; Verouden, K. J. F. M.; Vlugt, T. J. H.; Gascon, J.; Kapteijn, F. Adsorption-Driven Heat Pumps: The Potential of Metal–Organic Frameworks. *Chem. Rev.* 2015, 115, 12205–12250.

Journal Name

This article is licensed under a Creative Commons Attribution-NonCommercial 3.0 Unported Licence

Open Access Article. Published on 24 oktober 2025. Downloaded on 02.11.2025 08.53.33.

- 210. Mitsubishi Plastics, Inc. Low Temperature Heat Use. https://www.aaasaveenergy.com/products/001/temperature/. (Accessed on 16 April 25).
- 211. Madero-Castro, R. M.; Luna-Triguero, A.; González-Galán, C.; Vicent-Luna, J. M.; Calero, S. Alcohol-based adsorption heat pumps using hydrophobic metal—organic frameworks. *J. Mater. Chem. A* **2023**, *12*, 3434—3448.
- 212. Lu, Z. Comprehensive Investigation of Cooling, Heating, and Power Generation Performance in Adsorption Systems Using Compound Adsorbents: Experimental and Computational Analysis. *Sustainability* **2023**, *15*, 15202.
- 213. Wang, Z.; Xu, X. K.; Yan, T.; Zhang, H.; Wang, L. W.; Pan, W. G. Preparation and thermal properties of zeolite 13X/MgSO4-LiCl binary-salt composite material for sorption heat storage. *Appl. Therm. Eng.* 2024, 245, 122905.
- 214. Weckerle, C.; Dörr, M.; Linder, M.; Bürger, I. A Compact Thermally Driven Cooling System Based on Metal Hydrides. *Energies* **2020**, *13* (10), 2482.
- 215. Shabir, F.; Sultan, M.; Miyazaki, T.; Saha, B. B.; Askalany, A.; Ali, I.; Zhou, Y.; Ahmad, R.; Shamshiri, R. R. Recent Updates on the Adsorption Capacities of Adsorbent-Adsorbate Pairs for Heat Transformation Applications. Renewable Sustainable Energy Rev. 2020, 119, 109630.
- 216. Thommes, M.; Kaneko, K.; Neimark, A. V.; Olivier, J. P.; Rodriguez-Reinoso, F.; Rouquerol, J.; Sing, K. S. W. Physisorption of Gases, with Special Reference to the Evaluation of Surface Area and Pore Size Distribution (IUPAC Technical Report). Pure Appl. Chem. 2015, 87, 1051–1069.
- 217. Glaznev, I. S.; Ovoshchnikov, D. S.; Aristov, Y. I. Kinetics of Water Adsorption/Desorption under Isobaric Stages of Adsorption Heat Transformers: The Effect of Isobar Shape. Int. J. Heat Mass Transf. 2009, 52, 1774–1777.
- 218. Okunev, B. N.; Gromov, A. P.; Aristov, Y. I. Modelling of Isobaric Stages of Adsorption Cooling Cycle: An Optimal Shape of Adsorption Isobar. Appl. Therm. Eng. 2013, 53, 89– 95.
- 219. Kayal, S.; Baichuan, S.; Saha, B. B. Adsorption characteristics of AQSOA zeolites and water for adsorption chillers. *Int. J. Heat Mass Transfer* **2016**, *92*, 1120–1127.
- 220. Truong, B. N.; Borges, D. D.; Park, J.; Lee, J. S.; Jo, D.; Chang, J.-S.; Cho, S. J.; Maurin, G.; Cho, K. H.; Lee, U.-H. Tuning Hydrophilicity of Aluminum MOFs by a Mixed-Linker Strategy for Enhanced Performance in Water Adsorption-Driven Heat Allocation Application. Adv. Sci. 2023, 10, 2301311.
- 221. Abdullah; Duong, X. Q.; Shah, N. A.; Chung, J. D. Comparative study of various adsorbents for adsorption-based thermal energy storage. *J. Energy Storage* **2024**, *80*, 110332.
- 222. Builes, S.; Sandler, S. I.; Xiong, R. Isosteric Heats of Gas and Liquid Adsorption. *Langmuir* **2013**, *29*, 10416–10422.
- 223. Nuhnen, A.; Janiak, C. A Practical Guide to Calculate the Isosteric Heat/Enthalpy of Adsorption via Adsorption Isotherms in Metal—Organic Frameworks, MOFs. *Dalt. Trans.* **2020**, *49*, 10295–10307.
- 224. Cho, K. H.; Borges, D. D.; Lee, U.-H.; Lee, J. S.; Yoon, J. W.; Cho, S. J.; Park, J.; Lombardo, W.; Moon, D.; Sapienza, A.; Maurin, G.; Chang, J.-S. Rational design of a robust aluminum metal-organic framework for multi-purpose water-sorption-driven heat allocations. *Nat. Commun.* 2020, *11*, 5112.
- 225. Wongsuwan, W.; Kumar, S.; Neveu, P.; Meunier, F. A Review of Chemical Heat Pump Technology and Applications; 2001; Vol. 21.
- 226. Narayanan, S.; Yang, S.; Kim, H.; Wang, E. N. Optimization of Adsorption Processes for Climate Control and Thermal Energy Storage. *Int. J. Heat Mass Transf.* **2014**, *77*, 288–300.
- 227. Crank, J. The Mathematics of Diffusion, 2nd ed.; Clarendon Press: Oxford, 1979.
- 228. Narayanan, S.; Kim, H.; Umans, A.; Yang, S.; Li, X.; Schiffres, S. N.; Rao, S. R.; McKay, I. S.; Wang, E. N.; Rios Perez, C. A.; et

- al. A Thermophysical Battery for Storage-Based Climate Control. *Appl. Energy* **2017**, *189*, 31–4301: 10.1039/D5MH01794G
- 229. LaPotin, A.; Kim, H.; Rao, S. R.; Wang, E. N. Adsorption-Based Atmospheric Water Harvesting: Impact of Material and Component Properties on System-Level Performance. Acc. Chem. Res. 2019, 52, 1588–1597.
- 230. Alonso, M.; Sainz, E.; Lopez, F. A.; Shinohara, K. Void-Size Probability Distribution in Random Packings of Equal-Sized Spheres. Chem. Eng. Sci. 1995, 50, 1983–1988.
- 231. Huang, B.L.; Ni, Z.; Millward, A.; McGaughey, A. J. H.; Uher, C.; Kaviany, M.; Yaghi, O. Thermal conductivity of a metalorganic framework (MOF-5): Part II. Measurement. *Int. J. Heat Mass Transfer* **2007**, *50*, 405–411.
- 232. Erickson, K. J.; Léonard, F.; Stavila, V.; Foster, M. E.; Spataru, C. D.; Jones, R. E.; Foley, B. M.; Hopkins, P. E.; Allendorf, M. D.; Talin, A. A. Thin Film Thermoelectric Metal–Organic Framework with High Seebeck Coefficient and Low Thermal Conductivity. Adv. Mater. 2015, 27, 3453–3459.
- 233. Gunatilleke, W. D. C. B.; Wei, K.; Niu, Z.; Wojtas, L.; Nolas, G.; Ma, S. Thermal conductivity of a perovskite-type metalorganic framework crystal. *Dalton Trans.* 2017, 46, 13342– 13344.
- 234. Hoe, A.; Tamraparni, A.; Zhang, C.; Elwany, A.; Felts, J. R.; Shamberger, P. J. Design of Radially Variant Phase-Change Material Composites. Adv. Eng. Mater. 2022, 25, 2200841.
- 235. Shamberger, P. J.; Fisher, T. S. Cooling power and characteristic times of composite heatsinks and insulants, *Int. J. Heat Mass Transfer* **2018**, *117*, 1205–1215.
- 236. Tamraparni, A.; Hoe, A.; Deckard, M.; Zhang, C.; Elwany, A.; Shamberger, P. J.; Felts, J. R. Design and Optimization of Lamellar Phase Change Composites for Thermal Energy Storage, Adv. Eng. Mater. 2021, 23, 2001052.
- 237. Ma, H.; Aamer, Z.; Tian, Z.; Ultrahigh thermal conductivity in three-dimensional covalent organic frameworks. *Mater. Today Phys.* **2021**, *21*, 100536.
- 238. Freitas, S. K. S.; Borges, R. S.; Merlini, C.; Barra, G. M. O.; Esteves, P. M. Thermal Conductivity of Covalent Organic Frameworks as a Function of Their Pore Size. *J. Phys. Chem. C* **2017**, *121*, 27247–27252.
- 239. Boman, D. B.; Hoysall, D. C.; Pahinkar, D. G.; Ponkala, M. J.; Garimella, S. Screening of Working Pairs for Adsorption Heat Pumps Based on Thermodynamic and Transport Characteristics. *Appl. Therm. Eng.* **2017**, *123*, 422–434.
- 240. Makhanya, N.; Oboirien, B.; Ren, J.; Musyoka, N.; Sciacovelli, A. Recent Advances on Thermal Energy Storage Using Metal-Organic Frameworks (MOFs). J. Energy Storage 2021, 34, 102179.
- 241. Liu, Z.; Li, W.; Moghadam, P. Z.; Li, S. Screening Adsorbent-Water Adsorption Heat Pumps Based on an Experimental Water Adsorption Isotherm Database. *Sustain. Energy Fuels* **2021**, *5*, 1075–1084.
- 242. National Institute of Standards and Technology. NIST/ARPA-E Database of Novel and Emerging Adsorbent Materials. https://adsorption.nist.gov/isodb/index.php (Accessed on 17 April 2025).
- 243. Peng, X.; Lin, L.-C.; Sun, W.; Smit, B. Water Adsorption in Metal–Organic Frameworks with Open-Metal Sites. *AIChE J.* **2015**, *61*, 677–687.
- 244. Hamad, S.; Balestra, S. R. G.; Bueno-Perez, R.; Calero, S.; Ruiz-Salvador, A. R. Atomic Charges for Modeling Metal-Organic Frameworks: Why and How. *J. Solid State Chem.* **2015**, *223*, 144–151.
- 245. Nazarian, D.; Camp, J. S.; Sholl, D. S. A Comprehensive Set of High-Quality Point Charges for Simulations of Metal-Organic Frameworks. *Chem. Mater.* **2016**, *28*, 785–793.
- 246. Islamov, M.; Babaei, H.; Anderson, R.; Sezginel, K. B.; Long, J. R.; McGaughey, A. J. H.; Gomez-Gualdron, D. A.; Wilmer, C. E. High-throughput screening of hypothetical metal-organic

Journal Name ARTICLE

- frameworks for thermal conductivity. *npj Comput. Mater.* **2023**, 9, 11.
- 247. Zhao, G.; Brabson, L. M.; Chheda, S.; Huang, J.; Kim, H.; Liu, K.; Mochida, K.; Pham, T. D.; Prerna; Terrones, G. G.; Yoon, S.; Zoubritzky, L.; Coudert, F.-X.; Haranczyk, M.; Kulik, H. J.; Moosavi, S. M.; Sholl, D. S.; Siepmann, J. I.; Snurr, R. Q.; Chung, Y. G. CoRE MOF DB: A curated experimental metalorganic framework database with machine-learned properties for integrated material-process screening. *Matter*, 2025, 8, 102140.
- 248. Chung, Y. G.; Haldoupis, E.; Bucior, B. J.; Haranczyk, M.; Lee, S.; Zhang, H.Vogiatzis, K. D.; Milisavljevic, M.; Ling, S.; Camp, J. S.; Slater, B.; Siepmann, J. I.; Sholl, D. S.; Snurr, R. Q. Advances, Updates, and Analytics for the Computation-Ready, Experimental Metal—Organic Framework Database: CoRE MOF 2019. J. Chem. Eng. Data, 2019, 64, 5985–5998.
- 249. Zhang, H.; Snurr, R. Q. Computational Study of Water Adsorption in the Hydrophobic Metal–Organic Framework ZIF-8: Adsorption Mechanism and Acceleration of the Simulations. J. Phys. Chem. C 2017, 121, 24000–24010.
- 250. Datar, A.; Witman, M.; Lin, L.-C. Improving Computational Assessment of Porous Materials for Water Adsorption Applications via Flat Histogram Methods. *J. Phys. Chem. C* **2021**, *125*, 4253–4266.
- 251. Li, S.; Chung, Y. G.; Snurr, R. Q. High-Throughput Screening of Metal–Organic Frameworks for CO₂ Capture in the Presence of Water. *Langmuir* **2016**, *32*, 10368–10376.
- 252. Qiao, Z.; Xu, Q.; Jiang. Materials for Energy and Sustainability Computational Screening of Hydrophobic Metal-Organic Frameworks for the Separation of H₂S and CO₂ from Natural Gas. *J. Materials Chemistry A* **2018**, *6*, 18898.
- 253. Long, R.; Xia, X.; Zhao, Y.; Li, S.; Liu, Z.; Liu, W. Screening Metal-Organic Frameworks for Adsorption-Driven Osmotic Heat Engines via Grand Canonical Monte Carlo Simulations and Machine Learning. *iScience* **2021**, *24*, 101914.
- 254. Altintas, C.; Altundal, O. F.; Keskin, S.; Yildirim, R. Machine Learning Meets with Metal Organic Frameworks for Gas Storage and Separation. *J. Chem. Inf. Model.* **2021**, 61, 2131–2146.
- 255. Daglar, H.; Keskin, S. Combining Machine Learning and Molecular Simulations to Unlock Gas Separation Potentials of MOF Membranes and MOF/Polymer MMMs. ACS Appl. Mater. Interfaces. 2022, 14, 32134–32148.
- 256. Izadi, S.; Anandakrishnan, R.; Onufriev, A. V. Building Water Models: A Different Approach. J. Phys. Chem. Lett. 2014, 5, 3863-3871.
- 257. Erdős, M.; De Lange, M. F.; Kapteijn, F.; Moultos, O. A.; Vlugt, T. J. H. In Silico Screening of Metal-Organic Frameworks for Adsorption-Driven Heat Pumps and Chillers. ACS Appl. Mater. Interfaces 2018, 10, 27074–27087.
- 258. Li, W.; Xia, X.; Cao, M.; Li, S. Structure-Property Relationship of Metal-Organic Frameworks for Alcohol-Based Adsorption-Driven Heat Pumps via High-Throughput Computational Screening. J. Mater. Chem. A 2019, 7, 7470–7479.
- 259. Shi, Z.; Yuan, X.; Yan, Y.; Tang, Y.; Li, J.; Liang, H.; Tong, L.; Qiao, Z. Techno-Economic Analysis of Metal-Organic Frameworks for Adsorption Heat Pumps/Chillers: From Directional Computational Screening, Machine Learning to Experiment. J. Mater. Chem. A 2021, 9, 7656-7666.
- 260. Chung, Y. G.; Camp, J.; Haranczyk, M.; Sikora, B. J.; Krungleviciute, V.; Yildirim, T.; Farha, O. K.; Sholl, D. S.; Snurr, R. Q. Computation-Ready, Experimental Metal-Organic Frameworks: A Tool To Enable High-Throughput Screening of Nanoporous Crystals.
- 261. Chung, Y. G.; Haldoupis, E.; Bucior, B. J.; Haranczyk, M.; Lee, S.; Vogiatzis, K. D.; Ling, S.; Milisavljevic, M.; Zhang, H.; Camp, J. S.; et al. Computation-Ready Experimental Metal-Organic Framework (CoRE MOF) 2019 Dataset. 2019.

- 262. Wilmer, C. E.; Leaf, M.; Lee, C. Y.; Farha, O. K.; Hauser, B. G.; Hupp, J. T.; Snurr, R. Q. Large-Scale Screening of hypothesical Metal-Organic Frameworks. *Nat. Chem.* **2011**, *4*, 83–89.
- 263. Tong, M.; Lan, Y.; Qin, Z.; Zhong, C. Computation-Ready, Experimental Covalent Organic Framework for Methane Delivery: Screening and Material Design. J. Phys. Chem. C 2018, 122, 13009–13016.
- 264. Li, W.; Xia, X.; Li, S. Screening of Covalent–Organic Frameworks for Adsorption Heat Pumps. *ACS Appl. Mater. Interfaces* **2019**, *12*, 3265–3273.
- 265. Liang, T.; Li, W.; Li, S.; Cai, Z.; Lin, Y.; Wu, W. Performance Evaluation of Metal–Organic Frameworks in Adsorption Heat Pumps via Multiscale Modeling. *ACS Sustainable Chem. Eng.* **2024**, *12*, 2825–2840.
- 266. Cho, K. H.; Borges, D. D.; Lee, U.-H.; Lee, J. S.; Yoon, J. W.; Cho, S. J.; Park, J.; Lombardo, W.; Moon, D.; Sapienza, A.; et al. Rational Design of a Robust Aluminum Metal-Organic Framework for Multi-Purpose Water-Sorption-Driven Heat Allocations. *Nat. Commun.* 2020 111 2020, 11, 1–8.
- 267. Cadiau, A.; Lee, J. S.; Borges, D. D.; Fabry, P.; Devic, T.; Wharmby, M. T.; Martineau, C.; Foucher, D.; Taulelle, F.; Jun, C.-H.; et al. Design of Hydrophilic Metal Organic Framework Water Adsorbents for Heat Reallocation. Adv. Mater. 2015, 27, 4775–4780.
- 268. Rieth, A. J.; Wright, A. M.; Rao, S.; Kim, H.; LaPotin, A. D.; Wang, E. N.; Dincă, M. Tunable Metal—Organic Frameworks Enable High-Efficiency Cascaded Adsorption Heat Pumps. J. Am. Chem. Soc. 2018, 140, 17591—17596.
- 269. Rieth, A. J.; Wright, A. M.; Skorupskii, G.; Mancuso, J. L.; Hendon, C. H.; Dincă, M. Record-Setting Sorbents for Reversible Water Uptake by Systematic Anion Exchanges in Metal–Organic Frameworks. J. Am. Chem. Soc. 2019, 141, 13858–13866.
- 270. Wu, Y.; Kobayashi, A.; Halder, G. J.; Peterson, V. K.; Chapman, K. W.; Lock, N.; Southon, P. D.; Kepert, C. J. Negative Thermal Expansion in the Metal–Organic Framework Material Cu₃(1,3,5-Benzenetricarboxylate)₂. *Angew. Chemie Int. Ed.* **2008**, *47*, 8929–8932.
- 271. Zhang, J.; Cao, Z.; Huang, S.; Huang, X.; Han, Y.; Wen, C.; Walther, J. H.; Yang, Y. Solidification performance improvement of phase change materials for latent heat thermal energy storage using novel branch-structured fins and nanoparticles. Appl. Energy 2023, 342, 121158.
- 272. Rupam, T. H.; Tuli, F. J.; Jahan, I.; Palash, M. L.; Chakraborty, A.; Saha, B. B. Isotherms and kinetics of water sorption onto MOFs for adsorption cooling applications. *Therm. Sci. Eng. Prog.* 2022, 34, 101436.
- 273. Chao, J.; Xu, J.; Bai, Z.; Wang, P.; Wang, R.; Li, T. Integrated heat and cold storage enabled by high-energy-density sorption thermal battery based on zeolite/MgCl₂ composite sorbent. *J. Energy Storage* **2023**, *64*, 107155.
- 274. Rocky, K. A.; Pal, A.; Rupam, T. H.; Nasruddin; Saha, B. B.; Zeolite-graphene composite adsorbents for next generation adsorption heat pumps. *Microporour Mesoporous Mater.* **2021**, *313*, 110839.
- 275. Chaemchuen, S.; Xiao, X.; Klomkliang, N.; Yusubov, M. S.; Verpoort, F. Tunable Metal–Organic Frameworks for Heat Transformation Applications. *Nanomaterials* 2018, 8, 661.
- 276. Rönsch, S.; Auer, B.; Kinateder, M.; Gleichmann, K. Zeolite Heat Storage: Key Parameters from Experimental Results with Binder-Free NaY. Chem. Eng. Technol., 2020, 43, 2530– 2537.
- 277. van Alebeek, R.; Scapino, L.; Beving, M. A. J. M.; Gaeini, M.; Rindt, C. C. M.; Zondag, H. A. Investigation of a household-scale open sorption energy storage system based on the zeolite 13X/water reacting pair. *Appl. Therm. Eng.* **2018**, *139*, 325–333.

ARTICLE Journal Name

- 278. Wu, S.-F.; Yuan, B.-Z.; Wang, L.-W. MOF-ammonia working pairs in thermal energy conversion and storage. *Nat. Rev. Mater.* **2023**, *8*, 636–638.
- 279. AL-Dadah, R.; Mahmoud, S.; Elsayed, E.; Youssef, P.; Al-Mousawi, F. Metal-organic framework materials for adsorption heat pumps. *Energy* 2020, 190, 116356.
- 280. Zhang, Y.; Wang, R. Sorption thermal energy storage: Concept, process, applications and perspectives. *Energy Storage Mater.* **2020**, *27*, 352–369.
- 281. Ayaz, H.; Chinnasamy, V.; Yong, J.; Cho, H. Review of Technologies and Recent Advances in Low-Temperature Sorption Thermal Storage Systems. *Energies* 2021, 14, 6052.
- 282. Li, D.; Zeng, D.; Han, H.; Guo, L.; Yin, X.; Yao, Y. Phase Diagrams and Thermochemical Modeling of Salt Lake Brine Systems. I. LiCl + H₂O System. *Calphad* **2015**, *51*, 1–12.
- 283. Brünig, T.; Maurer, M.; Pietschnig, R. Sorbent Properties of Halide-Free Ionic Liquids for Water and CO₂ Perfusion. *ACS Sustainable Chem. Eng.* **2017**, *5*, 7228–7239.
- 284. Atkins, P. W.; De Paula, J. *Physical Chemistry*; W.H. Freeman and Co.: New York, **2010**.
- 285. Li, T. X.; Wang, R. Z.; Kiplagat, J. K.; Wang, L. W. Performance Study of a Consolidated Manganese Chloride–Expanded Graphite Compound for Sorption Deep-Freezing Processes. *Appl. Energy* **2009**, *86*, 1201–1209.
- 286. Veselovskaya, J. V; Tokarev, M. M.; Aristov, Y. I. Novel Ammonia Sorbents "Porous Matrix Modified by Active Salt" for Adsorptive Heat Transformation. 1. Barium Chloride in Various Matrices. *Appl. Therm. Eng.* **2010**, *30*, 584–589.
- 287. Wu, W. Low-Temperature Compression-Assisted Absorption Thermal Energy Storage Using Ionic Liquids. *Energy Built Environ.* **2020**, *1*, 139–148.
- 288. Kim, Y. J.; Gonzalez, M. Exergy Analysis of an Ionic-Liquid Absorption Refrigeration System Utilizing Waste-Heat from Datacenters. *Int. J. Refrig.* **2014**, *48*, 26–37.
- 289. Tanashev, Y. Y.; Krainov, A. V; Aristov, Y. I. Thermal Conductivity of Composite Sorbents "Salt in Porous Matrix" for Heat Storage and Transformation. *Appl. Therm. Eng.* 2013, 61, 401–407.
- 290. Wang, F.; Zhang, J.; Jia, S.; Chen, X.; Cheng, Z. A Review of Modification Strategies and Applications for Hydrated Salts: Insights from Energy Storage Materials Encapsulation Technology. Renewable Sustainable Energy Rev. 2025, 223, 115998.
- 291. Sun, Y.; Spieß, A.; Jansen, C.; Nuhnen, A.; Gökpinar, S.; Wiedey, R.; Ernst, S.-J.; Janiak, C. Tunable LiCl@UiO-66 Composites for Water Sorption-Based Heat Transformation Applications. J. Mater. Chem. A 2020, 8, 13364–13375.
- 292. Tan, B.; Luo, Y.; Liang, X.; Wang, S.; Gao, X.; Zhang, Z.; Fang, Y. Composite Salt in MIL-101(Cr) with High Water Uptake and Fast Adsorption Kinetics for Adsorption Heat Pumps. *Microporous Mesoporous Mater.* **2019**, *286*, 141–148.
- 293. Rehman, A. U.; Zhao, T.; Yun, S.; Xiao, Q.; Zhu, W.; Zhang, F. MgCl₂•6H₂O Supported on an NH₂-MIL-88(Fe)/MXene Hybrid Substrate to Enhance Thermochemical Heat Storage Performance. *J. Energy Storage* **2025**, *109*, 115186.
- 294. Qu, X.; Jain, A.; Rajput, N. N.; Cheng, L.; Zhang, Y.; Ong, S. P.; Brafman, M.; Maginn, E.; Curtiss, L. A.; Persson, K. A.; The Electrolyte Genome project: A big data approach in battery materials discovery. *Comput. Mater. Sci.* **2015**, *103*, 56–67.
- 295. Sewak, R.; Sudarsanan, V.; Kumar, H.; Accelerating discovery and design of high-performance solid-state electrolytes: a machine learning approach. *Phys. Chem. Chem. Phys.* **2025**, 27, 3834-3843.
- 296. Boev, A. O.; Fedotov, S. S.; Stevenson, K. J.; Aksyonov, D. A. High-throughput computational screening of cathode materials for Li-O₂ battery. *Comput. Mater. Sci.* **2021**, *197*, 110592.

- 297. Lu, Z.; Zhu, B.; Shires, B. W. B.; Scanlon, D. O.; Pickard, C. I. Ab initio random structure searching for battery waiting materials. *J. Chem. Phys.* **2021**, *154*, 174111.
- 298. Farmahini, A. H.; Krishnamurthy, S.; Friedrich, D.; Brandani, S.; Sarkisov, L. Performance-Based Screening of Porous Materials for Carbon Capture. Chem. Rev. 2021, 121, 10666–10741.
- 299. Liu, J.; Liang, L.; Su, B.; Wu, D.; Zhang, Y.; Wu, J.; Fu, C. Transformative strategies in photocatalyst design: merging computational methods and deep learning. *J. Mater. Inf.* **2024**, *4*, 33.
- 300. Priyanga, G. S.; Pransu, G.; Krishna, H.; Thomas, T. (2023). Discovery of Novel Photocatalysts Using Machine Learning Approach. In: Joshi, N.; Kushvaha, V.; Madhushri, P. (eds) *Machine Learning for Advanced Functional Materials*; Springer: Singapore, **2023**.
- 301. Luo S.; Li T.; Wang X.; Faizan M.; Zhang L. High-throughput computational materials screening and discovery of optoelectronic semiconductors. *WIREs Comput. Mol. Sci.* **2021.** *11*. e1489.
- 302. Dinic, F.; Neporozhnii, I.; Voznyy, O. Machine learning models for the discovery of direct band gap materials for light emission and photovoltaics. *Comput. Mater. Sci.* **2024**, *231*, 112580.
- 303. Pulido, A.; Chen, L.; Kaczorowski, T.; Holden, D.; Little, M. A.; Chong, S. Y.; Slater, B. J.; McMahon, D. P.; Bonillo, B.; Stackhouse, C. J.; Stephenson, A.; Kane, C. M.; Clowes, R.; Hasell, T.; Cooper, A. I.; Day, G. M. Functional materials discovery using energy-structure-function maps. *Nature* **2017**, *543*, 657–664.
- 304. Yin, X.; Gounaris, C. E. Computational discovery of Metal-Organic Frameworks for sustainable energy systems: Open challenges, *Comput. Chem. Eng.*, **2022**, *167*, 108022.
- 305. Daglar, H.; Keskin, S. Computational Screening of Metal–Organic Frameworks for Membrane-Based CO₂/N₂/H₂O Separations: Best Materials for Flue Gas Separation. *J. Phys. Chem. C.* **2018**, *122*, 17347–17357.
- 306. Kim, J.; Mok, D. H.; Kim, H.; Back, S. Accelerating the Search for New Solid Electrolytes: Exploring Vast Chemical Space with Machine Learning-Enabled Computational Calculations. *ACS Appl. Mater. Interfaces* **2023**, *15*, 52427–52435.
- 307. Chen, C.; Nguyen, D. T.; Lee, S. J.; Baker, N. A.; Karakoti, A. S.; Lauw, L.; Owen, C.; Mueller, K. T.; Bilodeau, B. A. Murugesan, V.; Troyer, M. Accelerating Ciomputational Materials Discovery with Machine Learning and Cloud High-Performance Computing: from Large-Scale Screening to Experimental Validation. J. Am. Chem. Soc. 2024, 146, 20009–20018.
- 308. Merchant, A.; Batzner, S.; Schoenholz, S. S.; Aykol, M.; Cheon, G.; Cubuk, E. D.; Scaling deep learning for materials discovery. *Nature* **2023**, *624*, 80–85.
- 309. Cai, R.; Bektas, H.; Wang, X.; McClintock, K.; Teague, L.; Yang, K.; Li, F. Accelerated Perovskite Oxide Development for Thermochemical Energy Storage by a High-Throughput Combinatorial Approach. Adv. Energy Mater. 2023, 13, 2203833.
- 310. Li, L.; Shi, Z.; Liang, H.; Liu, J.; Qiao, Z. Machine Learning-Assisted Computational Screening of Metal-Organic Frameworks for Atmospheric Water Harvesting. *Nanomaterials* **2022**, *12*, 159.
- 311. Kancharlapalli, S.; Gopalan, A.; Haranczyk, M.; Snurr, R. Q. Fast and Accurate Machine Learning Strategy for Calculating Partial Atomic Charges in Metal–Organic Frameworks. J. Chem. Theory Comput. 2021, 17, 3052–3064.
- 312. García, E. J.; Bahamon, D.; Vega, L. F. Systematic Search of Suitable Metal–Organic Frameworks for Thermal Energy-

Journal Name ARTICLE

- Storage Applications with Low Global Warming Potential Refrigerants. ACS Sustainable Chem. Eng. **2021**, *9*, 3157–3171.
- 313. Dubbeldam, D.; Torres-Knoop, A.; Walton, K. S. On the inner workings of Monte Carlo codes. *Mol. Simul.* **2013**, *39*, 1253–1292.
- 314. Myers, A. L.; Thermodynamics of adsorption in porous materials. *Thermodynamics* **2004**, *48*, 145–160.
- 315. Furukawa, H.; Gándara, F.; Zhang, Y.-B.; Jiang, J.; Queen, W. L.; Hudson, M. L.; Yaghi, O. M. Water Adsorption in Porous Metal-Organic Frameworks and Related Materials. *J. Am. Chem. Soc.* **2014**, *136*, 4369–4381.
- 316. Jeremias, F.; Lozan, V.; Henninger, S. K.; Janiak, C. Programming MOFs for water sorption: aminofunctionalized MIL-125 and UiO-66 for heat transformation and heat storage applications. *Dalton. Trans.* **2013**, *42*, 15967–15973.
- 317. Liu, Z.; Li, W.; Li, S. High-efficiency prediction of water adsorption performance of porous adsorbents by lattice grand canonical Monte Carlo molecular simulation. *RSC Appl. Interfaces* **2025**, *2*, 230–242.
- 318. Boyd, P. G.; Lee, Y.; Smit, B. Computational development of the nanoporous materials genome. *Nat. Rev. Mater.* **2017**, *2*, 17037.
- 319. Boyd, P. G.; Chidambaram, A.; Garcia-Diez, E.; Ireland, C. P.; Daff, T. D.; Bounds, R.; Gladysiak, A.; Schouwink, P.; Moosavi, S. M.; Maroto-Valer, M. M.; Reimer, J. A.; Navarro, J. A. R.; Woo, T. K.; Garcia, S.; Stylianou, K. C.; Smit, B. Data-driven design of metal-organic frameworks for wet flue gas CO₂ capture. *Nature* **2019**, *576*, 253–256.
- 320. Gomez-Gualdron, D. A.; Colon, Y. J.; Zhang, X.; Wang, T. C.; Chen, Y.-S.; Hupp, J. T.; Yildirim, T.; Farha, O. K.; Zhang, J.; Snurr, R. Q. Evaluating topologically diverse metal-organic frameworks for cryo-adsorbed hydrogen storage. *Energy Environ. Sci.* 2016, 3279–3289.
- 321. Wilmer, C. E.; Leaf, M.; Lee, C. Y.; Farha, O. K.; Hauser, B. G.; Hupp, J. T.; Snurr, R. Q. Large-scale screening of hypothetical metal-organic frameworks. *Nat. Chem.* **2012**, 83–89.
- 322.Ye, Z.; Liu, H.; Wang, W.; Liu, H.; Lv, J.; Yang, F. Reaction/sorption kinetics of salt hydrates for thermal energy storage. *Journal of Energy Storage* **2022**, *56*, 106122.
- 323. Koga, N.; Hotta, M.; Favergeon, L. Hydration Kinetics in Inorganic Salt–Water Vapor Systems: A Case of Lithium Sulfate. *J. Phys. Chem. C* **2024**, *128*, 15487–15504.
- 324. Bogdanovic, B.; Felderhoff, M.; Kaskel, S.; Pommerin, A.; Schlichte, K.; Schüth, F. Improved Hydrogen Storage Properties of Ti-Doped Sodium Alanate Using Titanium Nanoparticles as Doping Agents. *Adv. Mater.* **2003**, *15*, 1012–1015.
- 325. Xie, L.; Liu, Y.; Wang, Y. T.; Zheng, J.; Li, X. G. Superior hydrogen storage kinetics of MgH₂ nanoparticles doped with TiF₃. *Acta Mater.* **2007**, *55*, 4585–4591.
- 326. German, E.; Gebauer, R. Improvement of Hydrogen Vacancy Diffusion Kinetics in MgH₂ by Niobium- and Zirconium-Doping for Hydrogen Storage Applications. *J. Phys. Chem. C* **2016**, *120*, 4806–4812.
- 327. Shkatulov, A.; Miura, H.; Kim, S. T.; Zamengo, M.; Harada, T.; Takasu, H.; Kato, Y.; Aristov, Y. Thermochemical Storage of Medium-Temperature Heat Using MgO Promoted with Eutectic Ternary Mixture LiNO₃-NaNO₃-KNO₃. *J. Energy Storage* **2022**, *51*, 104409.
- 328. Hu, H.; Ma, C.; Chen, Q. Improved hydrogen storage properties of Ti₂CrV alloy by Mo substitutional doping. *Int. J. Hydrogen Energy* **2022**, *47*, 11929–11937.
- 329. Luo, Y.; Wang, Q.; Li, J.; Xu, F.; Sun, L.; Zou, Y.; Chu, H.; Li, B.; Zhang, K. Enhanced hydrogen storage/sensing of metal hydrides by nanomodification. *Mater. Today Nano* **2020**, *9*, 100071.

- 330. Cho, Y.; Cho, H.; Cho, E. S. Nanointerface Engineering of Metal Hydrides for Advanced Hydrogen Stores Phylogen Mater. 2023, 35, 366–385.
- 331. Chen, Z.; Muduli, R. C.; Xu, Z.; Guo, F.; Jain, A.; Isobe, S.; Wang, Y.; Miyaoka, H.; Ichikawa, T.; Kale, P. Exploring the cycling solid-state hydrogen storage performance in lithium Hydride-Porous silicon composite. *Chem. Eng. J.* **2025**, *512*, 162492.
- 332. Cho, Y.; Li, S.; Snider, J. L.; Marple, M. A. T.; Strange, N. A.; Sugar, J. D.; El Gabaly, F.; Schneemann, A.; Kang, S.; Kang, M.-h.; Park, H.; Park, J.; Wan, L. F.; Mason, H. E.; Allendorf, M. D.; Wood, B. C.; Cho, E. S.; Stavila, V. Reversing the Irreversible: Thermodynamic Stabilization of LiAlH₄ Nanoconfined Within a Nitrogen-Doped Carbon Host. *ACS Nano*, 2021, 15, 10163–10174.
- 333. Stavila, V.; Li, S.; Dun, C.; Marple, M. A. T.; Mason, H. E.; Snider, J. L.; Reynolds, J. E.; El Gabaly, F.; Sugar, J. D.; Spataru, C. D.; Zhou, X.; Dizdar, B.; Majzoub, E. H.; Chatterjee, R.; Yano, J.; Schlomberg, H.; Lotsch, B. V.; Urban, J. J.; Wood, B. C.; Allendorf, M. D. Angew. Chem. Int. Ed., 2021, 60, 25815–25824.
- 334. Abu EL-Maaty, A. E.; Abdalla, M. A.; Essalhi, M.; Abdelnaby, M. M.; Mahmoud, M. M.; Habib, M. A.; Antar, M.; Ben-Mansour, R. Kinetics of Water Adsorption in Metal-Organic Framework(MOF-303) for Adsorption Cooling Application. *Energy Convers. Manage.: X* 2024, 24, 100694.
- 335. Fuchs, A.; Knechtel, F.; Wang, H.; Ji, Z.; Wuttke, S.; Yaghi, O. M.; Ploetz, E. Water Harvesting at the Single-Crystal Level. *J. Am. Chem. Soc.* **2023**, *145*, 14324–14334.
- 336. Shi, L.; Kirlikovali, K. O.; Chen, Z.; Farha, O. K. Metal-organic frameworks for water vapor adsorption. *Chem* **2024**, *10*, 484–502.
- 337. Saha, D.; Wei, Z.; Deng, S. Equilibrium, kinetics and enthalpy of hydrogen adsorption in MOF-177. *Int. J. Hydrogen Energy* **2008**, *33*, 7479–7488.
- 338. Zeleňák V, Saldan I. Factors Affecting Hydrogen Adsorption in Metal-Organic Frameworks: A Short Review. Nanomaterials (Basel). 2021 Jun 22;11(7):1638.
- 339. Zondag, H.; Kikkert, B.; Smeding, S.; de Boer, R.; Bakker, M. Prototype Thermochemical Heat Storage with Open Reactor System. *Appl. Energy* **2013**, *109*, 360–365.
- 340. Houben, L.; Sögütoglu, L.; Donkers, P.; Huinink, H.; Adan, O. K₂CO₃ in closed heat storage systems. *Renewable Energy* **2020**, *166*, 35–44.
- 341. Zhang, Y. N.; Wang, R. Z.; Zhao, Y. J.; Li, T. X.; Riffat, S. B.; Wajid, N. M. Development and Thermochemical Characterizations of Vermiculite/SrBr₂ Composite Sorbents for Low-Temperature Heat Storage. *Energy* **2016**, *115*, 120–128.
- 342. Brancato, V.; Gordeeva, L. G.; Sapienza, A.; Palomba, V.; Vasta, S.; Grekova, A. D.; Frazzica, A.; Aristov, Y. I. Experimental Characterization of the LiCl/Vermiculite Composite for Sorption Heat Storage Applications. *Int. J. Refrig.* **2019**, *105*, 92–100.
- 343. Courbon, E.; D'Ans, P.; Skrylnyk, O.; Frère, M. New Prominent Lithium Bromide-Based Composites for Thermal Energy Storage. *J. Energy Storage* **2020**, *32*, 101699.
- 344. Shkatulov, A. I.; Houben, J.; Fischer, H.; Huinink, H. P. Stabilization of K₂CO₃ in Vermiculite for Thermochemical Energy Storage. *Renew. Energy* **2020**, *150*, 990–1000.
- 345. Aristov, Y. I.; Restuccia, G.; Cacciola, G.; Parmon, V. N. A Family of New Working Materials for Solid Sorption Air Conditioning Systems. Appl. Therm. Eng. 2002, 22, 191–204.
- 346. Chan, K. C.; Chao, C. Y. H.; Wu, C. L. Measurement of Properties and Performance Prediction of the New MWCNT-Embedded Zeolite 13X/CaCl₂ Composite Adsorbents. *Int. J. Heat Mass Transf.* **2015**, *89*, 308–319.

ARTICLE Journal Name

- 347. Veselovskaya, J. V; Critoph, R. E.; Thorpe, R. N.; Metcalf, S.; Tokarev, M. M.; Aristov, Y. I. Novel Ammonia Sorbents "Porous Matrix Modified by Active Salt" for Adsorptive Heat Transformation: 3. Testing of "BaCl₂/Vermiculite" Composite in a Lab-Scale Adsorption Chiller. *Appl. Therm. Eng.* **2010**, *30*, 1188–1192.
- 348. Gordeeva, L. G.; Grekova, A. D.; Krieger, T. A.; Aristov, Y. I. Adsorption Properties of Composite Materials (LiCl + LiBr)/Silica. *Microporous Mesoporous Mater.* **2009**, *126*, 262–267.
- 349. Johannes, K.; Kuznik, F.; Hubert, J.-L.; Durier, F.; Obrecht, C. Design and Characterisation of a High Powered Energy Dense Zeolite Thermal Energy Storage System for Buildings. *Appl. Energy* **2015**, *159*, 80–86.
- 350. Zhang, X.; Li, M.; Shi, W.; Wang, B.; Li, X. Experimental Investigation on Charging and Discharging Performance of Absorption Thermal Energy Storage System. *Energy Convers. Manag.* **2014**, *85*, 425–434.
- 351. Yu, N.; Wang, R. Z.; Wang, L. W. Sorption Thermal Storage for Solar Energy. Prog. Energy Combust. Sci. 2013, 39, 489–514.
- 352. Grekova, A.; Gordeeva, L.; Aristov, Y. Composite sorbents "Li/Ca halogenides inside Multi-wall Carbon Nano-tubes" for Thermal Energy Storage. Sol. Energy Mater. Sol. Cells 2016, 155, 176–183.
- 353. Gordeeva, L.; Frazzica, A.; Sapienza, A.; Aristov, Y.; Freni, A. Adsorption cooling utilizing the "LiBr/silica ethanol" working pair: Dynamic optimization of the adsorber/heat exchanger unit. *Energy* **2014**, *75*, 390-399.
- 354. Gaeini, M.; Rouws, A. L.; Salari, J. W. O.; Zondag, H. A.; Rindt, C. C. M. Characterization of Microencapsulated and Impregnated Porous Host Materials Based on Calcium Chloride for Thermochemical Energy Storage. *Appl. Energy* 2018, 212, 1165–1177.
- 355. Courbon, E.; D'Ans, P.; Permyakova, A.; Skrylnyk, O.; Steunou, N.; Degrez, M.; Frère, M. Further Improvement of the Synthesis of Silica Gel and CaCl₂ Composites: Enhancement of Energy Storage Density and Stability over Cycles for Solar Heat Storage Coupled with Space Heating Applications. Sol. Energy 2017, 157, 532–541.
- 356. Jabbari-Hichri, A.; Bennici, S.; Auroux, A. Enhancing the Heat Storage Density of Silica–Alumina by Addition of Hygroscopic Salts (CaCl₂, Ba(OH)₂, and LiNO₃). *Sol. Energy Mater. Sol. Cells* **2015**, *140*, 351–360.
- 357. Ristić, A.; Zabukovec Logar, N. New Composite Water Sorbents CaCl₂-PHTS for Low-Temperature Sorption Heat Storage: Determination of Structural Properties. *Nanomaterials* **2019**, *9*, 27.
- 358. Permyakova, A.; Wang, S.; Courbon, E.; Nouar, F.; Heymans, N.; D'Ans, P.; Barrier, N.; Billemont, P.; De Weireld, G.; Steunou, N.; et al. Design of Salt-Metal Organic Framework Composites for Seasonal Heat Storage Applications. *J. Mater. Chem. A* **2017**, *5*, 12889–12898.
- 359. Brancato, V.; Gordeeva, L. G.; Grekova, A. D.; Sapienza, A.; Vasta, S.; Frazzica, A.; Aristov, Y. I. Water Adsorption Equilibrium and Dynamics of LICL/MWCNT/PVA Composite for Adsorptive Heat Storage. Sol. Energy Mater. Sol. Cells 2019, 193, 133–140.
- 360. Grekova, A. D.; Gordeeva, L. G.; Aristov, Y. I. Composite "LiCl/Vermiculite" as Advanced Water Sorbent for Thermal Energy Storage. *Appl. Therm. Eng.* **2017**, *124*, 1401–1408.
- 361. Yu, N.; Wang, R. Z.; Lu, Z. S.; Wang, L. W. Development and Characterization of Silica Gel–LiCl Composite Sorbents for Thermal Energy Storage. *Chem. Eng. Sci.* **2014**, *111*, 73–84.
- 362. Whiting, G. T.; Grondin, D.; Stosic, D.; Bennici, S.; Auroux, A. Zeolite–MgCl₂ Composites as Potential Long-Term Heat Storage Materials: Influence of Zeolite Properties on Heats of Water Sorption. *Sol. Energy Mater. Sol. Cells* **2014**, *128*, 289–295.

363. D'Ans, P.; Courbon, E.; Permyakova, A.; Nouar, F.; Simonnet-Jégat, C.; Bourdreux, F.; Malet, L.; Serres, Oglobal Steunou, N. A New Strontium Bromide MOF Composite with Improved Performance for Solar Energy Storage Application. J. Energy Storage 2019, 25, 100881.